Diamond Cut:

A Foundation for Grading

GEMS & GEMOLOGY.

EDITORIAL _____

FEATURE ARTICLE _____

pg. 203

NOTES AND NEW TECHNIQUES _____

pg. 238

REGULAR FEATURES _____

pg. 249

pg. 261

GEMS & GEMOLOGY®

SUBSCRIPTIONS

Subscriptions to addresses in the U.S. are priced as follows: **$74.95** for one year (4 issues), **$194.95** for three years (12 issues). Subscriptions sent elsewhere are **$85.00** for one year, **$225.00** for three years. Canadian subscribers should add GST.

Special rates are available for GIA Alumni Association members and current GIA students. One year: **$64.95** to addresses in the U.S., **$75.00** elsewhere; three years: **$179.95** to addresses in the U.S., **$210.00** elsewhere. Please have your student or Alumni number ready when ordering.

Single copies of this issue may be purchased for **$19.00** in the U.S., **$22.00** elsewhere. Discounts are given for bulk orders of 10 or more of any one issue. A limited number of back issues are also available for purchase. Please address all inquiries regarding subscriptions and single copy or back issue purchases to the Circulation Coordinator (see above) or visit www.gia.edu.

To obtain a Japanese translation of *Gems & Gemology,* contact GIA Japan, Okachimachi Cy Bldg., 5-15-14 Ueno, Taitoku, Tokyo 110, Japan. Our Canadian goods and service registration number is 126142892RT.

MANUSCRIPT SUBMISSIONS

Gems & Gemology welcomes the submission of articles on all aspects of the field. Please see the Guidelines for Authors in this issue or on our Web site, or contact the Managing Editor for a copy. Letters on articles published in *Gems & Gemology* are also welcome.

COPYRIGHT AND REPRINT PERMISSIONS

ABOUT THE COVER

The standard round brilliant cut diamond is the staple of the modern jewelry industry. The lead article in this issue, by Thomas M. Moses and co-authors, is the third installment of GIA's research into the various aspects of diamond cut and how each affects overall cut appearance and quality. This report presents the results of extensive observation testing and describes the new GIA diamond cut grading system, which provides a useful assessment of cut quality in standard round brilliants.

The lenticular image on the cover shows a single round brilliant cut diamond as it moves through five different viewing angles (the individual images appear in the Editorial, on pp. 197–198). The lenticular was printed by Standard Register, Dayton, Ohio, using photographs © GIA and Harold & Erica Van Pelt.

Color separations for Gems & Gemology *are by PacificPreMedia, Carlsbad, California.*
Printing is by Fry Communications Inc., Mechanicsburg, Pennsylvania.

Unlocking the SECRETS

of the FOURTH C

When Richard T. Liddicoat created the now *de facto* international diamond grading system in the early 1950s, he was able to establish standards and nomenclature for color and clarity that would eventually become part of our everyday diamond lexicon. He was less confident in his ability to create a standardized system for cut that could adequately deal with both the scientific aspects and the multitude of tastes in the marketplace. Liddicoat therefore developed a system of "corrected weight" from which students could arrive at reasonably accurate diamond cut quality (and even pricing) determinations based on proportion deductions from the so-called American Ideal round brilliant. This system provided the basis for GIA's diamond training in cut for some three decades. However, when diamond prices skyrocketed in the late 1970s and subsequently crashed in the early '80s, the corrected weight system became less relevant.

GIA formally revised its diamond courses to reflect this change in the mid-1980s. For years afterward, some in the trade were still questioning our shift away from corrected weight toward a more generalized training system that did not hold the American Ideal cut as a standard to which all other round brilliants were compared. And yet another debate emerged: Some people wanted a cut grade, while others were vehemently against it. We knew, however, that fundamental to the concerns of this debate was the question of whether cut could be objectively assessed, and whether that assessment could be made scientifically, using modern resources.

Photos by Harold & Erica Van Pelt

Our commitment to contemporary research on cut reached a new level in the late 1980s, when computer technology had advanced to the point where we could analyze features of diamond appearance that heretofore had not been feasible to explore. As a result, in 1988 we made the critical decision to fund a substantial grant to a young mathematician then in graduate school at the California Institute of Technology (Caltech) in Pasadena. We had no idea at the time that a project to develop a highly technical three-dimensional computer model of a "virtual" diamond using sophisticated ray-tracing software would evolve into a 15-year, multi-million-dollar study of every aspect of cut appearance in round brilliant diamonds. What began as pure research has now resulted in a scientifically based, but eminently practical, grading system for categorizing cut in standard round brilliants.

The feature article in this issue, authored by Tom Moses and

a host of GIA professionals, is the third in a series of landmark articles on cut in round brilliants that we are proud to bring you in *Gems & Gemology*. The first, published in 1998, was from a group led by that "young mathematician" from Caltech, Scott Hemphill, and focused on what we called "weighted light return," a metric for reporting brilliance (which we have since determined is best described as *brightness*). The second article, published by Dr. Ilene Reinitz and co-authors in 2001, focused on dispersed colored light return, a metric for fire. These two articles formed the basis of our assessment of cut in round brilliants, but brightness and fire alone were not enough.

A third component, scintillation, needed to be examined before we could fully understand the factors that contribute to diamond cut appearance. Our researchers turned to observation testing with experienced people from different trade segments, as well as consumers, to explore this element. They found that although some aspects of scintillation (those related to sparkle) were included in the brightness and fire metrics, there was also an important underlying element that affected the appearance of scintillation itself. This element, called "pattern," represents the size and arrangement of bright and dark areas in a diamond, and is a key component of the extent to which observers find a diamond attractive. We found from our interaction with the trade that this phenomenon was considered part of the "life" of a diamond—a common term used to describe desirable stones.

Observation testing and interaction with the trade also established the importance of other aspects beyond cut appearance—design and craftsmanship—in the assessment of a diamond's overall cut quality. These include durability and "over-weight" concerns, as well as polish and symmetry. In addition, we used observation testing to fine-tune our original brightness and fire metrics, so they would more accurately reflect real-world conditions. The current article discusses all these elements of cut and describes how we validated the very sophisticated model we created.

Our authors aren't the first to use computer modeling to predict the effects of various proportion sets on the cut appearance of diamonds. To our knowledge, though, no other organization or research group has validated their models to the extent GIA has with observation testing of actual diamonds by experts in the field, a major part of the research described in the present article.

While GIA has studied cut in diamonds for decades, our concentrated effort—particularly over the past 10 years—has now yielded breakthrough research that will undoubtedly alter historical practices and traditional perceptions of many in the diamond industry. The main conclusions are as follows:

- Individual proportions must not be assessed on their own. It is the complex interrelationship of individual proportions that matters most in the face-up cut appearance and overall cut quality of a diamond.

- There is no one set of proportions that yields *the* most beautiful diamond. Similarly, the long-held view that expanding deviations from a fixed, arbitrary set of proportion values produces diamonds with increasingly poorer appearances is simply not valid.

- Truly consistent and accurate comparisons of cut in diamond require a standardized viewing and lighting environment that is representative of common environments used in the trade.

- Whereas other systems for assessing cut in round brilliants have from three to 11 different classification categories, our research found that most individuals could consistently discern five levels of different cut quality.

- For a grading system to be truly unbiased and objective, it must allow for personal and global preferences in diamond appearance.

Once we determined that a comprehensive system for assessing diamond cut in round brilliants could be developed, we were still left with the fundamental question of whether a diamond cut grade was useful for the public and the trade. Although there actually has been a tremendous amount of industry interest in the creation of an objective, scientifically based system for assessing diamond cut, ultimately the decisions on this project and the directions GIA has chosen were derived from its mission—*to ensure the public trust in gems and jewelry by upholding the highest standards of integrity, academics, science, and professionalism through education, research, laboratory services, and instrument development.* GIA firmly believes that the public interest is best served by creating such a system, and that its impact on the trade will also be positive.

Photos by Harold & Erica Van Pelt

As such, the authors and their colleagues have used this extensive research to develop a cut grading system for round brilliants that will be incorporated into GIA's diamond training in education and into diamond grading in the laboratory in mid-2005. For years, many in the trade have maintained that a wider set of proportions could yield an equally beautiful diamond; to some extent, these people are vindicated by the results of our research. Diamond manufacturers will be able to cut round brilliants to a wider range than the current norm and still achieve top-grade, great-looking diamonds. An even wider range of proportions can produce pleasing diamonds in the upper-middle to middle grade ranges. Each of these grades will, in many cases, allow for greater yield and weight retention from the rough.

Ultimately, the new GIA diamond cut grading system will provide answers to the long-debated questions about the fourth C in diamond grading. As a result, dealers and retailers will have definitive categories for cut in round brilliants and thus will be able to better serve their clients. And consumers will have access to information that was heretofore either nonexistent or unavailable as an international standard. GIA will soon propose that global standard.

Over the years, our research objectives evolved and expanded from first seeking a better understanding of cut, to establishing a system that would "flag" poorly cut diamonds, to building one that would also give credit to well-made stones. I am pleased to say that our objectives have been met with the creation of a truly unbiased scientific system to assess the cut grade of standard round brilliants; furthermore, the system has been validated by expert observers. We believe that this system will stand the test of time, like the color and clarity scales we created more than 50 years ago. While the process has been evolutionary, the end result may in fact be revolutionary. Only the future will tell. Research will certainly continue, and it may never stop. Cut is humankind's unique way of adding value to that finely crystallized carbon we have all come to know and love as the king of gems.

William E. Boyajian

William E. Boyajian, President
Gemological Institute of America

LETTERS

Issue Packaging

I wonder why, when you package the magazine, you conceal the cover photo. If everyone who handled *Gems & Gemology* on the way to delivery could see the cover, it might help to educate or create an interest—who knows? *[Anonymous]*

Reply: In mailing each issue, we deliberately conceal subject matter such as the cover photo. This is a security measure that was instituted at the request of several subscribers, who receive the journal at their homes. As a postscript, after we started this practice, we also saw a significant decrease in reports of issues that never quite made it into our readers' mailboxes.

Expressing Magnification in Photomicrographs

The use of simple numbers such as "30×" to describe the scale of photomicrographs is unheard of in the world of credible scientific publication. It is a meaningless number that is changed at any stage, from the camera itself to the digital file and the cropping of the photo, as well as in the adjustments made by the publisher for the column width, and so on. By the time this notation is seen by the reader, all the reader knows is that the microscope was set on 30× for visual observation at the time the photomicrograph was taken.

Respectable scientific journals in all other fields refer to the scale of a photomicrograph with an actual measured "field width" of the final image or a simple line in the image representing millimeters, decimals of millimeters, or other appropriate linear measurements.

That being said, I personally think the current iteration of *G&G* has done more for the science of gemology than any other single item or event, and I look forward to every issue.

> *Bob Hord*
> *Laguna Park, Texas*

Reply: This same point was raised by *G&G* reader Dr. William Hanneman in the Summer 1987 issue (Editorial Forum, pp. 111–112). Contributing editor and noted photomicrographer John I. Koivula responded to that letter, and we feel his reply—paraphrased here, with Mr. Koivula's permission—is just as appropriate today:

The purpose of printing photomicrographs in professional gemological publications is to convey useful information to the reader. When we say 45×, we immediately let the jeweler-gemologist know that this subject would be easily resolved using a standard gemological microscope with an upper magnification limit of 45× or greater. If the slide was cropped by the editor and then enlarged by a factor of 10 to fill the planned space, all the editor has done is increase the size of the image without gaining or increasing detail. In reality, if the same area was actually viewed at 450×, the scene could be significantly different, with the item in question totally distorted.

From my own experience in the use of precise measuring devices in petrology and chemical microscopy, I can understand some of these arguments. But each of the sciences has its own set of standard practices, and these may or may not apply to others. It is true that we could place a standard scale bar of a specified length in each photomicrograph as is done in some of the other sciences. However, gemology is more than just a science, it is also an art. As gemologists, we deal with beauty on a daily basis; it is perhaps the greatest appeal of our profession. And as long as there is no significant problem generated by the method of magnification designation as it is currently practiced in virtually all publications in the field, this writer sees no reason to detract from the artistic quality of the image by incorporating a size scale.

Use of Technical Terms

Quite often, with the exception of prefatory information and conclusions, the feature articles in *G&G* are difficult for me to understand because of the technical terms. The names of certain advanced instruments, geological terms, mining terms, etc. that are used by the authors are not found in my GIA course materials. I think it would be very helpful to have a comprehensive dictionary or encyclopedia that I could refer to when I encounter words or concepts that I don't understand.   *[Anonymous]*

Your Summer 2003 issue clearly explained on page 88 (of the article by J. L. Emmett et al., "Beryllium diffusion of ruby and sapphire") what SIMS is and how it works. In my opinion, a publication on non-standard identification techniques would be of interest. This summary should explain how each method works (e.g., EDXRF, photoluminescence spectroscopy, Raman, etc.) and why it is used. Do you think such a publication would be possible?

Heinz Kniess
Rodersdor, Switzerland

Reply: We know that our readers and authors alike come from many different backgrounds, with education and experience in a variety of disciplines. Within the journal, we make every attempt to define nonstandard terms when they are first used. In addition, for some articles on special topics (see, for example, the lead article in this issue, on diamond cut), we will include a glossary. GIA is also looking into updating and republishing the *Dictionary of Gems and Gemology*, which has been out of print for many years. In the interim, for geologic and mining terms, we strongly recommend the *Glossary of Geology*, 4th ed. (J. A. Jackson, Ed., American Geological Institute, Alexandria, VA, 1997). For descriptions of many of the advanced instruments and techniques currently used in gemology, we recommend the article by M. L. Johnson, "Technological developments in the 1990s: Their impact on gemology," Winter 2000 *G&G*, pp. 380–396. However, these two letters send a clear message that, given the rapid advances being made in gemology in the 21st century, we may need to publish such a review article more often than every 10 years.
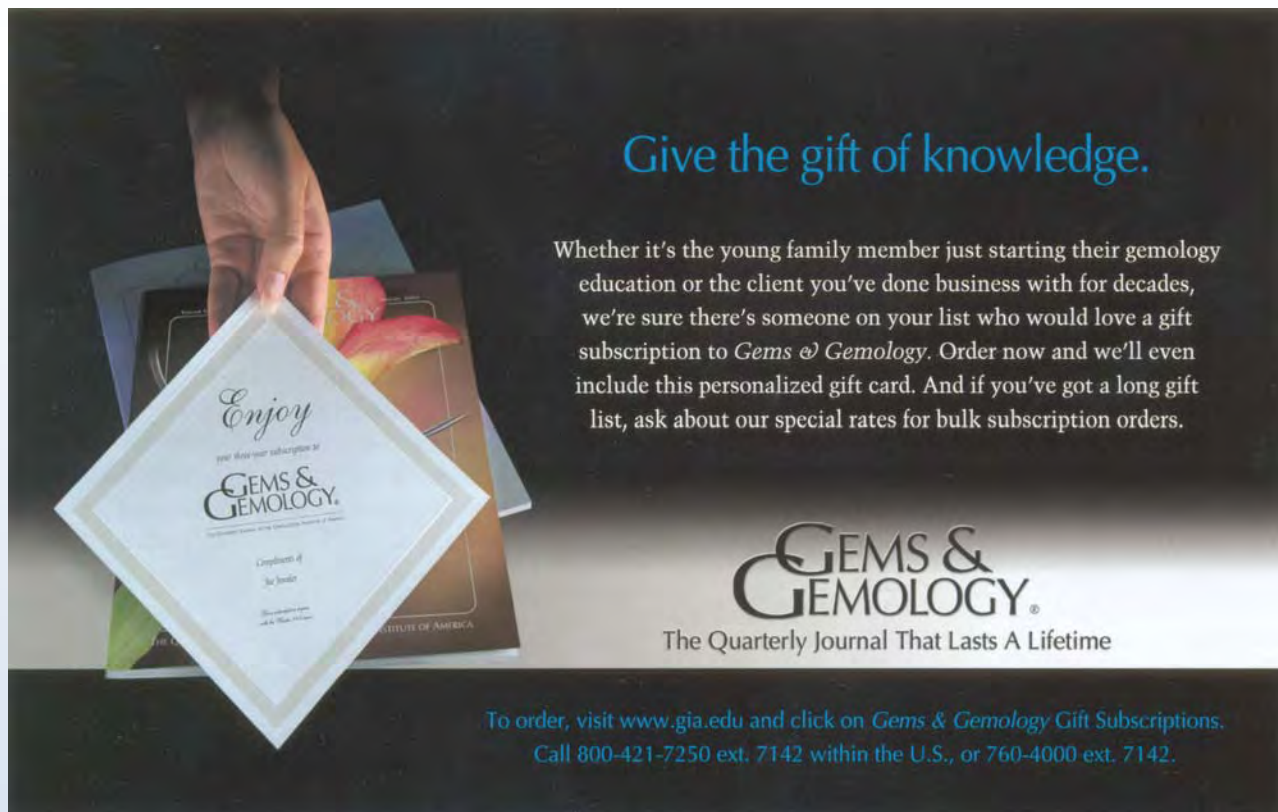
A FOUNDATION FOR GRADING THE OVERALL CUT QUALITY OF ROUND BRILLIANT CUT DIAMONDS

Thomas M. Moses, Mary L. Johnson, Barak Green, Troy Blodgett, Kim Cino, Ron H. Geurts,
Al M. Gilbertson, T. Scott Hemphill, John M. King, Lisa Kornylak, Ilene M. Reinitz, and James E. Shigley

GIA began its 15-year study of diamond cut by using a computer to model the way light behaves within a round brilliant cut diamond. From this model, GIA researchers developed proportion-based metrics to predict how diamonds would perform with regard to brilliance and fire. Continued research revealed several important variables that could not be evaluated effectively by computer modeling alone. Thus, the authors asked diamond manufacturers, dealers, retailers, and potential consumers to evaluate brightness (a term selected as more appropriate than *brilliance*), fire, and overall cut appearance of diamonds representing many different proportion combinations. These observations and discussions confirmed that additional factors, besides brightness and fire, contribute to diamond cut appearance, and that factors in addition to face-up appearance are important in assessing the quality of a diamond's cut. With the trade interactions as a foundation, the authors (1) tested the brightness and fire metrics to find the best fit with human observations, (2) identified and quantified factors in addition to brightness and fire that contribute to face-up appearance, (3) developed a standard viewing environment that mimics common trade environments, (4) created the foundation for a comprehensive diamond cut grading system, and (5) began development of reference software to predict the overall cut grade of a particular diamond. The GIA diamond cut grading system described here includes the components of brightness, fire, scintillation, polish, and symmetry, as well as weight and durability concerns, into a single overall grade for cut quality for standard round brilliants.

O f the Four Cs (color, clarity, cut, and carat weight), cut is the least understood—and least agreed upon—aspect of diamond appearance. Current claims about the superiority of certain round brilliant diamond cuts focus mostly on three approaches:

- The use of specific sets of proportions (e.g., those for the AGS 0, the AGA 1A, "Class 1" cuts [as previously taught by GIA Education], the HRD "Very Good" grades, "Ideal" cuts, and "Tolkowsky" cuts)
- The use of viewing devices to see specific patterns or pattern elements in diamonds (e.g., FireScope, Symmetriscope, IdealScope, and various "Hearts-and-Arrows"–style viewers)

- The use of proprietary devices, such as the GemEx BrillianceScope and ISEE2, which measure one or more of the following aspects of diamond appearance: brilliance, fire, scintillation, and/or symmetry

For GIA's research on the evaluation of diamond cut, we started with a different approach, based on the following questions: What makes a round brilliant cut (RBC, figure 1) diamond look the way it does? To what degree do differences among cutting

Figure 1. The round brilliant is the most popular diamond cut. Because of its popularity, assessment of this cut has been the subject of considerable research. This image shows a wide range of uses for this style in commercial jewelry, as well as loose polished diamonds and diamond crystals. The loose polished diamonds weigh 1.05–3.01 ct, and the rough crystals weigh 2.14–2.49 ct. Jewelry and loose polished diamonds courtesy of Ben Bridge Jewelers. Composite photo by Harold & Erica Van Pelt.

proportions create observable distinctions? Which proportion sets produce results that are deemed attractive by most experienced observers? The first stages of our research—which utilized advanced computer modeling—were described briefly by Manson (1991), and then in detail by Hemphill et al. (1998) and Reinitz et al. (2001).

Many other groups have used some form of computer modeling to predict appearance aspects of diamond proportion sets, including: Fey (1975), Dodson (1978, 1979), Hardy et al. (1981), Harding (1986), van Zanten (1987), Long and Steele (1988, 1999), Tognoni (1990), Strickland (1993), Shigetomi (1997), Shannon and Wilson (1999), Inoue (1999), and Sivovolenko et al. (1999). To our knowledge, however, few if any of these other studies validated their modeling results by using observation tests of actual diamonds, a major component of the research described in the present article. The validation of computer modeling by observations is essential in the evaluation of diamond cut appearance, as without this validation there is a risk of producing results that are not applicable to the real-world assessment of diamonds.

In this article, we discuss the key aspects of a well-cut diamond. We describe how we tested our previously published metrics (numerical values based on mathematical models) for brilliance and fire by conducting observations with actual diamonds in typical trade environments and then developed new metrics based on our results. We also explain how we validated these new metrics with further observation tests, and developed and tested additional methods, including environments and procedures, for evaluating other essential aspects of diamond appearance and cut quality. Finally, on the basis of the information gathered during this extensive testing, we constructed a comprehensive system for assessing the cut appearance and quality of round brilliant cut diamonds. The present article discusses the framework of this system, further details of which will be made available in later publications.

BACKGROUND AND TERMINOLOGY

The face-up appearance of a polished diamond is often described in terms of its brilliance (or brilliancy), fire, and scintillation (see, e.g., *GIA Diamond Dictionary*, 1993). Historically, however, diamond appearance has been described using other terms as well; even the addition of *scintillation* to this list has been a relatively recent development (see, e.g., Shipley, 1948).

Today, while brilliance, fire, and scintillation are widely used to describe diamond appearance, the definitions of these terms found in the gemological literature vary, and there is no single generally accepted method for evaluating and/or comparing these properties in diamonds. Further, experienced

members of the diamond trade use additional terms when they assess the appearance of diamonds. In the course of this study, we interviewed dozens of diamond manufacturers and dealers, in various international diamond cutting centers and at trade shows. (We also interviewed retailers and jewelry consumers, as described below.) We found that, in addition to *brilliance*, *fire*, and *scintillation*, they tended to use words such as *life*, *pop*, *lively*, *dull*, *bright*, or *dead* to describe a diamond's cut appearance, although they could not always explain precisely what they meant by such terms. In some cases, they would know whether or not they liked a diamond, but were unable to articulate exactly why.

To avoid potential confusion in describing cut appearance, we have refined and expanded the definitions of three essential terms, so that they more clearly and accurately reflect what experienced observers see in actual diamonds in everyday environments. Throughout this article, we will use the following definitions (see the glossary on p. 223 for a list of key diamond cut terms used in this article):

- **Brightness**—the appearance, or extent, of internal and external reflections of "white" light seen in a polished diamond when viewed face-up. *Note that although we originally used* brilliance *to describe this property (Hemphill et al., 1998; Reinitz et al., 2001), as we proceeded further with our study, we found that many individuals in the trade and general public include other appearance aspects (such as contrast) in their use of that term. Hence, we decided to use* brightness *instead.*

- **Fire**—the appearance, or extent, of light dispersed into spectral colors seen in a polished diamond when viewed face-up.

- **Scintillation**—the appearance, or extent, of spots of light seen in a polished diamond when viewed face-up that flash as the diamond, observer, or light source moves (*sparkle*); and the relative size, arrangement, and contrast of bright and dark areas that result from internal and external reflections seen in a polished diamond when viewed face-up while that diamond is still or moving (*pattern*).

Note that the definitions for *fire* and *scintillation* differ from those currently found for similar terms in the *GIA Diamond Dictionary* (1993) and those given in the two earlier *G&G* articles about this study. They replace those definitions, and *brightness*

replaces *brilliance*, for the purposes of this article and the forthcoming GIA diamond cut grading system.

Our interviews also confirmed that, in addition to brightness, fire, and scintillation, the design and craftsmanship of the diamond, as evidenced by its physical shape (e.g., weight and durability concerns) and its finish (polish and symmetry), are important indicators of a diamond's overall cut quality.

MATERIALS AND METHODS

This (third) stage of research evolved from that presented in our previous two articles on diamond appearance (Hemphill et al., 1998; Reinitz et al., 2001). Initially, we focused this stage on exploratory testing, to compare our computer-modeled predictions of brightness and fire with observations by experienced trade observers of selected actual diamonds. We found that the observers generally agreed with each other but, in many cases, not with our predictions. We used these findings to create and test additional brightness and fire metrics, using a broader group of observers and diamonds.

Extensive observation testing with diamonds was needed to: (1) determine how well the original and subsequent metric predictions compared to actual observations; (2) establish thresholds at which differences defined by the model are no longer discerned by an experienced observer; (3) see the broad range of effects that might be statistically significant with a large and varied sample of diamonds; (4) determine what additional factors must be considered when assessing diamond cut appearance and quality; and (5) supply enough data for overall preferences to be revealed amid the widely varied tastes of the participants.

Analysis of the observation data did reveal which metrics best fit our observation results. It also outlined discernible grade categories for our metric results by identifying those category distinctions that were consistently seen by observers. To determine what additional factors were not being captured by our computer model, we returned to the trade and asked individuals their opinions of diamonds that were ranked with our new brightness and fire metrics. Although a majority of these diamonds were ranked appropriately when metric results were compared to trade observations, many were not. By questioning our trade observers, and through extensive observations performed by a specialized team (the "Overall observation team"), we explored additional issues related to face-up appear-

ance (sparkle and pattern) and cut quality (design and craftsmanship) that proved to be essential when assessing a round brilliant's cut quality. These observation tests also supplied data that emphasized the importance of considering personal and global preferences when assessing and predicting diamond cut appearance and quality.

Last, we combined the findings of our observation testing and trade discussions with the predictive and assessment capabilities of our brightness and fire metrics to develop a comprehensive system comprised of all the factors identified in this latest phase of research. This became the framework of our diamond cut grading system.

Methods of Observation Testing. Testing for individual and market preferences is called *hedonics testing* (see, e.g., Ohr, 2001; Lawless et al., 2003) and is often used in the food sciences. Among the types of tests employed are acceptance tests (to determine if a product is acceptable on its own), preference tests (comparing products, usually two at a time), difference tests (to see whether observers perceive products as the same or different; that is, which levels of difference are perceptible), and descriptive analysis (in which observers are asked to describe perceptions and differences, and to what degree products are different). At various times throughout our research, we used each of these.

The observations focused on individual appearance aspects (such as brightness and fire) as well as on the overall cut appearance and quality of polished diamonds. The format and goal of each set of observation tests were determined by the questions we hoped to answer (e.g., Will pairs of diamonds ranked in brightness by our brightness metric appear in the same order to observers?), as well as by the findings of previous observation tests. In this way, as our study evolved, we varied the specific diamonds used in testing, the environments in which the diamonds were viewed, and the questions that we asked.

Our first observation tests for this project were performed in February 2001; since then, we have collected more than 70,000 observations of almost 2,300 diamonds, by over 300 individuals. (Approximately 200 observers were from all levels of the diamond trade or consumers, and about 100 were from the GIA Gem Laboratory and elsewhere at GIA, as described below.)

The trade press has reported on the use of diamond observations to test appearance models (e.g.,

Scandinavian Diamond Nomenclature [SCAN DN] in 1967, mentioned by Lenzen, 1983; Nahum Stern at the Weitzmann Institute of Science in Israel, circa 1978 ["Computer used . . .," 1978]), although to the best of our knowledge no results have been published. In addition, we at GIA have used statistical graphics in the past to explain observational results (see, e.g., Moses et al., 1997). Thus, this work is an application (and extension) of previously applied techniques.

Diamonds. We purchased and/or had manufactured a set of diamonds of various proportions (some rarely seen in the trade), so that the same set of samples would be available for repeated and ongoing observation tests. These 45 "Research Diamonds" made up our core reference set (see table 1). Some data on 28 of these diamonds were provided by Reinitz et al. (2001).

In our computer model, assumptions were made about color (D), clarity (Flawless), fluorescence (none), girdle condition (faceted), and the like. We recognized that actual diamonds seen in the trade would differ from their virtual counterparts in ways that would make the model less applicable. Therefore, to expand our sample universe, we augmented the core reference set with almost 2,300 additional diamonds (summarized in table 2) temporarily made available by the GIA Gem Laboratory. These diamonds provided a wide range of weights, colors, clarities, and other quality and cut characteristics. All of these diamonds were graded by the GIA Gem Laboratory and measured using Sarin optical measuring devices. In addition, we developed new methods for measuring critical parameters that previously had not been captured (for a description of the proportion parameters measured and considered, see figure 2).

Observers. Experienced diamond manufacturers and brokers make purchasing and cutting decisions based on aesthetic and economic considerations. To begin the verification process for our brightness and fire metrics, we watched these individuals as they examined some of our Research Diamonds, both in the environments where they usually make their daily decisions about diamond cut and appearance, and in a variety of controlled environments (detailed below). In general, we asked them what we thought were straightforward questions: "Which of these diamonds do you think is the brightest, the most fiery, and/or the most attractive overall? What differences do you see that help you make these decisions?"

TABLE 1. Properties of the core sample group of 45 Research Diamonds.[a]

RD no.	Weight (ct)	Crown angle (°)	Crown height (%)	Pavilion angle (°)	Table size (%)	Total depth (%)	Star length (%)	Lower girdle length (%)	Girdle thickness	Girdle condition	Culet size	Clarity	Color	Fluorescence	Polish	Symmetry
01	0.61	34.0	15.5	40.8	54	61.2	50	75	Thin to medium	Faceted	None	VS$_1$	E	None	Very good	Very good
02	0.64	33.0	13.0	41.6	59	61.5	55	75	Slightly thick to thick	Faceted	Very small	SI$_2$	E	Faint	Very good	Good
03	0.55	32.0	11.5	41.0	63	58.6	60	80	Medium to slightly thick	Faceted	None	VS$_2$	H	None	Good	Good
04	0.70	36.0	15.5	42.0	58	65.4	55	80	Slightly thick to thick	Faceted	None	VVS$_2$	E	None	Good	Very good
05	0.66	24.0	9.5	42.4	57	58.5	55	85	Medium to slightly thick	Faceted	None	VS$_2$	F	None	Very good	Good
06	0.59	23.0	9.5	42.0	56	57.2	60	80	Medium to slightly thick	Faceted	None	VVS$_2$	F	Faint	Very good	Very good
07	0.76	36.5	17.5	41.4	53	64.1	55	90	Thin to medium	Faceted	None	SI$_1$	F	None	Very good	Very good
08	0.50	33.5	14.0	41.2	57	61.1	55	85	Medium	Faceted	None	VVS$_1$	H	None	Very good	Very good
09	0.66	23.5	10.0	42.2	55	59.4	60	75	Medium to slightly thick	Faceted	None	IF	F	None	Very good	Good
10	0.68	34.5	16.0	41.0	54	62.1	55	75	Very thin to medium	Faceted	None	VS$_2$	G	None	Very good	Good
11	0.71	37.0	16.0	42.2	58	64.9	45	85	Medium to slightly thick	Bruted	None	VS$_2$	D	None	Good	Very good
12	0.71	35.0	15.0	41.0	57	62.6	55	75	Medium to slightly thick	Faceted	None	SI$_1$	F	None	Good	Very good
13	0.59	33.5	16.0	41.2	52	61.9	60	80	Thin to slightly thick	Faceted	None	VVS$_2$	E	None	Very good	Good
14	0.71	34.5	14.0	42.0	59	62.4	60	80	Very thin to slightly thick	Faceted	None	SI$_1$	G	None	Good	Good
15	0.67	25.5	10.0	40.8	59	55.6	55	75	Medium	Faceted	None	VS$_1$	H	None	Good	Good
16	0.82	33.5	15.5	40.6	53	61.2	50	75	Thin to medium	Faceted	Very small	VS$_1$	G	None	Good	Very good
17	0.75	26.0	10.0	38.6	59	53.2	50	75	Thin to medium	Faceted	None	VS$_2$	F	None	Very good	Very good
18	0.62	29.0	11.0	41.4	61	57.8	45	75	Medium to slightly thick	Faceted	None	VVS$_2$	H	None	Very good	Very good
19	0.72	29.0	10.5	39.6	62	54.5	50	75	Medium	Faceted	None	VS$_1$	H	None	Very good	Very good
20	0.62	34.5	13.5	40.8	61	59.6	55	80	Medium	Faceted	None	VVS$_1$	I	Strong blue	Very good	Very good
21	0.82	35.5	15.5	41.2	58	62.3	55	75	Thin to medium	Faceted	None	VVS$_1$	I	Strong blue	Very good	Good
22	0.81	35.5	16.5	39.4	54	60.6	55	75	Thin	Faceted	None	VS$_1$	K	None	Very good	Very good
23	0.72	36.5	17.0	40.6	54	63.7	55	80	Medium	Faceted	None	VVS$_2$	I	None	Very good	Good

[a] *Research Diamonds RD01–RD27 and RD29 were previously reported in Reinitz et al. (2001); variations in proportion values from that article are the result of recutting, measuring device tolerances, and/or the application of rounding. Verbal descriptions are used here for girdle thickness and culet*

Interactions with trade observers were used in two ways. First, they provided an initial direction for this stage of our research project, reinforcing which aspects of cut quality needed to be considered in addition to brightness and fire. Subsequently, they served as guidance; throughout our research, we returned to trade observers to compare against the findings we received from our internal laboratory teams.

A summary of our observers (including number and type) is given in table 3. Our core trade observers ("Manufacturers and Dealers" and "Retailers" in table 3) are experienced individuals from around the world who routinely make judgments on which their livelihoods depend about the quality of diamond manufacture. Many of these men and women have decades of experience in the dia-

RD no.	Weight (ct)	Crown angle (°)	Crown height (%)	Pavilion angle (°)	Table size (%)	Total depth (%)	Star length (%)	Lower girdle length (%)	Girdle thickness	Girdle condition	Culet size	Clarity	Color	Fluorescence	Polish	Symmetry
24	0.58	35.5	12.5	39.0	66	56.3	60	75	Thin to medium	Faceted	None	VVS_1	H	None	Very good	Good
25	0.82	40.0	13.0	42.0	69	60.2	55	75	Thin to medium	Faceted	None	VVS_2	H	None	Good	Very good
26	0.89	38.0	15.0	42.0	61	63.3	55	70	Medium	Faceted	None	VS_1	I	None	Very good	Very good
27	0.44	11.0	15.0	50.8	64	67.8	50	75	Thin to medium	Faceted	None	VS_2	G	Strong blue	Very good	Good
28[b]	n/a	n/a	n/a	n/a	n/a	n/a	n/a	n/a	n/a	n/a	n/a	n/a	n/a	n/a	n/a	n/a
29	0.69	37.5	15.5	42.2	60	62.9	50	75	Thin to medium	Bruted	Small	SI_1	F	Faint	Excellent	Excellent
30	0.64	34.5	15.5	40.8	55	60.9	50	75	Medium	Bruted	None	IF	I	None	Very good	Excellent
31	0.41	27.0	11.5	40.4	57	58.8	50	75	Slightly thick to thick	Faceted	Very small	VS_2	E	None	Very good	Good
32	0.64	35.0	16.5	41.0	53	60.5	45	60	Medium to thick	Faceted	Slightly large	VS_2	H	Medium blue	Very good	Good
33	0.64	37.0	16.5	44.0	56	68.0	55	70	Thin to medium	Faceted	None	VS_1	H	None	Very good	Very good
34	0.49	41.5	19.5	40.4	56	70.7	55	80	Very thick	Faceted	None	VS_1	H	None	Very good	Good
35	0.44	31.0	9.0	43.2	70	58.4	65	80	Thin to medium	Bruted	None	VS_2	D	None	Good	Good
36	0.65	37.0	16.5	43.4	57	67.9	55	75	Medium to thick	Faceted	None	VS_2	H	None	Excellent	Very good
37	0.50	33.5	9.5	40.2	70	56.9	60	80	Slightly thick to thick	Bruted	None	VS_2	F	None	Good	Good
38	0.70	37.0	16.5	41.6	57	69.1	60	85	Very thick	Faceted	None	VS_1	H	None	Very good	Good
39	0.70	35.5	15.5	41.2	57	74.0	55	80	Extremely thick	Faceted	None	SI_1	F	Medium blue	Good	Good
40	0.70	38.5	14.5	41.0	63	69.3	60	80	Very thick to extremely thick	Faceted	None	SI_1	G	None	Good	Good
41	0.71	37.0	17.0	40.2	55	67.3	55	85	Very thick	Faceted	None	VS_2	H	Medium blue	Good	Good
42	0.71	37.0	17.0	41.4	54	68.3	55	80	Thick	Faceted	None	VS_1	G	None	Good	Very good
43	0.50	38.5	17.5	41.8	57	71.5	55	80	Thick to very thick	Faceted	None	VVS_2	G	None	Good	Good
44	0.70	38.0	16.5	41.4	57	68.1	55	80	Medium to very thick	Faceted	None	VVS_2	I	Faint	Good	Good
45	0.62	37.0	14.5	45.2	62	69.3	60	85	Medium to very thick	Bruted	None	VS_1	F	None	Good	Good
46	0.54	37.0	14.5	37.2	62	54.5	60	85	Extremely thin to thick	Bruted	None	SI_2	F	None	Excellent	Good

size, as they are reported by the GIA Gem Laboratory. Listed properties were determined by the GIA Gem Laboratory.
[b] Not included in sample set for this research because it is a modified round brilliant.

mond trade, and most of them routinely handle thousands of polished diamonds per week. (Because retailers typically sell diamonds in different environments from those in which manufacturers and dealers evaluate them [see below], we generally analyzed their observations separately.) The results of these trade observations were used to define our initial quality ranges for brightness, fire, and overall face-up appearance, as well as to provide useful information on other essential aspects of diamond cut quality.

To expand our population of experienced diamond observers, we also established several teams of individuals from the GIA Gem Laboratory to carry out the numerous observations that we conducted. We developed a team of "Brightness

observers" who saw the same differences in bright-ness (within a five-diamond set of our Research Diamonds, RD01–RD05; again, see table 1) as our trade observers did in a comparable environment. We assembled a different group of specialized individuals to serve as our "Fire observers." Last, we assembled a team of six individuals from the GIA Gem Laboratory (our Overall observation team) who combined had more than 100 years of experience viewing diamonds. This team, whose members did not participate in any of the other teams, conducted several sets of tests that focused on judging diamonds for their overall cut appearance and quality. The GIA Gem Laboratory observers were asked to examine larger populations of selected diamonds and to answer the same kinds of questions as those posed to the trade observers. Early testing showed that the responses of the lab groups were consistent with those of the trade observers.

Two other groups who took part in observations were less experienced GIA personnel and consumers. In this way, we met our goal of considering observations from people at all levels of the diamond trade, as well as consumers.

Viewing Environments. To discover how individuals in the trade normally evaluate diamonds on a day-to-day basis, we asked them detailed questions about their working environments, and we observed them while they assessed diamonds in these environments. This revealed their everyday observation practices such as colors of clothing, colors of the backgrounds on which they viewed diamonds, light intensity, lighting and viewing geometry, light-source specification, and how they held and moved diamonds when viewing them.

Our observers examined diamonds in a number of different environments, some variable and some controlled, including:

- Their own offices and workplaces (using desktop fluorescent lamps)

- A conference room at the GIA offices in New York (using similar desk lamps and/or the viewing boxes described below)

- Retail showrooms (usually consisting of a mix of fluorescent and spot lighting)

- "Retail-equivalent" environments at GIA in Carlsbad and New York, set up according to recommendations by a halogen light-fixture manufacturer (Solux)

- Standardized color-grading boxes, including two commercially available boxes (the Graphic Technology Inc. "Executive Show-Off" Model PVS/M—the "GTI" environment—and the Macbeth Judge II Viewing Booth, both with daylight-equivalent D65 fluorescent lamps)

TABLE 2. Ranges of properties and proportions for 2,298 other diamonds used for verification testing.[a]

Parameter	Brightness and fire verification diamonds	Overall Verification Diamonds (OVDs)
No. of diamonds	688	1,610
Weight range	0.20–1.04 ct	0.25–14.01 ct
Clarity	Internally flawless–I_3	Internally flawless–I_3
Color	D–Z	D–Z
Fluorescence intensity	None to very strong	None to very strong[b]
Fluorescence color	Blue	Blue, white, yellow[b]
Table size	52–72%	46–74%
Crown angle	23.0–42.5°	22.5–42.0°
Pavilion angle	37.6–45.6°	37.2–44.0°
Lower-girdle facet length	60–95%	55–95%
Star facet length	40–70%	35–70%
Depth percent	51.5–71.2	52.8–72.0
Crown height	7.0–20.0%	6.5–19.5%
Polish	Excellent to fair	Excellent to fair
Symmetry	Excellent to fair	Excellent to fair
Culet size	None to very large	None to very large
Girdle thickness	Very thin to extremely thick	Very thin to extremely thick
Girdle condition	Faceted, polished, bruted	Faceted, polished, bruted
Total no. observations per diamond	9–29	3–15
Brightness observations per diamond	3–11	0[c]–3
Fire observations per diamond	5–15	0[c]–4
Overall appearance observations per diamond	1–3	3–8

[a] See figure 2 for a description of diamond proportions mentioned in this table.
[b] We saw only an extremely small number of fluorescent diamonds in the very strong range, or in white or yellow; we found the effects of these particular qualities to be insignificant for the diamonds observed.
[c] Brightness and/or fire observations were not conducted for some of the Overall Verification Diamonds.
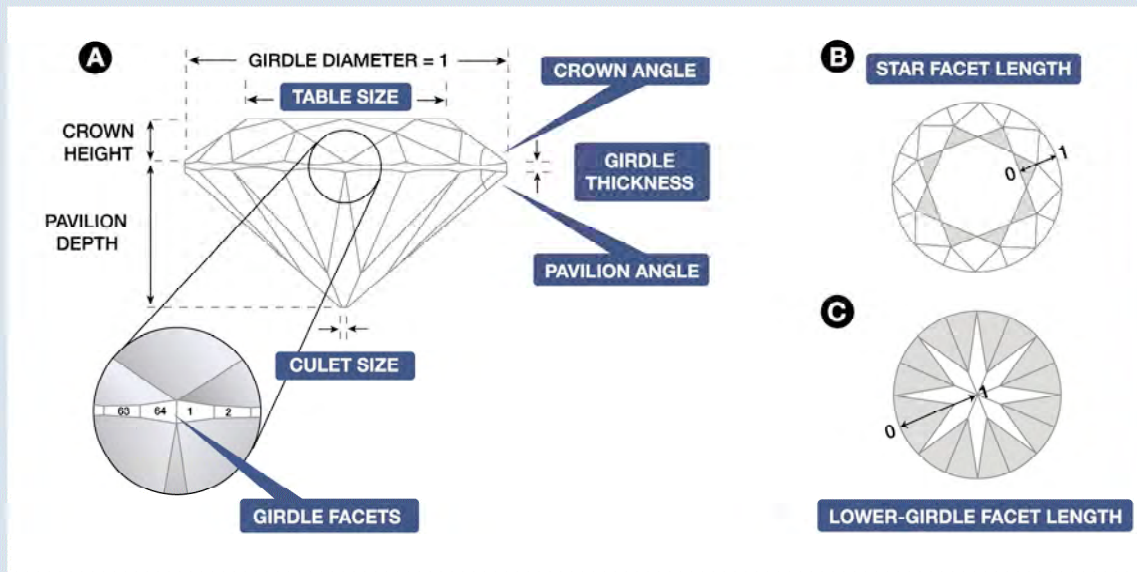
Figure 2. A round brilliant cut diamond can be described using eight proportion parameters: table size, crown angle, pavilion angle, star facet length, lower-girdle facet length, girdle thickness, culet size, and number of girdle facets. Other parameters (e.g., crown height) can be calculated from these eight. (A) All linear distances in this profile view can be described as a percentage of the girdle diameter, although at the GIA Gem Laboratory girdle thickness and culet size are described verbally based on a visual assessment. (B) In this face-up view of the crown, the star facet length is shown at 50%, so that the star facets extend half the distance from the table to the girdle (indicated here by 0–1). (C) In this table-down view of the pavilion, the lower-girdle facet length is shown at 75%, so that the lower-girdle facets extend three-fourths of the distance from the girdle to the culet center (0–1). Adapted from Reinitz et al. (2001).

• At least three versions of a standardized viewing box of our own design (the common viewing environment, or "CVE")

• A variety of patterned hemisphere environments (to imitate computer-modeled environments)

The same diamond can look quite different depending on the type and position of lighting that is used (figure 3). On the one hand, for cutting diamonds and for evaluating brightness and the quality of diamond cutting in general, most manufacturers use overhead fluorescent lights and/or desk lamps

TABLE 3. Summary of observers and types of observations.

| Observation group | Trade observers | | GIA Gem Laboratory observers[b] | | | | | |
	Manufacturers and dealers	Retailers[a]	Brightness team	Fire team	Overall observation team	Additional GIA personnel[c]	Consumers[d]	Total
No. of individuals	37	159	7	6	6	141	28	384
Types of observations	Brightness, fire, overall	Brightness, fire, overall	Brightness	Fire	Overall	Brightness, fire, overall	Brightness, fire, overall	

[a] Includes sectors of the trade that work with the public, such as appraisers.
[b] Each of these three teams was composed of members who were not part of other teams.
[c] Includes individuals from the Research department, the GIA Gem Laboratory, and GIA Education.
[d] Includes non-gemological individuals from trade shows and GIA.

Figure 3. A diamond looks different in different lighting and viewing environments. In these images, the same diamond was photographed in diffused lighting (left), mixed lighting (center), and spot lighting only (right). Photos by A. Gilbertson.

with daylight-equivalent fluorescent bulbs; dealers and brokers generally use similar desk lamps in their offices (figure 4). However, this type of diffuse lighting suppresses the appearance of fire (again, see figure 3). On the other hand, retail environments generally provide spot, or point source, lighting (usually with some overall diffuse lighting as well), which accentuates fire (figure 5).

Therefore, when we wanted solely to study the effects of brightness, we used dealer-equivalent

Figure 4. Diamond manufacturers and dealers typically view and assess diamond appearance and cut quality in offices with fluorescent desk lamps. Objects in the room, including the observer, can block or affect light shining on the crown of a polished diamond. Photo by A. Gilbertson.
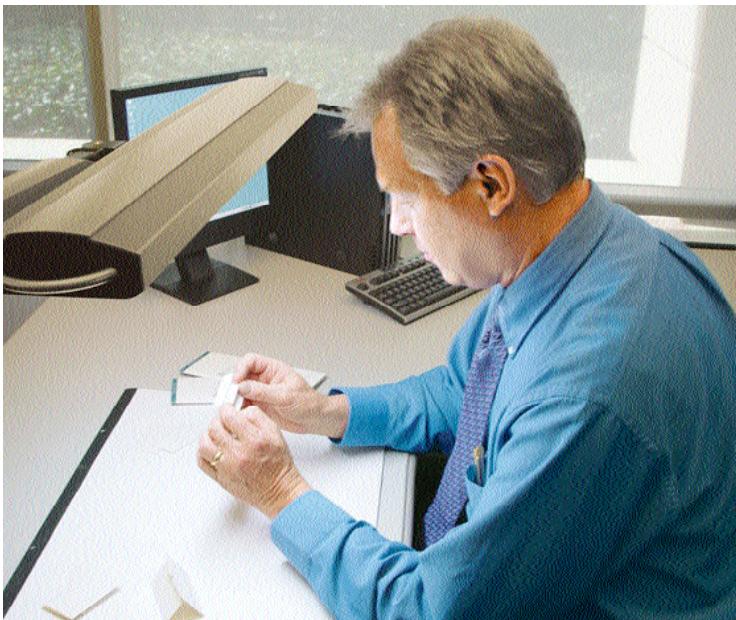
lighting, which consisted of daylight-equivalent fluorescent lights mounted in fairly deep, neutral-gray viewing boxes (e.g., the Macbeth Judge II, as is used for color grading colored diamonds; see King et al., 1994). Similarly, when we wanted to study only the effects of fire, we used our retail-equivalent lighting, which consisted of a series of three halogen lamps mounted 18 inches (about 46 cm) apart and six feet (1.8 m) from the surface of the work table, in a room with neutral gray walls that also had overhead fluorescent light fixtures.

For observation of overall cut appearance, we developed a GIA "common viewing environment" (CVE [patent pending]), a neutral gray box (shallower than the Macbeth Judge II or GTI environment) with a combination of daylight-equivalent fluorescent lamps and overhead white LEDs (light-emitting diodes; figure 6). We established the optimum intensity of the fluorescent lamps by observing when a set of reference diamonds showed the same relative amounts of brightness as they showed in the dealer-equivalent lighting. The intensity of the LEDs was determined by identifying a level at which fire was visible in diamonds but the relative amounts of brightness were still easy to observe accurately. In this way, we were able to observe brightness and fire in a single viewing environment that preserved the general qualities of both dealer and retail lighting.

We also investigated the effects of background color (that is, the color in front of which diamonds were observed). Our computer models for brightness and fire assumed a black background; yet we found that most people in the diamond trade use white backgrounds of various types (often a folded white business card) to assess diamond appearance. Our observation teams assessed diamonds for brightness and fire on black, white, and gray trays

Figure 5. Retail environments for diamonds typically use a combination of spot lighting and diffused or fluorescent lighting. Photo courtesy of Dale's Jewelry, Idaho Falls, Idaho; ©Instore.

to determine if tray color affected brightness and fire results. Additionally, the members of our Overall observation team observed diamonds on various color trays to determine their effect on overall cut appearance.

For the Brightness and Fire teams, additional viewing devices were sometimes employed, especially in the early stages of investigation. To test our axially symmetric (that is, hemisphere-like) brightness metrics, we built patterned hemispheres (figure 7; also, see table 1 in the *Gems & Gemology* Data Depository at www.gia.edu/gemsandgemology) of various sizes (6, 12, and 16 inches—about 15, 30, and 41 cm—in diameter) in which the diamonds were placed while observers evaluated their relative brightness. The results of these hemisphere observations were also compared to results from the more typical trade environments discussed above (table 4, "Brightness: verification;" see also box A). To be rigorous in our investigation, we examined a wider range of hemispheres than we believed were necessary solely to test our brightness metrics. In addition, we constructed a "fire training station," an environment consisting of a light source and a long tube (figure 8) that enabled Fire team observers to grow accustomed to seeing finer distinctions of dispersed colors in diamonds, and to distinguish among diamonds with different amounts of fire. Once they were comfortable with the fire training station, observers made evaluations of fire in our retail-equivalent lighting (described above) and, eventually, in our CVE (table 4, "Fire: verification").

Figure 6. The GIA common viewing environment (CVE) allows individuals to observe the brightness, fire, and overall cut appearance of a polished diamond. This CVE contains daylight-equivalent fluorescent lighting (to best display brightness) combined with the spot lighting of LEDs (to best display fire) in a neutral gray environment. Photo by Maha Tannous.
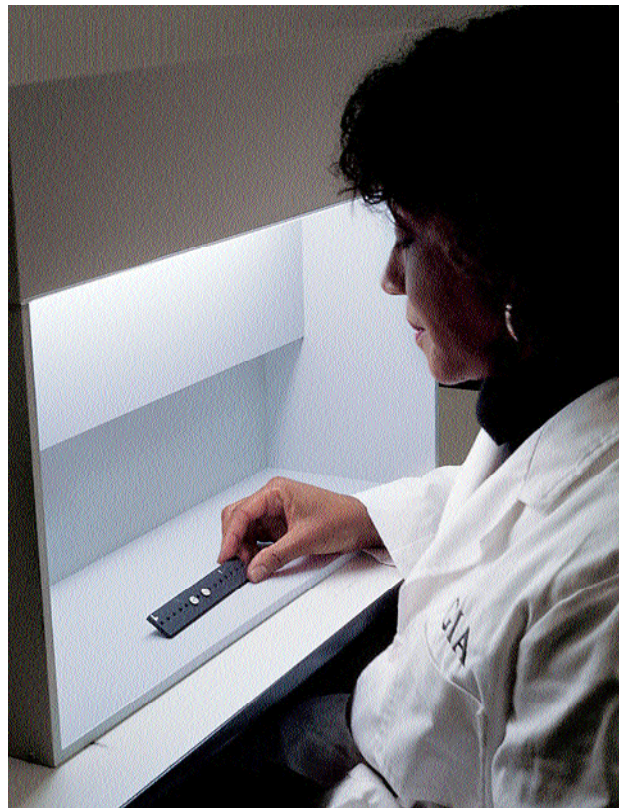
Figure 7. Shown here is a small assortment of the "patterned" hemispheres used in the testing of the brightness metrics. Inset: Using a hemisphere to observe diamonds. Photos by A. Gilbertson.

Early Observation Testing: Brightness and Fire. Our Brightness team examined a set of five Research Diamonds, RD01–RD05 (see table 1), for brightness differences in the dome environments described above. We confirmed that the predictions of a specific brightness metric (the relative brightness order of the five diamonds) matched the observations of the Brightness team in the environment for that metric. We then used relative observations of 990 pairs of Research Diamonds (our core reference set; see table 1 and box A) in dealer-equivalent lighting to select the appropriate brightness metric; that is, we adjusted the modeling conditions (e.g., lighting conditions or viewing geometry) of our brightness metrics until we found one that predicted brightness ranking in the same order as the observation results.

Next, we trained the Fire team to see relative amounts of fire consistently and asked them to compare the same 990 pairs of diamonds in a retail-equivalent environment that emphasized this appearance aspect. Then, as we did with the brightness metric, we varied the modeling conditions (in

this case, the threshold levels of discernment) of the Reinitz et al. (2001) fire metric to get the best fit with these observations in this environment.

As part of this early testing process, we also chose almost 700 diamonds with varying quality characteristics (i.e., with a wide range of clarity, color, symmetry, polish, fluorescence, etc.) and had both our Brightness and Fire teams observe them for brightness and fire in the dealer- and retail-equivalent environments. We compared these observations to brightness and fire metric results to determine whether any of these characteristics significantly affected the correlation between observation results and metric results.

Later Observation Testing: Overall Cut Appearance and Quality. We used several methodologies for observation testing of overall cut appearance and quality. One method was to ask observers to look at five diamonds at a time and rank them from brightest, most fiery, and/or best looking to least bright, least fiery, and/or worst looking (we also did this using three diamonds at a time). We conducted later

comparisons in a "binary" fashion (that is, comparing two diamonds at a time from a set, until each diamond had been compared to every other diamond in the set). We also conducted observations in which diamonds were compared against a small suite of Research Diamonds chosen from the core reference set. A fourth methodology consisted of asking observers to examine larger sets (10 to 24 diamonds) and order them by overall appearance into as many groups as they wished (for a summary of all observation tests, again see table 4).

In early sessions, participants were asked to observe diamonds face-up, without a loupe, while the diamonds were in the observation tray. However, we did not restrict their ability to move or tilt the diamonds, and in most cases participants

tilted or "rocked" them during their examination. Later, when we conducted observations on overall cut quality (as opposed to just face-up appearance), we allowed participants to examine the profiles of the diamonds (using a loupe and tweezers) *after* they had provided their first impressions of the diamonds. This process further helped us recognize the importance of craftsmanship and other factors in the assessment of overall cut quality.

In all of these observations, participants were asked to rate diamonds based solely on face-up appearance or on each diamond's overall cut quality. Participants were also asked to detail the reasons for their decisions (e.g., localized darkness in the face-up appearance or girdles that were "too thick"). These responses along with the participants' rank-

TABLE 4. Summary of observation tests.

Type of observation	Viewing environment[a]	Type of observer[b]	Diamond samples used[c]	Comparison method[d]	Total no. of observations
Brightness	Manufacturer-equivalent, retail-equivalent, Judge	M&D, GIA personnel, consumers, B-team	RD01–RD46	Binary, 3x rank, 5x rank	9,996
Brightness: metric verification	GTI and CVE	GIA personnel and B-team	Diamonds borrowed from other sources[e]	Binary with comparison "master" diamonds	11,418
Brightness: metric verification	Various domes	GIA personnel and B-team	RD01–RD46	Binary, 3x rank, 5x rank	17,843
Brightness: environment consistency	GTI, Judge	B-team	Set 1	Binary	280
Fire	Manufacturer-equivalent, retail-equivalent	GIA personnel, B-team, M&D	RD01–RD46	Binary, 5x rank	688
Fire: metric verification	Retail-equivalent and CVE	F-team	Diamonds borrowed from other sources[e]	Binary with comparison "master" diamonds	11,992
Scintillation	Retail-equivalent	GIA personnel, B-team, F-team	Set 1, set 2, diamonds borrowed from other sources[e]	5x rank	2,122
Overall	Retail-equivalent and CVE	GIA personnel, B-team, F-team, retailers, consumers	RD01–RD46	5x rank, Good/Fair/ Poor rank; dividing diamonds into groups	3,608
Overall: metric verification	CVE	Overall observation team	Diamonds borrowed from other sources[e]	Binary with comparison "master" diamonds	3,549
Overall: environment consistency	CVE with and without multiple light sources	Overall observation team	RD01–RD46	Binary with comparison "master" diamonds	396
Brightness, fire, scintillation, and overall	Retailer environments	Retailers	Set 1, set 2	5x rank	1,370
Overall verification (brightness, fire, overall) observations	CVE	F-team, B-team, Overall observation team	Diamonds borrowed from other sources[e]	Binary with comparison "master" diamonds	7,580

[a] As described in the Materials and Methods section: GTI = Graphic Technology Inc. "Executive Show-Off" Model PVS/M; Judge = Macbeth Judge II Viewing Booth; CVE = the GIA common viewing environment.
[b] Observers are listed as B-team (Brightness team), F-team (Fire team), and M&D (Manufacturers and Dealers). See Materials and Methods section and table 3 for a description of these teams.
[c] Set 1 consisted of RD01, RD02, RD03, RD04, and RD05; set 2 consisted of RD08, RD11, RD12, RD13, and RD14. See table 1 for properties.
[d] Comparison methods used were binary rank (two diamonds side-by-side), 3x rank (three diamonds side-by-side), and 5x rank (five diamonds side-by-side). "Master" diamonds were chosen from the Research Diamonds.
[e] Summarized in table 2.

ings were then used to develop a methodology for accurately predicting a diamond's overall cut appearance and quality.

Computer Modeling and Calculations. Our computational methods for the modeling of brightness and fire were essentially the same as those given in our two previous papers (Hemphill et al., 1998; Reinitz et al., 2001). Although our modeling software is custom and proprietary, it can be used on any computer that can run programs written in the C language; to calculate the metric results for almost one million proportion combinations, we ran them on sixteen 500 MHz Pentium III processors (later updated to sixteen 2.5 GHz Pentium IV processors) and two 2.4 GHz Pentium IV processors.

Metrics. We generated more than 75 different, yet related, brightness and fire metrics to compare with our ongoing observations (see table 2 in the *Gems & Gemology* Data Depository at www.gia.edu/gemsandgemology). To define an appearance metric, assumptions must be made about the modeled diamond, the modeled observer (position and angular spread of observation), the modeled environment (including illumination), and the property being quantified.

In the metrics for this work (compared to those presented in our two previous *G&G* articles), we varied:

- The position of the observer and the angular spread of observation for brightness.
- The distribution of dark and light in the environment for brightness.
- The absence or presence of front-surface reflections (specular reflection, or "glare") for brightness.
- The visual threshold for fire. (This was an explicitly variable factor in our fire metric; again, see Reinitz et al., 2001.)

BOX A: STATISTICAL EVALUATION OF BRIGHTNESS AND FIRE METRICS

We collected relative brightness and fire observations on diamonds in many environments, and we examined a number of possible brightness and fire metrics. To compare metric values with observation results, we had to convert both into rank orders.

Members of the Brightness and Fire teams compared each of the Research Diamonds to each other in pairs for brightness or fire, respectively; this gave 990 binary comparisons under each condition. As is typical with observation data, not all observers agreed on every result (although some results were unanimous). This makes sense if the relative ranking of two diamonds is not considered simply as a measurement, but as a measurement with some accompanying uncertainty; that is, a distribution of values. (For example, 4 is always a larger number than 3 which is a larger number than 2; but a number measured as 3 ± 1.2 could in fact be greater than 4 or less than 2.) We therefore assumed that the observed brightness (or fire) rank for each diamond could be represented by a probability distribution, and then found the relative order that maximizes the probability of obtaining the observational data we had.

Sometimes, the data showed that all observers saw one diamond to be better (or worse) than all the others. In such a case, all the pair-wise comparisons to that diamond were set aside from the rest of the data set; this process was repeated, if necessary, to determine the relative order of the remaining diamonds, from which overall rankings could then be made.

For both observed ranks (described above) and metric ranks (based on their metric values), we used scaled rank orders (i.e., the orders did not have to be an integer value, but the highest-ranking diamond came in first, and the lowest-ranking diamond came in 45th).

The scaled-rank data sets were compared using the Pearson Product Moment Correlation. This method produces the "r"-value seen in linear correlations (see, e.g., Kiess, 1996; Lane, 2003). The metric with the highest r-value to the observed data was selected as the best fitting metric.

We then used Cronbach's alpha (see, e.g., Cronbach, 1951; Nunnally, 1994; Yu, 1998, 2001) to test the reliability of the metric predictions relative to our observers. Cronbach alpha values range between 0 and 1, with near-zero values representing noncorrelated sets of data. Values of 0.70 and higher are considered acceptable correlations for reliability. More importantly, if results from a predictive system are added to a dataset as an additional observer and the alpha coefficient remains about the same, then that system is strongly correlated to (i.e., is equally reliable as) the observers.

As before, the proportions of the modeled diamonds were the input parameters that determined the metric values, so the proportion sets could vary without changing the fundamental nature of the metrics. Also as in our earlier articles, the computer-modeled diamonds were colorless, nonfluorescent, inclusion-free, and perfectly polished. Although at first we assumed the diamonds were completely symmetrical, later we measured all the facets on certain diamonds to input their exact shapes into metric calculations.

Comparison of the observation results with the metrics proved to be quite challenging, and details of some of the statistical methods we used are given in box A. These tools enabled us to decide which of our metrics were the most appropriate to predict levels of brightness and fire (i.e., the calculated appearance values that best matched results from observers looking at actual diamonds in realistic environments).

Our new metrics were based on the previously published WLR and DCLR metrics and then further developed by varying observer and environmental conditions, and the effect of glare, until we found sets of conditions that best fit the observation data in dealer- and retail-equivalent environments. The Hemphill et al. (1998) WLR (weighted light return) metric for brilliance and the Reinitz et al. (2001) DCLR (dispersed colored light return) metric for fire both assume a *distributed observer* who is positioned over the entire hemisphere, above the diamond, infinitely far away. The weighting for each possible angle of observation is determined by an angular relationship to the zenith of the hemisphere. (The zenith, looking straight down on the table of the diamond, is weighted the strongest in the final result; this is like someone who rocks the diamond, but allows the table-up view to create the strongest impression.)

To obtain stronger correlations with our diamond observation results, this time we also modeled a *localized observer*. This virtual observer only detected light from the diamond from a face-up position and within a narrow—3° angular spread—area (like a person who looks at a diamond from a mostly fixed position and from a reasonably close distance, in this case about 14–20 inches—roughly 35–50 cm—as we noted in most trade observations). Although the published WLR observer did not detect light reflected directly from the upper surfaces (that is, glare, or luster), for this work we considered brightness metrics both with and without

Figure 8. This configuration was used to train observers to see differences in fire in polished diamonds. Inset: In this schematic diagram, spot incandescent lighting from above is blocked and channeled into a long tube that shines a narrow beam of directed light onto a polished diamond. Photo by A. Gilbertson.

glare. As for previous metrics, we assumed our observer had normal color vision.

Another factor to consider when modeling an observer for fire is the visual threshold at which an individual can readily detect colored light. In our previous research (Reinitz et al., 2001), we determined visual thresholds by using a hemisphere on which chromatic flares from the crown of a polished diamond were reflected. With this hemisphere, we concluded that about 3,000 levels of intensity of the colored light could be observed. In the course of our observation tests for fire discernment, we found that an individual could

observe more levels of intensity with this hemisphere than when observing fire directly from the crown of a polished diamond. Thus, for the present work we varied this threshold in our metric until we found the best fit with observation results.

The *environment* for the WLR metric was assumed to be a hemisphere of uniform (that is, fully diffused) illumination above the diamond's girdle (everything below the diamond's girdle is dark). By contrast, for the present work we were trying to model environments and lighting conditions used in the trade to buy or sell diamonds. Real-life environments for observing brightness are considerably more complicated. For example, light around a diamond often is disrupted by objects in the room, and much of the light directly over a diamond's table is reflected off the observer (again, see figure 4). We modeled hemispheres with various patterns of light and dark (again, see figure 7) until we found a modeled environment that closely correlated with the brightness results from typical trade environments.

The *environment* for the DCLR metric was a uniformly dark hemisphere (again, above the diamond's girdle, with all space below the girdle plane also dark) with parallel rays of illumination coming from a point light source, centered over the table. This is a reasonable approximation of a single spot light (for an observer who is not blocking the light source, and who is rocking the diamond a lot) or of many, arbitrarily placed spot lights, including one above the diamond, for an observer who rocks the diamond only a little. For our current research, we

adjusted the visual discernment thresholds within the metric to improve correlation with actual observations of fire in retail-equivalent lighting and viewing environments. This change in metric thresholds was the only one needed to create a new fire metric that correlated well with fire observations.

Finally, the *property* being quantified by WLR (and our new brightness metric, discussed below) was the total amount of *white* light returned to the observer from the crown of the diamond (in the case of the new brightness metric, this includes glare); for DCLR, it was the amount of dispersed *colored* light (i.e., fire) returned to the observer (see table 5 for a summary of these model conditions).

Calculations Derived from Standard Proportion Parameters. From the eight proportion parameters describing a perfectly symmetrical round brilliant cut diamond with a faceted girdle (i.e., table size, crown angle, pavilion angle, star facet length, lower-girdle facet length, girdle thickness, culet size, and number of girdle facets; again, see figure 2), it is possible to calculate other proportions and interrelationships. These include not only commonly quoted proportions such as crown height, pavilion depth, and total depth, but also, for example:

- Facet geometry (e.g., facet surface areas and inter-facet angles)
- Extent of girdle reflection in the table when the diamond is viewed face-up (i.e., if too extensive, a "fisheye" effect)
- Extent of table reflection when viewed face-up
- Several parameters related to localized darkness in the crown when viewed face-up
- Weight-to-diameter ratio

We ran such calculations for all the Research Diamonds and for most of the diamonds in table 2; these were used to explore scintillation aspects (see below) and other factors related to the physical shape (e.g., weight concerns) of the diamonds.

Evaluation of Overall (Face-Up) Cut Appearance. Our initial observation tests revealed that, as we expected, our best brightness and fire metrics were able to predict specific observation results (i.e., brightness and fire), but they were not adequate to predict and evaluate a diamond's overall cut appearance and quality. An example of this can be seen in figure 9, which displays brightness and fire metric results for 165 randomly selected diamonds evaluat-

TABLE 5. Comparison of old and new model conditions for calculating brightness and fire.

| Property	Metric	Modeled observer	Modeled environment	Other factors
Brightness	Old	Spread over 180° above diamond and "weighted"	White hemisphere	No glare
	New	Localized 3° angular spread	Dark circle with radius of 23° around zenith	Glare included
Fire	Old	Spread over 180° above diamond and "weighted"	Dark hemisphere	Large threshold—3,000 brightness levels
	New	Spread over 180° above diamond and "weighted"	Dark hemisphere	Small threshold—18 brightness levels

OBSERVATIONS FOR OVERALL CUT APPEARANCE
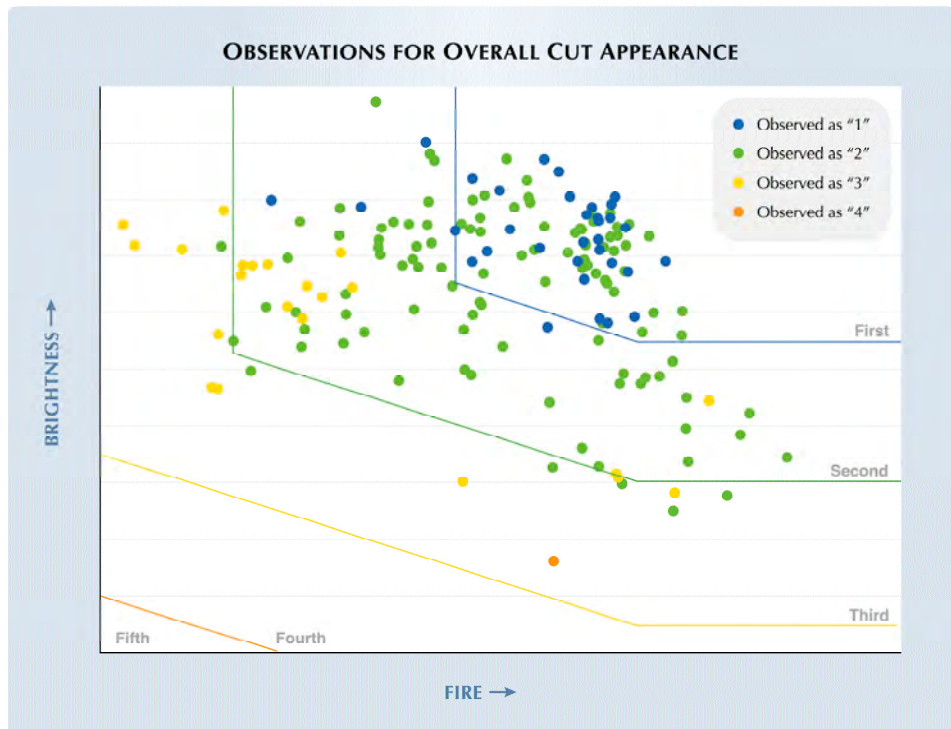
Figure 9. This plot shows 165 of the diamonds used for our overall observation tests plotted against their brightness and fire metric results. The five grading categories delineated are based on brightness and fire observation results obtained for the 45 Research Diamonds. Although many of these 165 diamonds were found to be predicted correctly by our brightness and fire metrics (when compared to overall observation results), many were not. This necessitated further research to determine what other factors might be influencing observers' assessments of face-up cut appearance.

ed by our Overall observation team for their overall face-up cut appearance. The boundaries on this plot delineate five discernible appearance categories, which were based on observation results for brightness and fire previously obtained for the Research Diamond set. Of these 165 diamonds, the overall cut appearance for 95 (58%) was accurately predicted using brightness and fire metrics alone. In addition, all the diamonds were within one category of the predicted result based only on a combination of calculated brightness and fire results.

Obviously, additional factors played a significant role in the observation results for the remaining 42% of these diamonds. Hence, the next stage of our investigation concerned how to identify and correctly evaluate those diamonds for which the brightness and fire metric results alone did not accurately predict overall cut appearance, without affecting the results for diamonds already adequately "predicted."

With this in mind, we looked at comments provided by trade observers and the Overall observation team on the visual appearance of every diamond they examined. In many cases, these comments supported the metric results (for example, that a diamond was dark overall). In other cases, the observers' comments described appearance effects

that caused the diamond to look worse than expected on the basis of brightness and fire alone. When we studied these additional appearance factors, we recognized them as various aspects of scintillation (see box B).

We used specific comments provided by the Overall observation team and by members of the diamond trade to develop methods of capturing scintillation aspects of overall (face-up) appearance that were not being addressed already by our brightness and fire metrics (again, see box B). We used several rounds of observation tests (listed together in table 4) to create and test a methodology for identifying, quantifying, and categorizing the various effects that indicate deficiencies in scintillation.

Members of our Overall observation team compared "Overall Verification Diamonds" (OVDs; again, see table 2), one at a time, to a suite of appearance comparison diamonds assembled from our Research Diamonds. (Some OVDs were looked at more than once, and some were also observed by the Brightness and Fire teams.) Observations were done in the CVE environment on gray trays (which, at this point, we had determined were most appropriate for assessing cut appearance; see Results). These observers were asked to rank the overall cut appearance of diamonds on a scale of 1 to 5, and to

BOX B: SCINTILLATION

In recent history, *scintillation* has been defined as the "flashes of white light reflected from a polished diamond, seen when either the diamond, the light source, or the observer moves" (see, e.g., *GIA Diamond Dictionary*, 1993, p. 200). This was widely recognized as the third essential appearance aspect that worked with brightness and fire to create the overall face-up appearance of a diamond.

However, we found through our interaction with members of the diamond trade and our overall observation tests that scintillation encompasses more than just this flashing of light. When asked about the face-up appearance of the diamonds they were observing, many trade members also mentioned the importance of the distribution of bright and dark areas seen in the crown of a diamond. Differences in this distribution, especially changes brought on when the diamond moves, were seen to underlie and influence the flashes of light described in the above definition of *scintillation.*

Thus, given the interdependence of flashing light and distribution, we decided to use two terms to represent these different aspects of scintillation. *Sparkle* describes the spots of light seen in a polished diamond when viewed face-up that flash as the diamond, observer, or light source moves. *Pattern* is the relative size, arrangement, and contrast of bright and dark areas that result from internal and external reflections seen in a polished diamond when viewed face-up while that diamond is still or moving. As such, patterns can be seen as positive (balanced and cohesive patterns; see figure B-1) or negative (e.g., fisheyes, dark centers, or irregular patterns; see figure B-2).

Figure B-2. These diamonds are viewed negatively by experienced members of the diamond trade, due to a variety of unattractive pattern-related traits such as a fisheye (left), dark upper-girdle facets (center), and a busy, broken overall pattern (right). Photos by A. Gilbertson and B. Green.

Many of these pattern-related aspects of scintillation are already taken into consideration by experienced individuals in the diamond trade. Often they were included in the general assessments of diamonds we recorded during observation tests, usually described with terms such as *dark spots* or *dead centers*, in addition to *fisheyes.* Our main finding was that pattern-related effects were often used to describe why a diamond did not perform as well as it otherwise should based on its brightness and fire.

Many sparkle-related aspects of scintillation are already included in our brightness and fire metrics. These consist of specular reflections from facet surfaces (now included in the brightness metric) and the dispersed light that exits the crown but has not yet fully separated, so is not seen as separate colors at a realistic observer distance (included in the fire metric). We also found that sparkle was strongly tied to our fire metric, in that those diamonds that displayed high or low fire were found to display high or low sparkle, respectively. Therefore, we concluded that we did not need to address sparkle any further. However, we developed proportion-based limits and pattern calculations to specifically predict and assess the pattern-related aspects of scintillation.

Figure B-1. These diamonds are, in general, viewed positively by experienced members of the diamond trade, due to the overall balance of their patterns and the lack of any negative pattern-related traits. Photos by A. Gilbertson and B. Green.

provide specific reasons for the rankings they gave. We used these reasons (which were in the form of descriptions about each diamond's appearance) to find ways to predict specific pattern-related scintillation aspects that caused a diamond to appear less attractive than expected from our brightness and fire metrics.

This developed into a system for addressing those diamond proportion sets that led to lower-than-expected appearance rankings (due to pattern-

related scintillation). We used proportion-range limits along with proportion-derived calculations to predict specific pattern-related effects.

As we completed each set of observations, we developed and refined our pattern-related methodology, so we could test its efficacy during the next set of observation tests. In this way, we refined proportion-range borders as appropriate, adding new predictive calculations as needed. Thus, we were able to use early test results to address the additional aspects that observers considered (either consciously or unconsciously) while assessing overall cut appearance in later tests. In addition, the tens of thousands of observations we conducted during this process have provided a real-world confirmation of our predictive system, allowing us to feel confident in predicted results, even in cases where we may not have seen a diamond with that specific set of proportions.

RESULTS

Brightness. In early observation experiments, we found that the WLR (weighted light return) metric of Hemphill et al. (1998), although an accurate predictor of a diamond's brightness when tested in an environment similar to the model, was not as effective at predicting the brightness observations by manufacturers and experienced trade observers in their own environments. Consequently, we developed a new brightness metric that included a more appropriate lighting condition, a more limited observer placement, and an additional observation factor (i.e., glare, the direct reflections off the facet surfaces).

We first confirmed that observations with hemispheres agreed with our predictions of the relative order of the diamonds based on the corresponding brightness metrics. We then used the statistical techniques described in box A to determine which of these metrics gave the best fit to observations of brightness in dealer-equivalent environments (e.g., the GTI, Judge, and CVE). Cronbach alpha values for our brightness testing were determined to be 0.74 for observers alone, and 0.79 for observers plus our brightness metric; the closeness of the two values shows that the brightness metric is at least as reliable as the average observer.

Our final brightness metric assumes a diffused, white hemisphere of light above the girdle plane of the diamond, with a dark circle located at the zenith of this hemisphere (see figure 10). The area
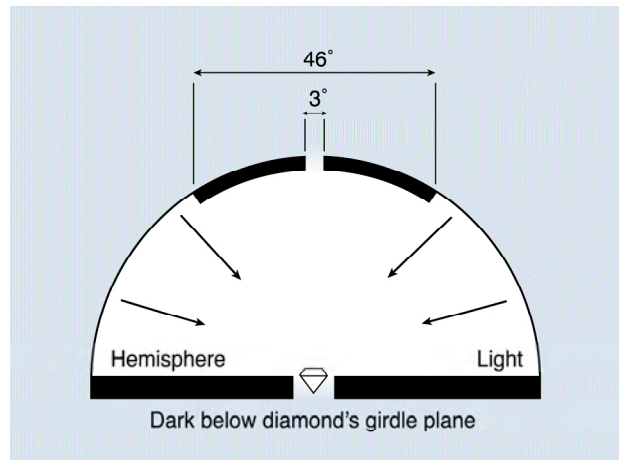

Figure 10. This diagram shows the environment and viewing conditions for our brightness metric. It assumes a diffused, white hemisphere of light above the girdle plane of the diamond, with a dark circle located at the zenith of this hemisphere that has a radius formed by a 23° angle from the centered normal of the diamond's table. The area below the girdle plane is dark, and the angular spread of observation is 3°, located directly over the center of the diamond's table.

below the girdle plane is dark. The total angular spread of observation is 3°, located directly over the center of the diamond's table. In addition, glare is included in the final metric results.

Fire. Also as described above, the DCLR (dispersed colored light return) metric of Reinitz et al. (2001) did not correlate well with the collected fire observations in standard lighting and viewing conditions. This is probably because it assumed a greater ability to discern fire than observers demonstrated when they looked at diamonds instead of projected dispersed-light patterns (see Materials and Methods). Therefore, we varied the threshold for readily observable fire to find the best fit. Again using statistical methods mentioned in box A, we found that the best match to the observation data was for a threshold of $10^{1.25}$, which gives about 18 distinct levels of light intensity for observed fire.

Cronbach alpha values for our fire observations were determined to be 0.72 for observers alone, and 0.75 for observers plus our fire metric; again, the closeness of the two values shows that the fire metric is at least as reliable as the average observer. Since the final fire metric correlated well with the fire observation data, we did not vary any of the other model assumptions.

The Effect of Other Diamond Properties and Conditions on Brightness and Fire. Our Brightness and Fire teams evaluated the brightness and fire of 688 diamonds with a range of color, clarity, polish and symmetry grades, girdle condition (bruted, polished, or faceted), and blue fluorescence[1] intensity (from none to very strong), as given in the first column of table 2. From these evaluations, we assessed the interaction of these properties or conditions with apparent brightness and fire (by comparing the predicted metric values of these diamonds). We found, as would be expected, that apparent brightness decreases as the color of the diamond becomes more saturated in the GIA D-to-Z range (including browns). Grade-determining clouds in the SI_2 and I clarity grades diminish the appearance of fire. Fair or Poor polish causes both apparent brightness and fire to diminish; and Fair or Poor symmetry negatively affects apparent brightness. Neither fluorescence nor girdle condition showed any effect on apparent brightness or fire.

Addressing Overall Cut Appearance. The next step was to compare brightness and fire metric results with observer assessments of overall appearance. For this exercise, we used the experienced observers who comprised our Overall observation team and a set of 937 diamonds borrowed from various sources (a subset of the 1,610 Overall Verification Diamonds). We also conducted observation tests with trade observers using the core reference set of Research Diamonds. Based on tests that placed diamonds into groups, these two observer populations distinguished five overall appearance levels. A number of additional results emerged:

1. Differences in body color did not influence the ability of observers to assess overall cut appearance.
2. To be ranked highest by the observers, a diamond had to have both high brightness and high fire metric values.
3. Not all diamonds with high values for either or both metrics achieved the highest rank.

For the subset of 937 Overall Verification Diamonds for which we had measurements, quality information, system predictions, and a detailed set of observations, the observer ranks for about 73% corre-

sponded to the ranks that would be anticipated based on brightness and fire alone; most of the rest were ranked one level lower than would be expected solely based on those two metrics. An additional factor—perhaps more than one—was contributing to overall face-up appearance.

Scintillation. At this point, we did not believe that developing a specific "scintillation metric" was the right approach. (Recall that most of the sparkle aspect of scintillation was already being captured in our metrics for brightness and fire; again, see box B.) Instead, we needed to find a methodology for capturing and predicting the *pattern*-related effects of scintillation. We accomplished this using a dual system of proportion-based deductions and calculations for specific negative pattern-based features such as fisheyes. (For example, we downgraded diamonds with pavilion angles that were very shallow or very deep because these proportions generally changed the face-up appearance of the diamond in ways that made it less desirable to experienced trade observers.)

Based on the results of the OVD examinations, we found that some overall cut appearance categories were limited to broad, yet well-defined, ranges of proportions. Changes in table size, crown angle, crown height, pavilion angle, star facet length, lower-girdle facet length, culet size, girdle thickness, or total depth could lead to less desirable appearances. Therefore, based on our observation testing, we determined limits for each of these proportions for each of our overall cut quality categories. We also developed calculations to predict pattern-related effects of scintillation (based on proportion combinations) that included the fisheye effect, table reflection size, and localized dark areas in the crown when the diamond is viewed face-up (see examples at the end of the Discussion section). A diamond has to score well on each of these pattern-related factors to achieve a high grade.

Design and Craftsmanship. After speaking with diamond manufacturers and retailers, we verified a number of additional aspects of a diamond's physical attributes as important: A diamond should not weigh more than its appearance warrants (i.e., diamonds that contain "hidden" weight in their girdles or look significantly smaller when viewed face-up than their carat weights would indicate; figure 11); its proportions should not increase the risk of damage caused by its incorporation into jewelry and

---

[1] Less than 2% of all diamonds that fluoresce do so in colors other than blue.

Figure 11. These two diamonds are fairly similar in diameter and face-up appearance. However, the diamond on the right contains extra, or "hidden," weight located in the thickness of the girdle. The diamond on the left weighs 0.61 ct, while the diamond on the right weighs 0.71 ct. Photos by A. Gilbertson and Maha Tannous.

everyday wear (i.e., it should not have an extremely thin girdle); and it should demonstrate the care taken in its crafting, as shown by details of its finish (polish and symmetry). Diamonds that displayed lower qualities in these areas would receive a lower overall cut quality grade.

Putting It All Together. Each of these factors (brightness, fire, scintillation, weight ratio, durability, polish, and symmetry) individually can limit the overall cut quality grade, *since the lowest grade from any one of them determines the highest over-all cut quality grade possible*. When taken together, these factors yield a better than 92% agreement between our grading system and Overall observation team results (for comparison, observers in our Overall observation team averaged a 93% agreement). Similar to our brightness and fire metrics, these results confirm that our grading system is as reliable as an average observer. Such high agreement percentages are considered a reliable measure of correlation in the human sciences; this is especially true in those studies influenced by preference (Keren, 1982). We found that many diamonds in the remaining percentage were often "borderline" cases in which they could be observed by our team as a certain grade one day, and as the adjacent grade the next. The difficulties inherent in the assess-

ment of cut for "borderline" samples are similar to those faced in the assessment of other quality characteristics. Observation testing with members of the retail trade and consumers confirmed these findings as well.

Grading Environment. When diamonds are being assessed for overall cut appearance, a standardized environment is essential. Therefore, we developed the GIA common viewing environment, which includes the diffused lighting used by manufacturers and dealers to assess the quality of a diamond's cut, and the directed lighting used by many retailers, within an enclosed neutral gray viewing booth. Our CVE contains a mix of fluorescent daylight-equivalent lamps (to best display brightness) and LEDs (to best display fire). Observation tests and trade interaction confirmed that this environment is useful for consistently discerning differences in overall cut appearance.

After testing with laboratory observers who wore either white or black tops, we determined that observers provided more consistent results for assessing brightness (that is, independent observers were more likely to reach the same results) when they wore a white shirt. Shirt color did not influence fire and overall appearance observations.

During our observation testing with trade

members and our Overall observation team, we also found that in many cases background color could affect the ease with which observers distinguished the face-up appearance of one diamond from another. We determined that white trays (which mimic the white folded cards and white display pads often used in the trade) can sometimes cause a diamond to look brighter by hiding or masking areas of light leakage (areas where light is not returned from the diamond because it exits out of the pavilion rather than back to the observer). Alternately, black trays were shown to demonstrate possible areas of light leakage, but in many cases they overemphasized them so the diamond looked too dark. We found that a neutral gray tray (similar in color to the walls of our CVE) was the most appropriate choice for assessing a round brilliant's overall face-up appearance.

DISCUSSION

Through our research (computer modeling, observation testing, and trade interaction) we found that to be attractive, a diamond should be *bright*, *fiery*, *sparkling*, and have a pleasing *overall appearance*, especially as can be seen in the pattern of bright and dark areas when viewed face-up.

Aspects of overall face-up appearance seen as positive features include facet reflections of even, balanced size, with sufficient contrast between bright and dark areas of various sizes so that some minimal level of crispness (or sharpness) of the faceting is displayed in the face-up pattern. There are also appearance aspects that are considered negative traits: For example, a diamond should not display a fisheye or large dark areas in its pattern.

In the same manner, we recognized that more than just face-up attractiveness should be incorporated into evaluating overall diamond cut quality. Quality in design and craftsmanship (as evidenced by a diamond's weight ratio, durability, polish, and symmetry), even if face-up appearance is barely affected, also should be evident in a diamond's fashioning.

Overall Cut Grade: Components of the GIA Diamond Cut Grading System. Seven components (brightness, fire, scintillation, weight ratio, durability, polish, and symmetry) are considered together to arrive at an overall cut grade in our system. These seven components are considered

equally in the system, as the lowest result from any one component determines the final overall cut grade (e.g., a diamond that scores in the highest category for all components except durability, in which it scores in the second highest category, would only receive the second highest overall cut grade; see the pull-out chart for examples). Using this approach ensures that each diamond's overall cut grade reflects all critical factors, including aspects of face-up appearance, design, and craftsmanship.

In practice, the GIA diamond cut grading system [patent pending] operates by first establishing the diamond's light-performance potential through metric calculations of brightness and fire (i.e., the best grade possible considering the combination of average proportions and how well they work together to return white and colored light to the observer). That potential is then limited by pattern-, design-, and craftsmanship-related determinations based on calculations, proportion-range limits, and polish and symmetry, so that the grade takes into account any detrimental effects. These determinations work together with the brightness and fire metrics as a system of checks and balances; the cut grade of a diamond cannot be predicted by either the metric calculations or any of the other components alone.

We found through our observation tests that most experienced individuals can consistently discern five levels of overall cut appearance and quality. Thus, the GIA diamond cut grading system is composed of five overall grade categories.

Design and Craftsmanship. "Over-weight" diamonds are those with proportions that cause the diamond, when viewed face-up, to appear much smaller in diameter than its carat weight would indicate. Consider, for example, a 1 ct diamond that has proportions such that its diameter is roughly 6.5–6.6 mm; this diamond will have the face-up appearance of a relatively typical 1 ct round brilliant. A comparable 1 ct diamond with a diameter of, for example, only 5.7 mm should sell for less. A person who contemplates buying one of these diamonds might believe that the latter was a "bargain" (since both diamonds weigh 1 ct, but the latter costs less). However, that person would end up with a diamond that appeared smaller when viewed face-up because much of the weight would be "hidden" in the overall depth of the diamond. Such diamonds are described in the trade as

GLOSSARY

Brightness the appearance, or extent, of internal and external reflections of "white" light seen in a polished diamond when viewed face-up.

Brightness team the team of individuals used in observation testing to validate the brightness metric.

Common viewing environment (CVE) for this study, a neutral gray box with a combination of daylight-equivalent fluorescent lamps and overhead white LEDs (light-emitting diodes), used to view the overall cut appearance and quality of diamonds.

Computer model a computer program that re-creates the properties and characteristics of an object, along with the key factors in its interaction with specified aspects of its environment.

Craftsmanship a description of the care that went into the crafting of a polished diamond, as seen in the finish (polish and symmetry) of a diamond.

Design decisions made during the fashioning process that determine a diamond's physical shape, as seen in a diamond's proportions, weight ratio, and durability.

Durability the characteristic of a polished diamond that accounts for the risk of damage inherent in its proportions (i.e., the risk of chipping in a diamond with an extremely thin girdle).

Face-up appearance the sum appearance (brightness, fire, and scintillation) of a polished diamond when it is viewed in the table-up position. This appearance includes what is seen when the diamond is "rocked" or "tilted."

Fire the appearance, or extent, of light dispersed into spectral colors seen in a polished diamond when viewed face-up.

Fire team the team of individuals used during observation testing to validate the fire metric.

Metric a calculated numerical result obtained through computer modeling; for the GIA diamond cut research project, metrics were calculated for brightness and fire for both hypothetical and actual diamonds.

Overall cut appearance and quality a description of a polished diamond that includes the face-up appearance, design, and craftsmanship of that diamond.

Overall observation team the team of six individuals (who combined had over 100 years of diamond experience) used during observation testing to discover additional aspects related to face-up appearance, as well as to validate the predictions of the GIA cut grading system.

Overall Verification Diamonds diamonds used in this study to validate the predictive accuracy of the GIA diamond cut grading system. Each of these diamonds was observed for its overall cut appearance and quality by the members of the Overall observation team.

Research (reference) Diamonds (RD) the core set of 45 polished diamonds (which represented a wide range of proportion combinations) that were purchased and/or manufactured to be used as a consistently available sample group during the course of the diamond cut study.

Scintillation the appearance, or extent, of spots of light seen in a polished diamond when it is viewed face-up that flash as the diamond, observer, or light source moves (**sparkle**); and the relative size, arrangement, and contrast of bright and dark areas that result from internal and external reflections seen in a polished diamond when viewed face-up while that diamond is still or moving (**pattern**).

Weight ratio a description of a diamond's overall weight in relation to its diameter.

"thick" or "heavy." A similar difference in value would apply if two diamonds had roughly the same diameter but one weighed significantly more (again, see figure 11).

Often, an assessment of a diamond as over-weight can be deduced from the combination of its crown height, pavilion depth, total depth, and/or girdle thickness. We developed a calculation that

combines the effects of all these factors into one value (the *weight ratio* of a diamond). This ratio compares the weight and diameter of a round brilliant to a reference diamond of 1 ct with a 6.55 mm diameter, which would have a fairly standard set of proportions (see the pull-out chart for examples).

Durability is another trait of overall diamond cut quality that was emphasized throughout our interaction with members of the diamond trade. Diamonds fashioned in such a way that they are at greater risk of damage (i.e., those with extremely thin girdles) receive a lower grade in the GIA diamond cut grading system.

Finish (that is, the *polish* and *physical symmetry* of a diamond) also affects cut appearance and quality. Much like weight ratio and durability, polish and symmetry were highlighted by trade observers as important indicators of the care and craftsmanship that went into the fashioning of a diamond, and therefore had to be considered in any comprehensive grading system. These are assessed based on standard GIA Gem Laboratory grading methodology, and lower qualities of either can bring the grade of the diamond down (again, see the pull-out chart for examples). Note, however, that unlike other traits, there is not a direct correlation between a finish grade and an overall cut grade (e.g., a diamond with a "Very Good" finish may receive a top cut grade).

Other Diamond Quality Factors. Our observer tests enabled us to examine the effects of other diamond quality factors (e.g., color, clarity, fluorescence, and girdle condition) on overall cut appearance. Although in cases of very low color or clarity, we found some impact on overall appearance, in general observers were able to separate these factors out of their assessments. Therefore, we determined that the GIA diamond cut grading system does not need to take these factors into consideration in its final overall cut quality grades; it applies to all standard round brilliant cut diamonds, with all clarities, and across the D-to-Z color range as graded by the GIA Gem Laboratory.

Optical Symmetry. One aspect of pattern-related scintillation that has gained more attention in recent years is often called "optical symmetry" (see, e.g., Cowing, 2002; Holloway, 2004). Many people in the trade use this term for "branded" diamonds that show near-perfect eight-fold symmetry by displaying eight "arrows" in the face-up position (and

typically eight "hearts" table-down) when observed with specially designed viewers. To investigate the possible benefits of optical symmetry, we included several such diamonds in our observation testing. We found that although many (but not all) diamonds with distinct optical symmetry were rated highly by our observers, other diamonds (with very different proportions and, in many cases, no discernible optical symmetry) were ranked just as high. Therefore, both types of diamonds can receive high grades in our system.

Examples from the GIA Diamond Cut Grading System. On the enclosed pull-out chart, we have provided three examples (from our core set of Research Diamonds) for each of five categories in the GIA diamond cut grading system, including their proportions and other grade-determining factors. For the purposes of this article only, categories are listed as "first" through "fifth," with "first" representing the best; this nomenclature *does not in any way reflect future nomenclature* of the GIA diamond cut grading system.

In the first category, we see a relatively wide range of proportions. For these three examples, brightness and fire metric values indicated that they could belong in the top category. Also, none of these diamonds were subject to downgrading based on proportion values or calculated pattern-related scintillation problems. Finally, these diamonds all had polish and symmetry grades that were Very Good. These factors combined to create diamonds that would receive the highest grade.

Our research found that the top grade included even broader proportion ranges than are shown in the chart. For example, we have established that diamonds in this category could have crown angles ranging from roughly 32.0° to 36.0° and pavilion angles ranging from 40.6° to 41.8°. *It is important to note, however, that not all proportions within these ranges guarantee a diamond that would rate a top grade.* As we have previously stated, it is not any one proportion, but rather the interrelationship of all proportions, that determines whether a particular diamond will perform well enough to receive a top grade.

By further studying the data in the pull-out chart, one can see various reasons why particular diamonds would receive a lower cut grade in the GIA system. For example, **RD07** falls in the second category based on its fire and scintillation, its total depth of 64.1% and crown height of 17.5%,

and its weight ratio. This is a good example of a diamond where the proportion values cause lower light performance and a less-than-optimal face-up appearance.

We have found through our research that proportion ranges for the second category are much wider than those considered by other cut grading systems. Likewise, our trade observers were often surprised when they learned the proportions of diamonds they had ranked in this near-top-level category, although they supported our findings. Here, crown angles can range from roughly 27.0° to 38.0°, and pavilion angles can range from roughly 39.8° to 42.4°. Tables also can range from roughly 51% to 65% for this grade category. Once again, it is important to note that not all individual proportions within these ranges guarantee a diamond that would fall into the second category.

RD06 on the pull-out chart falls into the third category in the GIA diamond cut grading system for at least two reasons: It has a crown height of 9.5% and a crown angle of 23.0°. These factors combine in this diamond to produce a shallow crown, which negatively affects overall appearance. In addition, this diamond is downgraded for a lack of contrast in its scintillation and a localized darkness in the crown area (especially in the table), which results from the interaction of the shallow crown with this particular pavilion angle. Therefore, this is a good example of a diamond that scores high on our brightness and fire metrics, yet is down-graded based on individual proportion values that cause undesirable pattern-related scintillation effects.

It is interesting to note that many in the trade would not consider cutting a diamond with a crown angle this shallow. Yet our research has shown that diamonds with these proportions score in the middle category overall, and might be a very useful alternative for diamond cutters in some circumstances. Typical ranges for this grade category are roughly 23.0° to 39.0° for crown angles, 38.8° to 43.0° for pavilion angles, and 48% to 68% for table sizes.

An example of a diamond that would fall in the fourth category is **RD37**, which has low brightness and fire metric scores, a table size of 70%, and downgrading for a fisheye that becomes more prominent when the diamond is tilted slightly. Here is another example of a "shallow" diamond, but this one is less attractive because of the fisheye produced by the combination of a large table

and a shallow crown height (9.5%) with a pavilion angle of 40.2%.

RD39 is an interesting example of a diamond that would receive the lowest grade. Its brightness and fire metric results—and polish and symmetry grades (each was assessed as Good)—would place it in the second category, and a calculated prediction for localized darkness would place it in the third category. However, it falls into the fifth category in the GIA diamond cut grading system based on its total depth (74.0%) and its weight ratio (which was calculated to be 1.52—that is, 52% more "hidden" weight than a diamond with this diameter should have). Although these proportions may seem extreme, this diamond was purchased in the marketplace. This diamond might be considered better in a less comprehensive system that only accounted for brightness, fire, and finish; however, we believe that this diamond's overall cut quality (which includes its excess weight) is properly accounted for and appropriately graded in our system.

Please examine the pull-out chart for additional examples of diamonds in the various grade categories.

Personal Preferences and Their Effect on Diamond Grading. Although a diamond's performance is quantifiable, "beauty" remains subjective. (That is, metrics are not subjective but individual taste is.) No cut system can guarantee that everyone will prefer one set of proportions over another; instead, as you move down the cut grade scale, the diamonds in the grade categories change from those that almost everyone likes, to those that only some people might like, to those that no one prefers. A grading system that fails to acknowledge differences in taste is neither practical nor honest in terms of human individuality and preference.

We have found through our research and extensive interaction with the trade that even for diamonds within the same grade, some individuals will prefer one face-up appearance over another (figure 12). Individual preferences have even greater impact in the lower categories. The inherent role of personal preference in diamond assessment will often lead to a situation in which some observers will not agree with the majority; thus, no cut grading system should expect to assess perceived diamond cut quality perfectly for everyone. Instead, what we have tried to accomplish with our grading system is to "capture" within each

Figure 12. Both of these diamonds would score in the top category of the GIA diamond cut grading system, yet we found that different observers prefer one or the other based on face-up appearance. Since personal preference plays such an important role in perceived cut quality, it is essential that the purchaser examine the actual diamond (and not rely solely on its proportions or its cut grade). Photos by A. Gilbertson and B. Green.

grade category those diamonds that, in general, most individuals would consider better in appearance and cut quality than diamonds in the next lower category.

CONCLUSIONS

During the 15 years of our research into the relationship of proportions and overall cut quality, we have accomplished a great deal: developed a computer model and created metrics to predict brightness and fire; developed a methodology to validate those metrics and assess other aspects of cut appearance and quality using observation testing; created a common "standardized" viewing environment; and, finally, combined all of these elements to create a comprehensive system for grading the cut appearance and quality of round brilliant diamonds.

In the course of this research (including research described in our earlier articles by Hemphill et al., 1998, and Reinitz et al., 2001), we arrived at many conclusions. Among them:

- Proportions need to be considered in an interrelated manner. The combination of proportions is more important than any individual proportion value.
- Attractive diamonds can be manufactured in a wider range of proportions than would be suggested by historical practice or traditional trade perception.
- For consistent comparisons between diamonds, cut grading requires a standardized viewing environment that is representative of common environments used by the trade.

- Personal preference still matters. Diamonds with different appearances can be found within each cut grade, so individuals need to look at the diamond itself, not just its grade, to choose the one they like the best.

Our research and trade interaction also necessitated the further refinement of the terms we use to describe the appearance of a polished diamond when it is viewed face-up. Our definitions of these terms are:

- **Brightness**—the appearance, or extent, of internal and external reflections of "white" light
- **Fire**—the appearance, or extent, of light dispersed into spectral colors
- **Scintillation**—the appearance, or extent, of spots of light that flash as the diamond, observer, or light source moves (sparkle); and the relative size, arrangement, and contrast of bright and dark areas that result from internal and external reflections seen while that diamond is still or moving (pattern)

The GIA Diamond Cut Grading System. We believe that to best serve the public and the trade, an effective diamond cut grading system should ensure that well-made diamonds receive the recognition they deserve for their design, craftsmanship, and execution. Conversely, it should ensure that diamonds that are not pleasing in appearance, or that warrant a discount for weight or durability reasons, are rated appropriately. In addition, the individual categories in this system should allow for personal and global differences in taste.

Extensive observation testing and trade interaction made it very clear that for a diamond cut grading system to be useful and comprehensive, it had to consider more than just brightness, fire, and scintillation (i.e., more than only face-up appearance). For these reasons, we decided that our system should also include elements of design and craftsmanship (which can be seen in a diamond's physical shape and finish respectively). Therefore, the GIA diamond cut grading system, which applies to standard round brilliant diamonds on the GIA D-to-Z color scale, encompasses the following seven components: brightness, fire, scintillation, weight ratio, durability, polish, and symmetry.

Brightness and fire, including aspects of sparkle-related scintillation, are assessed using computer-modeled calculations that have been refined and validated by human observations. Pattern-related aspects of scintillation are assessed using a combination of determinations based on proportion ranges and calculations developed to predict specific detrimental patterns (both derived from observation testing). Weight ratio (which is used to determine whether a diamond is so deep that its face-up diameter is smaller than its carat weight would usually indicate) and durability (in the form of extremely thin girdles that put the diamond at a greater risk of damage) are calculated from the proportions of each diamond. Polish and symmetry are assessed using standard GIA Gem Laboratory methodology. The grading scale for each of these components was validated through human observations; these individual grades are considered equally when determining an overall cut grade.

In summary, our research has led us to conclude that there are many different proportion sets that provide top-grade diamonds, and even wider ranges of proportions that are capable of providing pleasing upper-middle to middle-grade diamonds. Although it is important to consider many components when assessing the overall cut appearance and quality of a round brilliant diamond, an individual's personal preference cannot be ignored. The GIA cut grading system provides a useful assessment of a diamond's overall cut quality, but only individuals can say which particular appearance they prefer. With this system of cut grading, the diamond industry and consumers can now use cut along with color, clarity, and carat weight to help them make balanced and informed decisions when assessing and purchasing round brilliant diamonds.

GIA Diamond Cut Grading Reference System. During our research and trade interaction, it became clear that for our grading system to be useful to all levels of the diamond trade (including manufacturers, dealers, retailers, and appraisers), as well as consumers, we needed to provide a method for individuals to predict the cut grade of a polished diamond (even if that diamond was only in the "planning" stage of fashioning) from that diamond's proportion parameters. To this end, we began the process of developing reference software.

This software [patent pending] will provide a predicted overall cut grade from proportion values input by the user, with different versions allowing variation of some or all relevant proportions. Final results will be in the form of an estimated overall cut grade by itself (in the basic version of the application) or the estimated overall cut grade presented within a larger grid that would allow a user to explore possible alternative proportion sets that might provide an improved final result. GIA plans to release several versions of this software (as well as a printed version) concurrently with the release of the new cut system.

Next Steps. We plan to incorporate the findings from this research, as well as the foundations and framework of our cut grading system, into future GIA Education courses, GIA Alumni and Research presentations, and Institute informational brochures. In addition, we plan to incorporate some of this information (e.g., expanded proportion data and an overall cut grade) into future GIA Diamond Grading Reports and the GIA Diamond Dossier®. To this end, we are also planning to publish future articles on other aspects of the cut grading system, reference software, and changes to GIA Gem Laboratory grading reports.

Although a primary goal of this research project has been to develop a cut grading system for round brilliant diamonds, there are other benefits that we have gained from this work. Most importantly, this research project has allowed us to create and validate a method of modeling the behavior of light in a polished diamond along with a methodology to verify the findings from that modeling using observation testing by experts in the field. We can now apply these technologies and methods to other shapes, cutting styles, and colors of diamond to determine whether similar grading systems can be developed. We will continue to identify new goals and questions related to diamond cut as we move forward in our research, beyond the standard round brilliant.

REFERENCES

Computer used to set standard of gem beauty (1978) *Retail Jeweller*, January 19, p. 40.

Cowing M., Yantzer P., Tivol T. (2002) Hypothesis or practicality: The quest for the ideal cut. *New York Diamonds*, Vol. 71, July, pp. 40, 42, 44.

Cronbach, L.J. (1951) Coefficient alpha and the internal structure of the tests. *Psychometrika*, Vol. 16, pp. 297–334.

Dodson J.S.(1978) A statistical assessment of brilliance and fire for polished gem diamond on the basis of geometrical optics. *Optica Acta*, Vol. 25, No. 8, pp. 681–692.

Dodson J.S. (1979) The statistical brilliance, sparkliness, and fire of the round brilliant-cut diamond. *Diamond Research 1979*, pp. 13–17.

Fey E. (1975) Unpublished research completed for GIA.

GIA Diamond Dictionary, 3rd ed. (1993) Gemological Institute of America, Santa Monica, CA, 275 pp.

Harding B. (1986) GemRay [unpublished computer program].

Hardy A., Shtrikman S., Stern N. (1981) A ray tracing study of gem quality. *Optica Acta*, Vol. 28, No. 6, pp. 801–809.

Hemphill T.S., Reinitz I.M., Johnson M.L., Shigley J.E. (1998) Modeling the appearance of the round brilliant cut diamond: An analysis of brilliance. *Gems & Gemology*, Vol. 34, No. 3, pp. 158–183.

Holloway G. (2004) The Ideal-Scope. *Precious Metals*, http://www.preciousmetals.com.au/ideal-scope.asp [accessed June 22, 2004].

Inoue K. (1999) Quantification and visualization of diamond brilliancy. *Journal of the Gemmological Society of Japan*, Vol. 20, No. 1–4, pp. 153–167.

Keren G., Ed. (1982) *Statistical and Methodological Issues in Psychology and Social Sciences Research*. L. Erlbaum Associates, Hillsdale, NJ, 390 pp.

Kiess H.O. (1996) *Statistical Concepts for the Behavioral Sciences*. Allyn and Bacon, Boston, 604 pp.

King J.M., Moses T.M., Shigley J.E., Liu Y. (1994) Color grading of colored diamonds in the GIA Gem Trade Laboratory. *Gems & Gemology*, Vol. 30, No. 4, pp. 220–242.

Lane D.M. (2003) Pearson's correlation (1 of 3). *Hyperstat Online*, http://davidmlane.com/hyperstat/A34739.html [accessed Aug. 23, 2004].

Lawless H., Chapman K., Lubran M., Yang H. (2003) FS410: Sensory evaluation of food. Cornell University, Fall, http://zingerone.foodsci.cornell.edu/fs410 [accessed Sept. 11, 2003].

Lenzen G. (1983) *Diamonds and Diamond Grading*. Butterworths, London, p. 164.

Long R., Steele N. (1988) Ray tracing experiment with round brilliant. *Seattle Faceter Design Notes*, January.

Long R., Steele N. (1999) *United States Faceters Guild Newsletter*, Vol. 9, No. 4.

Manson D.V. (1991) Proportion considerations in round brilliant diamonds. In A. S. Keller, Ed., *Proceedings of the International Gemological Symposium 1991*, Gemological Institute of America, Santa Monica, CA, p. 60.

Moses T.M., Reinitz I.M., Johnson M.L., King J.M., Shigley J.E. (1997) A contribution to understanding the effect of blue fluorescence on the appearance of diamonds. *Gems & Gemology*, Vol. 33, No. 4, pp. 244–259.

Nunnally J.C. (1994) *Psychometric Theory*, 3rd ed. McGraw-Hill, New York, 752 pp.

Ohr L.M. (2001). Formulating with sense. *Prepared Foods*, February; http://www.preparedfoods.com/CDA/ArticleInformation/features/BNP__Features__Item/0,1231,114431,00.html [accessed Aug. 23, 2004]

Reinitz I.M., Johnson M.L., Hemphill T.S., Gilbertson A.M., Geurts R.H., Green B.D., Shigley J.E. (2001) Modeling the appearance of the round brilliant cut diamond: An analysis of fire, and more about brilliance. *Gems & Gemology*, Vol. 37, No. 3, pp. 174-197.

Shannon P., Wilson S. (1999) The great cut debate rages on. *Rapaport Diamond Report*, Vol. 22, No. 5 (February 5), pp. 89–90, 95.

Shigetomi G.T. (1997) Diamond industry breakthrough. *Bangkok Gems & Jewellery*, Vol. 10, No. 8, pp. 97, 98, 100.

Shipley R.M. (1948, date approximate) Assignment 2-30: The critical angle and comparative brilliancy. *Diamonds Course*, Gemological Institute of America, Los Angeles, p. 1.

Sivovolenko et al. (1999) http://www.gemology.ru/cut/english/document4.htm [accessed Dec. 15, 2003].

Strickland R. (1993) GEMCAD [computer program]. Austin, Texas.

Tognoni C. (1990) An automatic procedure for computing the optimum cut proportions of gems. *La Gemmologia*, Vol. 25, No. 3–4, pp. 23–32.

van Zanten P.G. (1987) Finding angles for optimal brilliance by calculation. *Seattle Faceter Design Notes*, November.

Yu C.H. (1998) Using SAS for item analysis and test construction, http://seamonkey.ed.asu.edu/~alex/teaching/assessment/alpha.html [accessed Aug. 23, 2004].

Yu C.H. (2001) An introduction to computing and interpreting Cronbach Coefficient Alpha in SAS. In *Proceedings of the 26th SAS Users Group International*, April 22–25, 2001, Long Beach, California, Paper 246-26, http://www2.sas.com/proceedings/sugi26/p246-26.pdf [accessed Aug. 23, 2004].

AMETHYST FROM FOUR PEAKS, ARIZONA

Jack Lowell and John I. Koivula

For more than a century, the Four Peaks mine in Maricopa County, Arizona, has produced gem-quality amethyst from crystal-lined or crystal-filled cavities and fractures in a brecciated quartzite host rock. Crystals from the deposit exhibit a range of purple colors, uneven color zoning, and variable transparency, which present challenges for obtaining a steady supply of material suitable for faceting. Faceted material may display fluid inclusions and tiny reddish brown hematite flakes, growth zoning, and Brazil-law twinning, all of which provide visual clues to separating the Four Peaks material from synthetic amethyst. Recovery of amethyst at this deposit continues at this time on a limited basis.

The most important commercial source of gem-quality amethyst in the United States is the Four Peaks mine in Maricopa County, Arizona (figure 1). Discovered by accident in the early 1900s by a gold prospector, this deposit has been worked intermittently on a small scale ever since. Good-quality amethyst from a U.S. occurrence has special value in the marketplace, but the challenge at this deposit has been to produce sufficient quantities of commercial-grade material on a continuing basis to satisfy market demand.

The mine's restricted accessibility and remote location in the rugged Mazatzal Mountains of central Arizona, combined with the low market value of amethyst from all sources, has limited production in the past. In the late 1990s, the mine was reopened with the prospect of providing a regular supply of calibrated material in a range of sizes and shapes (Lurie, 1998, 1999; Johnson and Koivula, 1998). Currently, it is owned and operated by Four Peaks Mining Co. LLC of Ocean Grove, New Jersey. The deposit is again producing good-quality amethyst, with some of the cut stones exceeding 20 ct.

This article provides a brief description of the geologic occurrence of amethyst at the deposit and summarizes the gemological properties of this material. Although previous descriptions of the deposit and local geology can be found in Sinkankas (1957, 1976, pp. 373–374), Lowell and Rybicki (1976), Estrada (1987), Chronic (1989, pp. 174–175), and Lieber (1994, p. 122), this article provides the first gemological characterization of Four Peaks amethyst.

LOCATION AND ACCESS

The Four Peaks mine is named for the mountain area where it is located. The Four Peaks are four prominent, steep-sided mountains aligned north-south near the southern end of the 80-km-long Mazatzal mountain range (figure 2). This area is approximately 75 km (46 miles) east-northeast of Phoenix (and is visible from the city) within the Four Peaks Wilderness area of the Tonto National Forest (figure 3). The amethyst deposit is located on a 20-acre patented mining claim that lies below the second peak from the south (again, see figure 2) at an elevation of 1,980

Figure 1. These two cut stones (19.25 and 17.02 ct) are excellent examples of the fine-quality amethyst obtained from the Four Peaks mine in Maricopa County, Arizona. Courtesy of Jack Lowell; photo © Jeff Scovil.

m (6,500 ft) above sea level. The area has sparse vegetation and an arid, high-desert climate.

The workings consist of an elongate open cut and a tunnel that penetrates about 10 m into the mountainside (figures 4 and 5). Because of the very rugged terrain and location in a wilderness area, access is limited to foot travel or helicopter. Except during the winter months, when the peaks are sometimes covered with snow, the area can be approached by vehicle on U.S. Forest Service roads from State Route 188 or Highway 87. A narrow trail then climbs approximately 760 m over a distance of 7.2 km to the mine. Entrance to the tunnel is closed when the mine is not in operation, and at all times prior permission from the mine owners is required to enter the property.

GEOLOGY

The Four Peaks are eroded remnants (what geologists call "roof pendants") of Precambrian-age metasedimentary rocks that were intruded from below by a granitic batholith. The amethyst mineralization occurs within one stratigraphic unit of

Figure 2. This aerial photograph, taken in 1994 toward the northeast, shows the Four Peaks mountains at the southern end of Mazatzal Range. The tallest, on the far left, is known as Browns Peak. The trail and mine are visible in the right foreground. Photo by Todd Photographic Services; courtesy of Commercial Mineral Co.

Figure 3. The amethyst deposit is located within the Four Peaks Wilderness area, approximately 75 km east-northeast of Phoenix.

these rocks: the Mazatzal Formation, a light-colored quartzite consisting of a tough, closely packed aggregate of cemented, angular quartz fragments. This quartzite and other sedimentary units were uplifted during the intrusion of the batholith in the middle Proterozoic; the uplifting was accompanied by faulting and brecciation of zones in the quartzite.

Figure 4. An elongate open cut (in the center and upper right) can be seen from the trail approaching the Four Peaks mine. Rugged outcrops are formed by the Mazatzal quartzite. Photo by J. E. Shigley.

Erosion since Precambrian times has exposed portions of both the granite batholith and the overlying Mazatzal Formation.

Quartz deposition (colorless and smoky quartz, as well as amethyst) is thought to have occurred in several stages along fractures and cavities in the brecciated quartzite. These crystal-lined spaces are irregular in form and can vary from several centimeters to a few meters in maximum dimension. Smaller openings are completely filled with interlocking amethyst crystals (figure 6), whereas larger cavities often contain either crystal druses attached to cavity walls, or loose crystals suspended in a vug-filling alteration material. The amethyst appears to have formed along fractures by crystallization of silica-containing hydrothermal solutions thought to have been derived from the cooling granite batholith. Fractured zones within the quartzite exhibit evi-

Figure 5. A short tunnel penetrates about 10 m from this entrance. All the Four Peaks amethyst produced in the past seven years has come from the underground workings. Courtesy of Commercial Mineral Co.
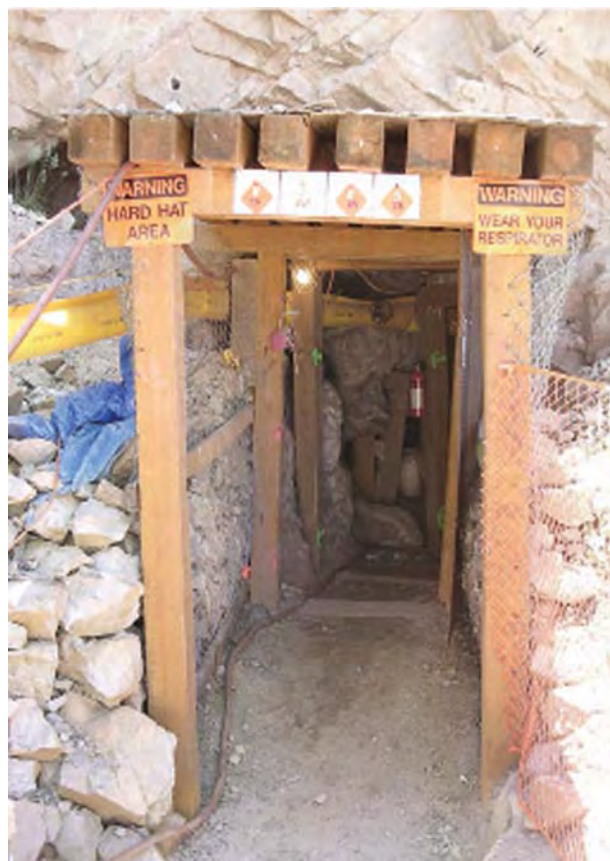
dence of hydrothermal alteration from these or other solutions. This evidence includes not only the quartz mineralization, but also the occurrence of fine-grained apatite, hematite, and unidentified clay minerals within open spaces (Sinkankas, 1957).

MINING

Recovery of amethyst for both mineral specimens and gemstones has taken place on a limited scale and intermittent basis. Initial work was carried out from surface outcrops of the amethyst-mineralized zones. Later, mining by open-pit methods employed hand tools and (unsuccessfully) a bulldozer. More recently, a tunnel was driven by hand to access productive areas of the deposit. Several measures have recently been implemented so that the operation is legally compliant with mine safety regulations. A crew of three miners is working the deposit within the horizontal tunnel. Explosives are rarely used, and only to break up boulders when needed. Otherwise, the miners use a hand-held pneumatic chisel for digging. Challenging conditions are caused by the remoteness of the location as well as hot summer temperatures and the lack of water and power at the mine. Gem material is taken out on foot or by helicopter.

Since 1998, Commercial Mineral Co. of Scottsdale, Arizona, has had an exclusive arrangement with the mine owner to acquire the mined

Figure 6. Amethyst mineralization occurs along fractures and cavities in the brecciated quartzite, as shown in this May 2004 image. Courtesy of Commercial Mineral Co.

material. However, a certain amount of illegal mining has occurred over the years, with the material periodically sold to local gem cutters.

DESCRIPTION OF THE AMETHYST

The amethyst crystals from this locality display a morphology that is typical of gem amethyst worldwide. Rhombohedral faces are predominant, while the prism faces are either poorly developed or absent (figure 7). This habit is common for quartz crystals

Figure 7. Amethyst crystals from the Four Peaks mine display a typical morphology for amethyst, consisting mainly of rhombohedral faces. Facetable material varies from light to dark purple, and generally only small portions of the crystals are suitable for faceting. The cut stones shown here range from 3.83 to 13.00 ct. Courtesy of Commercial Mineral Co.

that grew simultaneously on the walls of open cavities. The best cutting material shows dissolution basal pinacoid (c) faces, which are rare in natural amethyst. Euhedral crystals of good form and with lustrous faces are seen rarely at this deposit; when found, they range from a few centimeters to about 20 cm in maximum dimension. More typically, crystals (or crystal fragments) are etched and corroded due to attack from late-stage hydrothermal solutions. These solutions appear to have preferentially attacked the joints between adjacent crystals, thereby loosening the crystals and perhaps causing them to break away from a small point of attachment at the base. Crystal faces are normally frosted or coated by apatite or hematite. Some display internal areas that have a hazy or translucent fog-like appearance.

Four Peaks amethyst crystals show great variability in the distribution and quality of color, which can range from light to dark purple and includes some purplish red material. Most crystals display an uneven color distribution (figure 8), with darker purple areas separated by sharp boundaries from areas that are lighter or near-colorless. Color banding is oriented parallel to the rhombohedral crystal faces, with most crystals showing the strongest color zones under the larger rhombohedral faces.

Figure 8. Distinctive color zoning is evident in this amethyst crystal fragment (5 cm in diameter). Virtually all the material from the Four Peaks mine shows color zoning in certain orientations. Photo by J. Lowell.

Figure 9. This 68.39 ct amethyst from Four Peaks is the largest faceted stone from the deposit known to the authors. Photo by J. Lowell.

MANUFACTURING AMETHYST FOR JEWELRY PURPOSES

Four Peaks amethyst crystals also vary in size and quality. The rough is cobbed or trim sawn to produce relatively clean, darker pieces suitable for faceting. Because of the color zoning, even large crystals often contain only small portions that are of suitable color and transparency for faceting. The cuttable areas are usually near the pyramidal crystal terminations. These areas can sometimes be best examined after acid cleaning and application of mineral oil. More commonly, however, because of the corroded or encrusted nature of the crystal faces, the gem material is judged after the crystal has been sawn or broken into pieces. Only a small percentage of the total production exhibits intense, even coloration and good clarity. Polished stones of good color can also be created by positioning the zones of best color in the culet. A significant amount of Four Peaks material shows red overtones and/or a deep reddish purple bodycolor when faceted; these stones are known in the gem trade as "Siberian" quality.

All of the material cut by Commercial Mineral Co. has come from the underground workings and is faceted overseas. Material not suitable for faceting is stockpiled for future carving or cabbing. According to Mike Romanella (pers. comm., 2004), vice president of Commercial Mineral Co., the amethyst is faceted in both calibrated and free sizes. The non-calibrated amethyst ranges from 4 to 15 ct;

fine-quality stones in the 15–20 ct range are quite rare. The calibrated goods range from 4 mm (0.25 ct) to 8–10 mm (~3 ct). The material is classified into three quality grades, and at press time the company had thousands of carats of the high-quality faceted stones in its inventory. The largest faceted stone known to the authors weighs 68.39 ct (figure 9). A few pieces have been carved to utilize the color zoning to good effect.

Like amethyst from other localities (e.g., Brazil), some material from Four Peaks is heated to lighten the color. According to Mr. Romanella (pers. comm., 2004), 20–30% of the amethyst he has faceted is over-dark, so this material is heated to 350–450°C. The treatment has about a 50% success rate; the remainder becomes unsalable due to fracturing. Although Sinkankas (1957) reported that heating of some Four Peaks amethyst can result in a pale green color, the present authors have been unable to verify or reproduce this behavior.

MATERIALS AND METHODS

Gemological properties were measured on five faceted amethyst samples using standard gem-testing instruments. These samples, ranging from 1.25 to 3.71 ct (figure 10), are representative of the material currently being produced from the Four Peaks mine.

Refractive indices were obtained with a Duplex II refractometer and a near-monochromatic light source. Birefringence reactions were observed with a polariscope and a calcite dichroscope. Reactions to ultraviolet radiation were checked in a darkened room with conventional four-watt long-wave (366 nm) and short-wave (254 nm) Ultra-Violet Products lamps. Observation of absorption spectra was made with a Beck prism spectroscope. The visual features of the study samples were observed with a gemological microscope. Photomicrographs were taken with a Nikon SMZ-10 photomicroscope under various lighting conditions. A polished amethyst plate oriented perpendicular to the optic axis was prepared to allow for better observation of twinning patterns.

A solid mineral inclusion was identified using a Raman Renishaw 1000 microspectrometer. Mid-infrared absorption spectra for two of the samples were recorded at room temperature with a Nicolet Magna-IR Fourier-transform infrared (FTIR) spectrometer over the range 400–6000 cm^{-1}, with a resolution of 1.0 cm^{-1}. Qualitative chemical analyses of the same two samples were obtained with a Kevex (now Thermo-Electron) Omicron X-ray fluorescence (EDXRF) system operating at accelerating voltages of 10, 25, and 35 kV, and beam currents of 1.70, 2.15, and 3.30 mA.

RESULTS AND DISCUSSION

The refractive indices of each of the seven samples studied were 1.543 (ω) and 1.551 (ε). The birefringence calculated from these values is 0.008. With the polariscope, a uniaxial "bull's-eye" optic figure was seen in all samples; slight distortions of this optic figure were seen near the edges of twinning boundaries (a feature noted before in amethyst). Purple and bluish purple dichroic colors were seen

Figure 10. These faceted samples of Four Peaks amethyst (1.25–3.71 ct) were examined for this study. The amethyst is typically faceted to minimize the appearance of color zoning in the face-up position (left). When viewed table-down (right), the color zoning of these samples becomes apparent. Photos by Maha Tannous.

Figure 11. Primary fluid inclusions, such as those shown here, were common in the Four Peaks amethyst examined. The largest inclusion measures 0.7 mm long. Photomicrograph by J. I. Koivula.
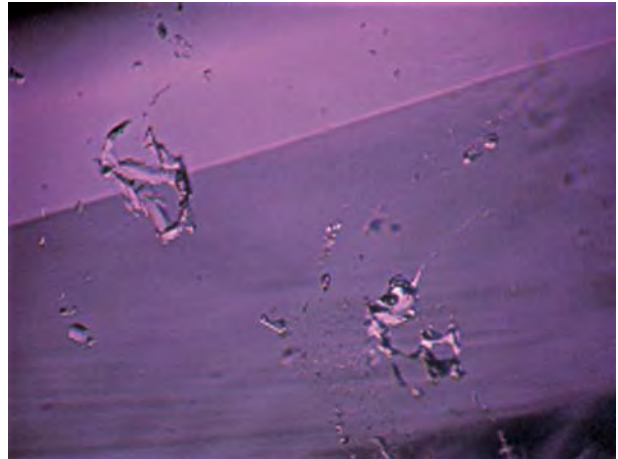

Figure 12. Many of the primary fluid inclusions in the amethyst samples examined also contained tiny anhedral solid phases, as shown in the lower right of this image. Photomicrograph by J. I. Koivula; magnified 25×.

through a calcite dichroscope. All the samples were inert to both long- and short-wave UV radiation, and they displayed no absorption spectra when examined with a Beck spectroscope.

Both primary and secondary fluid inclusions were observed in the samples studied. The former were relatively small, the largest being 0.7 mm in length (figure 11), and they showed minimal negative crystal form. While some of the primary fluid inclusions appeared to be two-phase with liquid and gas components, many others appeared to con-

tain tiny anhedral solid phases (figure 12). No birefringence was evident in these solid phases when they were examined in transmitted light between crossed polarizers. The secondary fluid inclusions exhibited typical veil-like patterns, and they were often seen in association with the larger primary fluid inclusions (figure 13).

Other than the tiny anhedral solid phases in fluid inclusions, the only mineral inclusions observed within the amethysts were small reddish

Figure 13. Veil-like patterns of secondary fluid inclusions were commonly observed in the amethyst samples studied. Photomicrograph by J. I. Koivula; magnified 20×.

Figure 14. Where dense accumulations of reddish brown hematite flakes were seen, the host amethyst material tended to be a lighter purple. Photomicrograph by J. I. Koivula; magnified 15×.
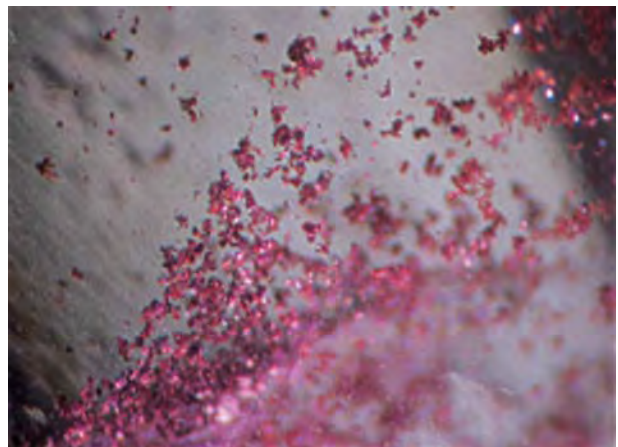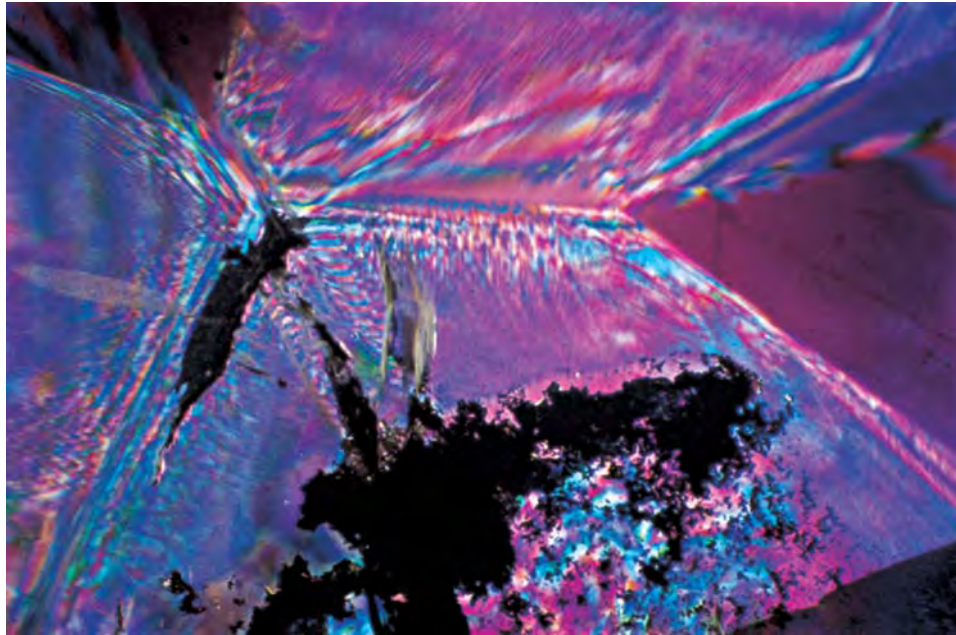
Figure 15. This photomicrograph, taken in transmitted light between crossed polarizers, shows the Brazil-law twinning pattern observed in a polished plate oriented perpendicular to the optic axis of the amethyst. The opaque areas are dense accumulations of hematite inclusions. Photomicrograph by J. I. Koivula; magnified 2×.

brown grains of hematite (identified by Raman analysis). These either occurred in dense accumulations (figure 14) or were sparsely scattered. To the best of our knowledge, such dense accumulations of hematite inclusions have not been reported in amethyst from other localities. Where hematite was present in considerable amounts, the color of the amethyst tended to be lighter purple, whereas darker-color material had fewer of these inclusions.

In transmitted light between crossed polarizers, Brazil-law twinning was obvious in all the samples studied (see, e.g., figure 15). In many of the Brazil-law-twinned crystals and faceted stones, there were sufficiently large untwinned areas to suggest that it would be possible to cut Four Peaks amethysts that would not show this form of optically active twinning.

The most unusual visual feature was a white, wedge-shaped zone that was seen oriented parallel to the rhombohedral direction in a 27.13 ct heart-shaped faceted stone (figure 16). While only slightly visible in darkfield illumination, this zone became

Figure 16. This 27.13 ct cut stone (inset; photo by J. Lowell) displayed an unusual white, wedge-shaped growth zoning pattern that was especially visible in reflected light when the sample was illuminated with a fiber-optic light source. Photomicrograph by J. I. Koivula; magnified 5×.

Figure 17. The Four Peaks amethyst mine has supplied attractive material for the gem trade. This white gold jewelry features a 6.89 ct Four Peaks amethyst in the ring. Courtesy of Commercial Mineral Co.

much more apparent in reflected light from a fiber-optic light source. The cause of this unusual type of decorated growth zoning is unknown, and such fog-like inclusions have not been reported in amethyst from other localities.

EDXRF analysis of two faceted amethyst samples detected silicon (as expected for quartz) and a weak fluorescence peak due to iron. IR spectra of these same two samples did not show the 3543 cm^{-1} peak that is characteristic of most synthetic amethyst (although also seen in some natural amethyst, such as that from Caxarai, Brazil; Kitawaki, 2002).

The Four Peaks amethyst tested exhibited inclusions, growth zoning, and Brazil-law twinning that should enable gemologists to separate this material from its synthetic counterpart. If needed, infrared spectroscopy can provide additional evidence that the material is not laboratory grown (Balitsky et al., 2004). When present, dense accumulations of reddish brown hematite platelets and wedge-shaped fog-like zones (again see figures 14 and 16) not only prove that an amethyst is natural, but they also strongly suggest that it originates from the Four Peaks deposit.

CONCLUSION

The Four Peaks mine in Maricopa County, Arizona, has sporadically produced fine-quality amethyst since the early 1900s, and it continues to supply commercial quantities of amethyst for the jewelry industry (figure 17). Usually the color is typical of material from most other localities, but a small percentage of Four Peaks amethyst exhibits red overtones and/or a deep reddish purple body color, a color sometime described in the trade as "Siberian." Future production will likely remain limited due to the small size of the deposit and its remote location.

REFERENCES

Balitsky V.S., Balitsky D.V., Bondarenko G.V., Balitskaya O.V. (2004) The 3543 cm^{-1} infrared absorption band in natural and synthetic amethyst and its value in identification. *Gems & Gemology*, Vol. 40, No. 2, pp. 146–161.

Chronic H. (1989) *Roadside Geology of Arizona*. Mountain Press Publishing Co., Missoula, MT, 322 pp.

Estrada J.J. (1987) Geology of the Four Peaks area, Arizona. M.S. thesis, Arizona State University, 76 pp.

Johnson M.L., Koivula J.I., Eds. (1998) Gem News: Amethyst from Arizona. *Gems & Gemology*, Vol. 34, No. 3, pp. 219–220.

Kitawaki H. (2002) Natural amethyst from the Caxarai mine, Brazil, with a spectrum containing an absorption peak at 3543 cm^{-1}. *Journal of Gemmology*, Vol. 28, No. 2, pp. 101–108.

Lieber W. (1994) *Amethyst–Geschichte, Eigenschaften, Fundorte*. Christian Weise Verlag, Munich, 188 pp.

Lowell J., Rybicki T. (1976) Mineralization of the Four Peaks amethyst deposit, Maricopa County, Arizona. *Mineralogical Record*, Vol. 7, No. 2, pp. 72–77.

Lurie M. (1998) Amethyst venture breathes new life into old mine. *Colored Stone*, Vol. 11, No. 3, pp. 72–73.

Lurie M. (1999) Uphill battle. *Lapidary Journal*, Vol. 53, No. 2, pp. 290–293, 328.

Sinkankas J. (1957) "Green" amethyst from Four Peaks, Arizona. *Gems & Gemology*, Vol. 9, No. 3, pp. 88–95.

Sinkankas J. (1976) *Gemstones of North America*, Vol. 1. Van Nostrand Reinhold, New York.

GEMS & GEMOLOGY®
Challenge Winners

This year, 253 dedicated readers participated in the 2004 GEMS & GEMOLOGY Challenge. Entries arrived from all corners of the world, as readers tested their knowledge on the questions listed in the Spring 2004 issue. Those who earned a score of 75% or better received a GIA Continuing Education Certificate recognizing their achievement. The participants who scored a perfect 100% are listed below. Congratulations!

ARGENTINA *Buenos Aires:* Ricardo Angel Tuccillo • **AUSTRALIA** *Slacks Creek, Queensland:* Ken Hunter • **BELGIUM** *Diegem:* Guy Lalous. *Diksmwide:* Honoré Loeters. *Ghent:* Jan Loyens. *Hemiksem:* Daniel De Maeght. *Koksijde:* Christine Loeters. *Overijse:* Margrethe Gram-Jensen. *Ruiselede:* Lucette Nols. *Tervuren:* Vibeke Thur • **CANADA** *Calgary, Alberta:* Diane Koke. *Bobcaygeon, Ontario:* David Lindsay. *Kingston, Ontario:* Brian Randolph Smith. *St. Catherines, Ontario:* Alice Christianson. *Montreal, Quebec:* Tricia Anderson, Marie-France Rosiak. • **ENGLAND** *Tenterden, Kent:* Linda Anne Bately • **FINLAND** *Oulu:* Petri Tuovinen • **FRANCE** *Paris:* Pierre-Henri Boissavy • **GREECE** *Athens:* Gihan Zohdy • **MALAYSIA** *Pasir Puteh, Kelantan:* Kiam Kui Yang • **THE NETHERLANDS** *Rotterdam:* E. Van Velzen • **PORTUGAL** *Figueira:* Johanne Jack • **SCOTLAND** *Edinburgh:* James Heatlie • **SPAIN** *Vitoria, Alava:* Ignacio Borras Torra • **SWITZERLAND** *Rodersdorf:* Heinz Kniess. *Zurich:* Doris C. Gerber, Eva Mettler • **THAILAND** *Bangrak, Bangkok:* Somapan Asavasanti, Siriya Siripanich, Pattarat Termpaisit, Anchalee Udomkhunatham • **UNITED ARAB EMIRATES** *Dubai:* Iamze Salukvadze • **UNITED STATES Arizona** *Chandler:* Gary Dutton, LaVerne Larson. *Gilbert:* Margaret Hodson. *Sun City:* Anita Wilde. *Tucson:* Dave Arens. **California** *Burlingame:* Sandra MacKenzie-Graham. *Burney:* Willard C. Brown. *Carlsbad:* Cindi Doyle, Michael Evans, Mark Johnson, Thorsten Strom, Ric Taylor, Jim Viall, Lynn Viall, Michael Wobby, Marisa Zachovay. *Marina Del Rey:* Veronika Riedel. *Orange:* Alex Tourubaroff. *San Rafael:* Robert Seltzer. *Ukiah:* Charles "Mike" Morgan. *Watsonville:* Janet Mayou. **Colorado** *Aurora:* Ronda Gunnett. *Denver:* Mary Shore, Alan Winterscheidt. **Florida** *Clearwater:* Tim Schuler. *Satellite Beach:* Consuelo Schnaderbeck. *Tampa:* R. Fred Ingram. **Illinois** *Bethany:* Richard Gallagher. *Chicago:* Linda Nerad. *Joliet:* Christopher Shumard. *Northbrook:* Frank Pintz. **Indiana** *Carmel:* Mark Ferreira. *Indianapolis:* Wendy Wright Feng. **Maine** *Braintree:* Arthur Spellissy, Jr. **Maryland** *Baltimore:* Alissa Ann Leverock. *Patuxent River:* Pamela Dee Stair. **Massachusetts** *Braintree:* Alan Howarth. *Brookline:* Martin Haske. *Lynnfield:* John Caruso. *Uxbridge:* Bernard Stachura. **Minnesota** *Paw Paw:* Ellen Fillingham. **Missouri** *Chesterfield:* Leslie Faerber. *Perry:* Bruce Elmer. **New Jersey** *Fort Lee:* Wendi Mayerson. **New York** *City Island:* Marjorie Kos. *Clifton Park:* Sarah A. Horst. *New York:* Anna Schumate. **North Carolina** *Advance:* Donna Cranfill. *Asheville:* Christian Richart. *Creedmoor:* Jennifer Jeffreys-Chen. *Kernersville:* Jean Marr. **Ohio** *Cuyahoga Falls:* Catherine Lee. *Holland:* Mary Jensen. *Toledo:* Nicholas Licata. **Pennsylvania** *Schuylkill Haven:* Janet Steinmetz. *Yardley:* Peter Stadelmeier. **South Carolina** *Sumter:* James Markides. **Tennessee** *Clarksville:* Kyle Hain. **Texas** *Corpus Christi:* Warren Rees. *Katy:* Christine Schnaderbeck. **Virginia** *Herndon:* Lisa Marsh-Vetter. *Newport News:* Shannon Smith. *Reston:* Beth Carter. *Vienna:* Eugene May, Jr. **Washington** *Ferndale:* Candi Gerard. *Seattle:* Janet Suzanne Holmes, A. Samsavar. *Sumner:* Lois Henning. **Wisconsin** *Milwaukee:* William Bailey.

Answers (see pp. 89–90 of the Spring 2004 issue for the questions): 1 (d), 2 (a), 3 (c), 4 (b), 5 (c), 6 (c), 7 (a), 8 (b), 9 (b), 10 (a), 11 (d), 12 (c), 13 (b), 14 (a), 15 (b), 16 (c), 17 (b), 18 (d), 19 (c), 20 (d), 21 (a), 22 (c), 23 (d), 24 (a), 25 (a)

LAB NOTES

2004

Large CORAL Bead Necklace

Sought after as a gem material for more than 2,000 years, today coral is one of the most popular organic gems in the marketplace, next to pearls ("Coral: More than seasonal," *The Guide*, May/June 2003, pp. 7–8, 13). Coral's enduring appeal may be due to its broad range of color saturation, from vivid "ox-blood" red, through the softer pinkish orange of "salmon," further to the pale pink of "angel skin," and beyond even that to white. Combined with a Moh's hardness of 3.5, it is not surprising that coral is a favorite carving material for use as *objets d'art* and in jewelry, as well as fashioned into cabochons and beads.

Figure 1. The 11 coral beads in this necklace, which graduated in size from 34.45 to 24.45 mm, were found to be untreated.

The coral used as a gem material is actually the accumulated calcium carbonate secreted by colonies of tiny anemone-like sea animals. Coral polyps are fairly delicate sea creatures, sensitive to changes in water depth, temperature, and clarity, as well as to modern hazards such as pollution and overfishing (see, e.g., R. Webster, *Gems*, 5th ed., rev. by P. G. Read, Butterworth-Heinemann, Oxford, 1994, pp. 559–564). These modern hazards and quotas imposed to protect endangered corals have led to shortages, particularly of the finer material.

The East Coast laboratory was therefore very fortunate to have the opportunity to identify a necklace containing 11 large round pinkish orange beads that were graduated in size from 34.45 to 24.45 mm (figure 1). All had a high polish, and only a few contained minor blemishes, which were almost hidden close to their drill holes. Each bead displayed coral's classic wavy parallel fibrous structure. Standard gemological testing identified the beads as coral, and swabbing with acetone in tiny inconspicuous places did not reveal any dye. Fourier-transform infrared (FTIR)

spectroscopy found no evidence of polymer impregnation. Thus, we concluded that these beads were, in fact, of natural color and not impregnated—an impressive result for such a well-matched, highly polished set of beads this size. Alternating with yellow metal spheres pavé set with numerous transparent yellow round brilliants, these coral beads were the highlight of a stunning necklace.

Wendi M. Mayerson

DIAMOND

Four Blue Diamonds from a Historic Necklace

The Cullinan blue diamond necklace (figure 2) holds a special place in the history of African diamond mining. While its classic style, workmanship, and rare blue diamonds have made it famous, it started as a personal memento—a gift to celebrate a special event. This Edwardian gold back, silver top, festoon necklace was presented by Thomas Cullinan, then chairman of the Premier mine, to his wife Annie in 1905 to commemorate the gift of the 3,106 ct Cullinan diamond to England's King Edward VII and Cullinan's subsequent knighthood. Mr. Cullinan could not have known at the time that blue diamonds such as those in the necklace would one day become as synonymous with the Premier (recently renamed Cullinan) mine as the famous large colorless crystals it has produced. Nor would he have known that blue diamonds would remain rare and among the most highly valued of all diamonds.

The exhibition of the Cullinan blue diamond necklace at GIA's museum in Carlsbad this fall presented a welcome opportunity to examine the necklace for the first time in many years, and to do so in detail for the first time ever. For this occasion, the current owner requested that detailed gemological information accompany the exhibition of the piece so as to better inform the public about this unique necklace. For our examination,

Figure 2. The Cullinan blue diamond necklace dates back to 1905 and contains several rare type IIb blue diamonds, the largest of which is 2.60 ct. Courtesy of S. H. Silver Co., Menlo Park, California.

the four principal blue diamonds (an oval shape weighing 2.60 ct—referred to as the Cullinan blue diamond—and three Old European cut brilliants weighing 0.75 ct, 0.73 ct, and 0.42 ct) were removed from the mounting for grading (figure 3), and the necklace itself was given a thorough inspection. Three of the four blue diamonds (all except the 0.42 ct) had been previously graded by GIA, most recently in 1993. That grading took place prior to the 1995 enhancements to GIA's colored diamond color grading system. Additionally, the 0.75 ct and 0.73 ct Old European brilliants had been graded in the mounting, which did not allow a precise assessment. Thus, this was an important opportunity to review the grading of these diamonds.

The 2.60 ct oval-shaped center stone was described as Fancy Intense blue. The three Old European brilliants were each color graded Fancy grayish blue. The range of color in which blue diamonds occur is rela-

tively compressed in saturation, and varies more widely in tone. Therefore, appearance differences are often differences in lightness to darkness rather than the strength or purity of the color. The four blue diamonds are relatively similar in tone, which explains their selection for the necklace. It is the stronger saturation of the 2.60 ct oval that accounts for its Fancy Intense grade.

Other gemological properties were consistent with those of typical type IIb natural-color blue diamonds (see J. M. King et al., "Characterizing natural-color type IIb blue diamonds," Winter 1998 *Gems & Gemology*, pp. 246–268). None of the diamonds showed a noticeable reaction to long- or short-wave ultraviolet radiation, and all of them were electrically conductive. Electrical conductivity is measured by placing the stone on a metal base plate and touching a probe carrying an electrical current to various surfaces of the

Figure 3. The four main blue diamonds are shown here removed from the necklace. The Fancy Intense blue oval at top weighs 2.60 ct, while the three Fancy grayish blue Old European brilliants weigh, from left to right, 0.75 ct, 0.42 ct, and 0.73 ct.

diamond. The conductivity value can vary with direction, so a number of measurements are made and the highest value is recorded. As noted in previous studies (again, see King et al., 1998), the highest electrical conductivity value can vary widely within and between color grades. We found this to be the case with these diamonds, as each showed a range of values. Interestingly, the Fancy Intense blue oval—the most strongly colored—displayed the lowest value.

It is common for type IIb blue diamonds to phosphoresce after exposure to short-wave UV radiation, and this characteristic was noted for all four stones. Although the best-known phosphorescent reaction in blue diamonds is that of the famous Hope diamond, the Hope's long-lasting strong red phosphorescence is actually quite rare. It is much more common for phosphorescence to be very weak to weak blue or yellow and of short duration; this more common reaction was exhibited by the diamonds from the necklace.

Microscopic examination revealed characteristics consistent with other type IIb blues. Such diamonds frequently have an uneven color distribution, which was observed here. It is also typical for them to have relatively few solid inclusions, with fractures and indented naturals being more common. This was also consistent with our findings. As would be expected, the blue diamonds, as well as other diamonds in the necklace, exhibited minor chips and abrasions consistent with the necklace's nearly 100-year history (figure 4).

Examination of these historic stones also gave us an important opportunity to study spectroscopic features of known natural IIb diamonds. Infrared spectroscopy showed absorptions in all four stones at 2801 and 2454 cm^{-1}, which are typical features of type IIb diamonds. Photoluminescence spectra collected using an argon laser (at 488 nm excitation) revealed emission features characteristic of natural diamonds. A relatively strong 3H emission (503.5 nm) was detected in all four stones.

Luminescence imaging is a useful way to study diamond growth, and was performed using the De Beers DiamondView. As shown in figure 5, blue luminescence and networks of polygonized dislocations are evident. Similar dislocation features were observed in all four stones. This type of dislocation network is a specific feature of natural diamond, and has never been observed in synthetic diamond.

*John M. King, TMM,
and Wuyi Wang*

Figure 4. Minor chips and abrasions such as those seen here on the 0.42 ct Old European brilliant are often encountered on diamonds that have been worn over a long period of time.

Figure 5. This luminescence image of the 2.60 ct oval-shaped diamond was collected using the De Beers DiamondView. A blue luminescence and networks of polygonized dislocations are evident; such dislocation networks are characteristic of natural diamond.

Irradiated Blue Diamond Crystal

Irradiation with or without annealing is a common technique used to enhance the color of diamonds, and those suspected of being treated in this manner are routinely submitted to the laboratory for origin-of-color testing. Most such stones are treated after faceting, and depending on the type of treatment, diagnostic color distribution features are sometimes seen. Among the few laboratory-irradiated rough diamonds we have examined was a 2.95 ct well-formed bluish green octahedron (Winter 1989 Lab Notes, pp. 238–239).

Recently, a large crystal that resembled the sample in the 1989 Lab Note was submitted to the East Coast laboratory for origin-of-color determination. The experienced client who brought the stone to our attention was suspicious of its origin even though it was represented as coming directly from the mine in central Africa.

The 11.60 ct crystal (figure 6), which measured 13.11 × 12.85 × 9.09 mm, exhibited typical octahedral crystal morphology and showed obvious resorption features on its surface. It also showed a distinct greenish blue coloration. In contrast to similarly colored natural diamonds, no green or brown radiation stains were observed with magnification. However, a slight color concentration was evident at the edges of the crystal faces (again, see figure 6). We observed a strong blue fluorescence to long-wave UV radiation and a weak green-yellow reaction to short-wave UV.

Infrared spectroscopy revealed features typical of a type Ia diamond with very high nitrogen content and a weak absorption due to hydrogen impurities. In rare cases, a high concentration of structurally bonded hydrogen in diamond could produce blue coloration, but that definitely was not the case for this crystal. A weak H1a absorption was present (at 1450 cm^{-1}), but there were no H1b, H1c, or H2 absorptions. In the UV-visible spectrum collected when the diamond was cooled by liquid nitrogen (figure 7), strong N3 (415

Figure 6. The strong blue coloration in this 11.60 ct diamond octahedron proved to be the result of laboratory irradiation.

nm), moderate N2 (478 nm), weak H3 (503 nm), and weak 595 nm absorptions were detected; a strong and broad GR1 (741 nm) absorption also was apparent.

These gemological and spectroscopic features led to the conclusion that this crystal was artificially irradi-

ated without subsequent annealing. Considering the large size of the crystal, it is possible that the radiation-related color does not penetrate evenly throughout, as is suggested by the concentration of color along the edges.

Wuyi Wang and TMM

Irradiated Type IIb Diamond

Type IIb diamonds are often blue, due to small amounts of boron impurities. Depending on the occurrence of other defects (e.g., plastic deformation), some type IIb diamonds exhibit a gray or, more rarely, a brown color (see, e.g., King et al., 1998, cited in earlier entry). Blue also can be produced in an otherwise colorless diamond by exposure to radiation (either naturally or in a laboratory) to create a vacancy defect. Although it is technically possible to enhance the blue color of a type IIb diamond by irradiation, mixing of two different color-causing mechanisms in the same diamond may not necessarily produce an attractive color. Brown natural

Figure 7. A strong and broad GR1 absorption (741 nm), together with a weak absorption at 595 nm, indicated that the 11.60 ct greenish blue diamond was irradiated in a laboratory. The pre-existence of relatively strong Cape absorptions (e.g., N3 and N2) resulted in the green modifier.
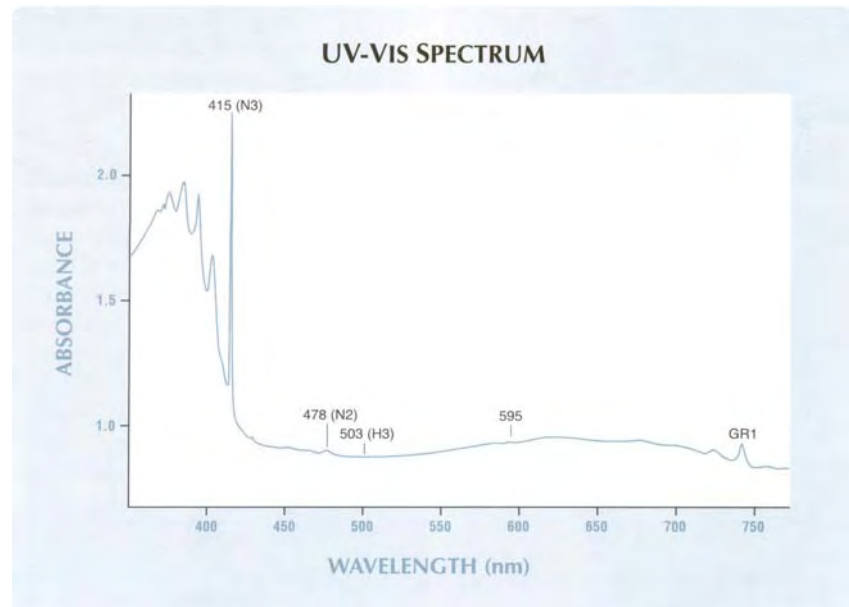
Figure 8. This 2.00 ct Fancy Dark green-gray type IIb diamond was found to have been laboratory irradiated.

radiation stains were reported on an unusual type IIb blue diamond (Fall 1991 Lab Note, pp. 174–175), but the radiation did not appear to have had any effect on the color of this faceted stone. An artificially irradiated type IIb diamond recently submitted to

Figure 9. When examined with a microscope and diffused light, the diamond in figure 8 revealed a strong concentration of blue near the culet, which proved that it had been artificially irradiated. Field of view is 6.0 mm high.
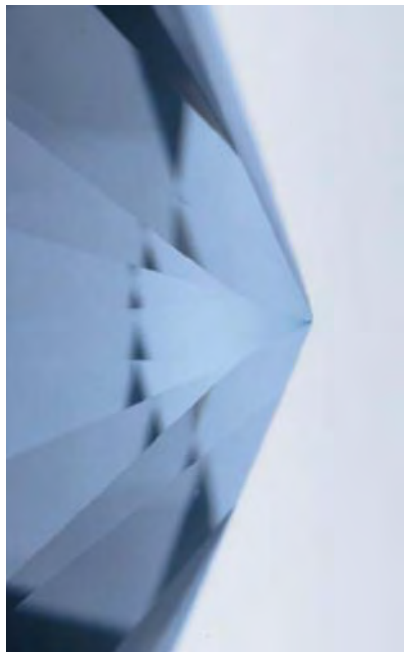
the East Coast laboratory gave us an extremely rare opportunity to examine a sample of this nature.

The 2.00 ct oval brilliant cut (10.52 × 7.14 × 4.21 mm) in figure 8 was color graded Fancy Dark green-gray. Although this hue was not outside the range of hues we have seen in natural-color type IIb diamonds, the cause of the color was not immediately obvious. No green or brown natural radiation stains were observed on the surface with magnification and darkfield illumination. Nor did the diamond have any notable internal characteristics such as solid inclusions or fractures, or any distinct colored graining. We did not see fluorescence to either long- or short-wave UV radiation, but very weak yellow phosphorescence was detected after exposure to short-wave UV. Infrared absorption spectroscopy only showed features typical of a type IIb diamond (e.g., strong and clear absorptions at 2801 and 2454 cm^{-1} due to substitutional boron impurities). However, when the

diamond was examined more carefully with low-power binocular magnification and diffused light, a distinct blue color concentration was noted near the culet (figure 9). This type of color zoning is typical for diamonds that have been artificially irradiated with a low-energy source, as is usually done today with an electron beam.

Absorption spectroscopy collected at liquid nitrogen temperature in the ultraviolet-visible range (figure 10) showed a strong GR1 band (vacancy, 741 nm) and several other lines of the GR series (GR2 through GR8). A clear TR12 absorption at 469.9 nm also was detected. It is very rare for a natural-color type IIb diamond to show any detectable GR1 or TR12 absorption with UV-Vis absorption spectroscopy. In addition, in the photoluminescence spectrum seen with a laser Raman microspectrometer, the intensity of the 3H defect with a zerophonon line at 503.5 nm (another typical radiation-related defect in diamond) was significantly stronger than

Figure 10. This UV-Vis absorption spectrum of the green-gray diamond shows a strong GR1 band and some additional lines from the GR series. A clear TR12 band also was detected. A gradual increase in absorption at higher wavelengths is attributed to the presence of boron impurities.
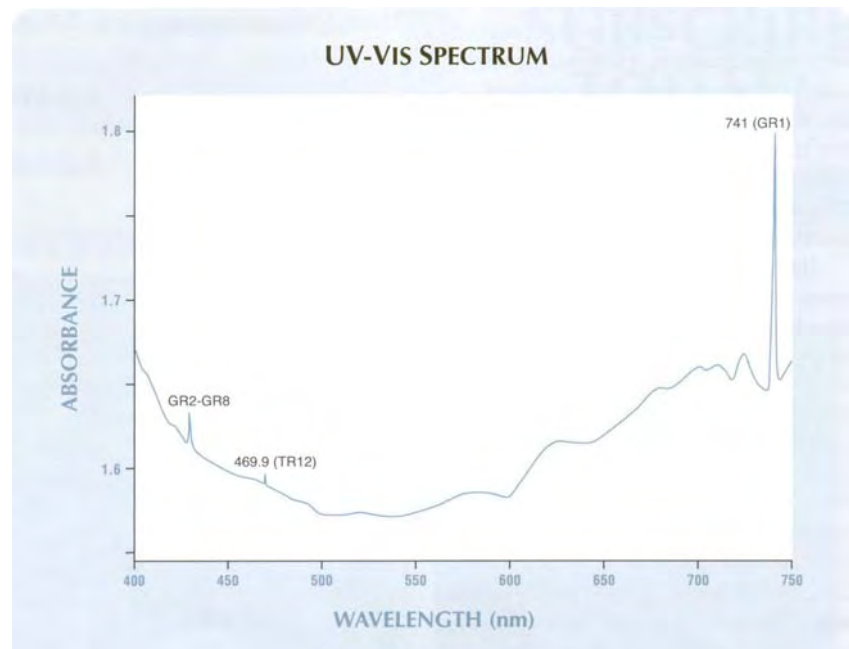
Figure 11. The color appearance of the 12+ ct Very Light blue type IaB oval modified brilliant in the center is due to scattering of light and not to any of the typical causes of natural blue color. The 6+ ct pear-shaped diamond on the left is colorless (D-color); the 5.5+ ct type IIb on the right is Fancy Light blue.

that in any natural-color type IIb diamonds we have examined. All these observations led to the conclusion that this type IIb diamond had been treated by irradiation in a laboratory.

Little is known about the interaction between vacancies and boron in diamond and the possible impact on color. The color of this specific sample is not very attractive. A possible reason is that prior to irradiation the stone may have had a strong brown component. This also would explain the green coloration after treatment.

Wuyi Wang, TMM,
and Thomas Gelb

Unusual Cause of
Blue Color in a Diamond

It is unusual for the laboratory to encounter natural blue diamonds with a cause of color other than boron impurities, natural irradiation, or the presence of hydrogen (see, e.g., E. Fritsch and K. Scarratt, "Natural-color nonconductive gray-to-blue diamonds," Spring 1992 *Gems & Gemology*, pp. 35–42; and King et al., 1998, cited above). Thus, it was quite a surprise when the East Coast lab recently tested an oval diamond over 12 ct (figure 11, center) with a blue color typical of that produced by boron but none of the other properties one would expect for such diamonds.

When color graded, the oval was classified as Very Light blue. On testing for electrical conductivity, the

diamond was found to be nonconductive. We observed a moderate blue reaction to both long- and short-wave UV radiation. Infrared spectroscopy proved that the diamond was type IaB and did not show any elevated levels of hydrogen. Spectroscopic analysis further ruled out any possibility that this stone was irradiated in a laboratory. However, microscopic examination revealed clouds of pinpoints and internal whitish graining.

In this case, we believe the color was caused by a scattering of light in the diamond from the clouds of pinpoint inclusions. This effect is similar to the one that causes cigarette smoke to appear blue, a phenomenon often referred to as the Tyndall effect. Named after its discoverer, 19th-century British physicist John Tyndall,

Figure 12. More typically, the scattering of light from micro inclusions produces a predominantly white (as shown in this 7.00 ct marquise) or gray color in diamond.

this effect is caused by reflection and/or scattering of light by very small particles in suspension in a transparent medium. It is often seen from the dust in the air when sunlight enters a room through a window or comes down through holes in clouds. Most diamonds that have dense clouds and also show scattering have a predominantly white or gray appearance (e.g., figure 12). The difference in color is probably related to the size of the particles and the density of the cloud.

We have documented diamonds with these properties from a few different geographic locations, including India and Australia. This unusual stone indicates that micro-inclusions in diamond can generate colors other than black, gray, and white. The nature of the micro-inclusions (chemistry, particle size, density, and distribution) and the size of the stone, along with the light source and its distribution of output, are all factors in determining the final color appearance of the diamond.

John M. King, Wuyi Wang, TMM

NEPHRITE that Mimics Serpentine

Because of their similar appearances, some nephrite and serpentine can be impossible to distinguish by visual observation alone. Although the two mineral species usually can be readily separated on the basis of their refractive index and specific gravity values, in some cases even these physical properties can be misleading. The West Coast laboratory recently received a 142.27 ct translucent mottled green-gray carving of a water buffalo that exhibited both an artificial water-soluble reddish stain outlining details of the carving, and a light brownish yellow coating that partially concealed the underlying host material (figure 13).

Microscopic examination revealed that the host was a fine-grained aggregate. When tested in an inconspicuous area, the coating dented and scratched easily with a metal probe, similar to the response of a wax.

Figure 13. This nephrite carving (43.95 × 30.35 × 9.98 mm) could be confused with serpentine due to the effects of an unidentified coating.

istry, S.G., and FTIR and Raman spectra were all consistent with nephrite.

In an attempt to confirm or explain the uncharacteristically low R.I. values, the thin film that coated the specimen was polished off in a small inconspicuous area to better expose the host material. A higher vague R.I. reading between 1.60 and 1.61 was then obtained, indicating that the coating was responsible for lowering the apparent R.I. This piece was a valuable reminder of the care and diligence that should be exercised when obtaining physical properties for gem identification.

CYW

However, it did not melt readily when exposed to a thermal reaction tester; instead it merely yielded more easily and turned brown under the microscope with prolonged contact. It also did not react to a dilute HCl solution. This coating may have been an attempt at "antiquing" the carving; however, it is not known whether the coating was natural or an artificially applied substance. In addition, a very thin coating, which may have been separate from—or an extension of— the built-up areas, created an invisible film over the host material. It too could be scratched off, possibly deceiving an unwary observer into believing that the host material was soft. However, only the thin film yielded to the tip of the probe, whereas the material beneath was harder than the metal point.

The R.I. of the greenish areas was approximately 1.58, varying from 1.57 to 1.59. The higher value was obtained on a small area where the thin coating had been removed with solvent; areas with the thicker brownish yellow coating had lower R.I. values than areas where the green-gray host material was clearly visible.

The reaction to long-wave UV radiation was a combination of an inert background mottled with medium chalky green-yellow fluorescence that appeared weak to medium yellow on the areas with the thicker brownish yellow coating. The reaction to short-wave UV was also a combination of an inert background with a mottled very weak to weak yellow fluorescence on the coating. There was no significant visible-light spectrum.

With only this initial examination—the appearance of the carving, the illusory "soft" nature of the material, and the low R.I. values rarely attained by nephrite—a hasty evaluation could lead a gemologist to misidentify this material as serpentine. However, further testing revealed its true composition. The specific gravity, measured hydrostatically, was approximately 2.96; the FTIR spectrum was consistent with those of other nephrites; and the Raman spectrum of the greenish areas was consistent with the nephrite reference in the database. To characterize the material further, EDXRF analysis was performed by GIA senior research associate Sam Muhlmeister. The major elements present were Si, Ca, and Mg, with a trace of Mn and Fe. The presence of Ca in the structure excluded serpentine, while the chem-

Pink OPAL

This past summer, the East Coast laboratory received for identification two pairs of partially drilled translucent to semi-translucent variegated pink drops (figure 14). The larger pair measured 35.90 × 13.95 × 13.90 mm and 35.60 × 13.95 × 13.90 mm and had a total weight of 64.73 ct; the smaller pair had a total weight of 29.28 carats.

At first glance, the drops resembled conch pearls in their coloration. However, they did not exhibit any flame-like structure; nor were they the standard shape of conch pearls. In fact, their symmetrical shape indicated they were not pearls at all. They also resembled massive rhodochrosite, but they lacked the botryoidal structure and distinctive color zoning commonly associated with that mineral. Standard gemological testing revealed spot refractive indices of 1.45, weak-to-medium whitish fluorescence to long-wave UV, very weak yellow to no reaction to short-wave UV, and specific gravities ranging from 2.16 to 2.23. With a desk-model spectroscope, all four drops showed a weak band at approximately 490 nm, a weak line at approximately 550 nm, and a cutoff from 430 nm. These properties suggested opal, but glass could not be ruled out.

A Fall 1982 Lab Note (pp. 172–173) described a variegated light pink and

Figure 14. These four variegated pink drops, which range from 14.01 to 32.68 ct, were identified as pink opal.

gray carving of a bird that was identified as opal by the West Coast laboratory. Not until the Winter 1991 issue (pp. 259–260) did information become available in *G&G* regarding the location of the mines that reportedly were producing this translucent-to-opaque pink material, along with blue opal: the Acari copper mining area near Arequipa, Peru. It was said that some of the pink material even "exhibits a color reminiscent of rhodochrosite" (p. 259).

Our next step was to use energy-dispersive X-ray fluorescence (EDXRF) to investigate the chemistry of the four drops and compare the findings to a sample of known pink opal from Peru. EDXRF revealed the presence of Mg, Al, Si, K, Ca, Mn, and Fe. As opal is amorphous silica, the other elements can be attributed to mineral impurities, such as palygorskite, that are commonly associated with this type of opal (see J. Hyrsl, "Gemstones of Peru," *Journal of Gemmology*, Vol. 27, No. 6, 2001, pp. 328–334, and the Fall 1982 Lab Note). The spectra were nearly identical, clearly identifying these drops as pink opal, possibly from Peru.

Wendi M. Mayerson
and David Kondo

## RUBIES, Clarity Enhanced with a Lead Glass Filler

Heat treatment of natural rubies frequently leaves a glassy residue within surface-reaching fractures and cavities. This filling is produced during the heating process and can facilitate the partial healing of fractures within the rubies. It is often detectable with magnification by observing the difference in luster compared to the surrounding corundum (see, e.g., Fall 2000 Lab Notes, pp. 257–259). This type of glass residue has a relatively low R.I. compared to corundum and is usually not considered to

be a clarity enhancement on its own.

Earlier this year, however, the Gemmological Association of All Japan (GAAJ) issued a lab alert describing rubies that had not been heat treated, but that showed a flash effect in their fractures caused by a clarity enhancement similar to that traditionally used in diamonds ("Lead glass impregnated ruby," *GAAJ Lab Alert*, 2004, GAAJ Research Laboratory, http://www.gaaj-zenhokyo.co.jp/ researchroom/kanbetu/2004/gaaj_ alert-040315en.html). Their EDXRF chemical analyses revealed the presence of elevated levels of lead (Pb) in the material filling the fractures in these stones. The results were later confirmed by the AGTA ("New ruby treatment arrives in the United States," AGTA Gemstone Update, http://www.agta.org/consumer/news/ 20040702rubytreatment.htm).

Recently, the West Coast laboratory had the opportunity to examine two purplish red mixed-cut oval stones (3.19 and 2.76 ct) that contained numerous large surface-reaching fractures and cavities filled with a glassy substance (figure 15). Both gems were identified as natural ruby by their inclusions, R.I., and visible absorption spectra in a desk-model spectroscope. Unlike the stones described by GAAJ, the presence of thermally altered inclusions showed that these rubies had been heated. The glassy fillings contained numerous flattened gas bubbles or voids (figure 16), and showed a

Figure 15. These two rubies contain numerous fractures filled with a high-lead-content glass that undoubtedly significantly improved their apparent clarity.
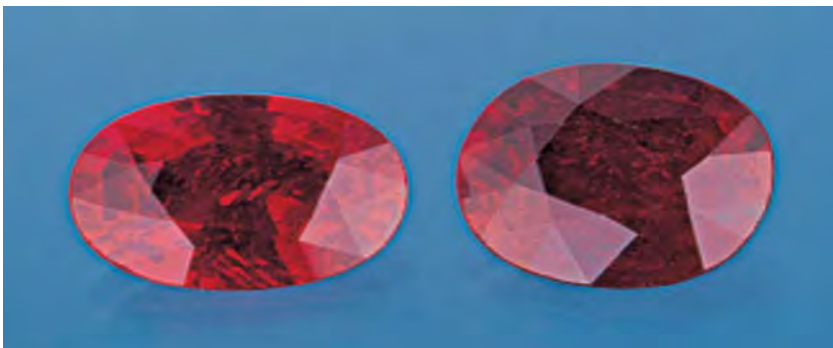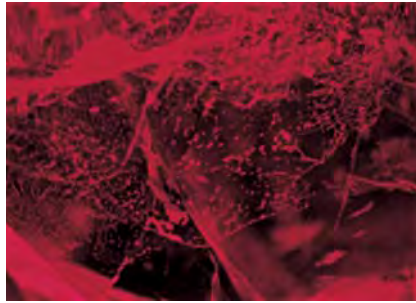
Figure 16. The glassy fillings in these clarity-enhanced rubies all contained numerous flattened gas bubbles (left) and elongated and irregular voids (right). Magnified 27×.

distinctly higher surface luster than the corundum (figure 17). The filled fractures were very low relief in all viewing directions and displayed weak to moderate blue-to-violet and orange flash effects. In some directions, the fractures had a slightly hazy appearance (figure 18). The 3.19 ct ruby, in particular, had several large filled cavities.

The filling material in the largest cavity was translucent, yellow in color, and contained many spherical gas bubbles (figure 19). In another large filled cavity, the filling material was also yellow, but transparent with no visible gas bubbles. The filling material in the fractures did not have a visible body color, but this was undoubtedly because of the small amount of material present. All the filled cavities showed poor polish at the surface, indicating a much lower hardness than the surrounding corundum (again, see figure 17). Unlike the residues we have seen previously in heat-treated rubies, the nature and abundance of the fillings in these two stones suggested an intent to hide the fractures and improve the apparent clarity of the gems.

To learn more about the filling material, we employed EDXRF analysis, Raman spectroscopy, and fluorescence imaging. EDXRF, performed by GIA senior research associate Sam Muhlmeister, showed elements typical of ruby (Al, Cr, and Fe) and elevated levels of Pb similar to those reported by GAAJ. None of the other elements that have been reported in glass-like ruby fillings (Si, P, Ca, and Ti) were detected (again, see the Fall 2000 Lab Note). It is important to note that lighter elements such as boron cannot be measured using EDXRF.

Raman spectroscopy was performed to compare the glass filler in these two rubies with five different glass samples known to contain significant Pb. Although the spectrum for this filler was not a match for any of the glasses in our collection, it had many of the same luminescence features as a sample of lead borate glass.

Last, we observed reactions to high-energy short-wave UV radiation using the De Beers DiamondView instrument. The filling material responded very strongly, fluorescing bright blue in contrast to the red reaction (caused by chromium) of the surrounding corundum. For comparison, traditional glass-filled cavities in rubies show an inert to dull gray reaction (figure 20, left and right). None of the glass samples from our collection showed any reaction in the DiamondView.

Key gemological identification features of this new filler include a distinct luster, flash effects, haziness, gas bubbles and voids, together with very low relief of the fractures in all viewing directions. In addition, elevated Pb and the absence of other significant ele-
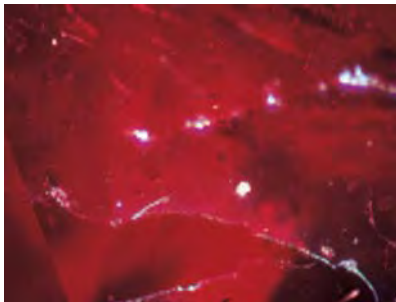
Figure 17. The luster of this filler material was actually higher than the ruby, which is the opposite of what is typically seen with glassy residues. Surface cavities filled with this lead glass also showed a poor polish compared to the surrounding corundum, indicating a much lower hardness. Magnified 40×.

Figure 18. In some directions, the filled fractures showed a slightly hazy appearance. Magnified 36×.

Figure 19. In one large filled cavity, the filler was translucent and yellow in color. One of the many spherical gas bubbles that were present can be seen in the center of this image. Magnified 27×.
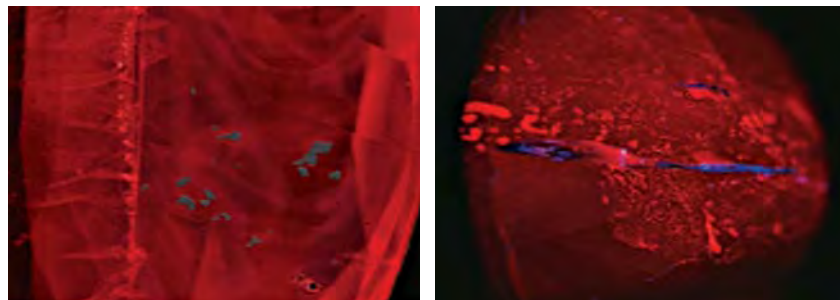
Figure 20. These DiamondView images show the inert to dull gray reaction of a traditional glass filler (left) compared to the bright blue reaction of the new lead glass filler (right).

ments attributable to the filler in the EDXRF analysis are characteristic of the samples we have seen thus far. Blue fluorescence in the DiamondView may also be useful for identification.

Kimberly M. Rockwell and
Christopher M. Breeding
GIA Gem Laboratory, Carlsbad

Unusual SYNTHETIC RUBY Triplet Displaying Asterism

The identification of loose assembled stones is relatively straightforward. However, when they are mounted in jewelry (often bezel set), almost all signs of assembly can be hidden. Frequently only the top portion of the assemblage can be identified, with few indications as to the identity of the bottom part possible because of the restrictions the mounting places on testing procedures (as was the case with the assembled stone reported in the Fall 1993 Lab Notes, p. 205).

Recently, the New York laboratory was asked to identify a large red double cabochon that displayed a weak six-rayed star; it was set in a yellow metal ring with 22 transparent near-colorless brilliants (figure 21). A 1.76 spot R.I. reading, characteristic absorption spectrum, and the presence of curved striae and gas bubbles seen with magnification identified the top of the cabochon

as synthetic ruby manufactured by a melt process. Further examination through the top of this mounted cabochon revealed a deeper layer of colorless cement with numerous oval gas bubbles, followed by another layer that exhibited the hexagonal growth structure typical of natural corundum.

Although at this point the cabochon appeared to be a simple assembled stone consisting of a synthetic ruby top and a natural ruby bottom, held together by a near-colorless cement layer, closer inspection of the convex bottom with a fiber-optic light and magnification revealed the presence of curved striae. This indicated that the bottom piece was *also* a melt-grown synthetic ruby. This was very unusual, but to fully identify the parts of this assemblage it would have to be removed from the mounting. Fortunately, the cabochon was held in place by only four small prongs, so with the client's permission we had it unmounted for further analysis.

The bottom piece exhibited diagnostic properties identical to those of the synthetic ruby top. Immersion of the cabochon in methylene iodide revealed a thin grayish blue layer completely encapsulated within a thick layer of colorless cement (figure 22). Due to its location within the glue, it was not possible to definitively identify this layer. However, the hexagonal growth structure seen in figure 23

Figure 21. The red asteriated cabochon in this ring (13.00 × 11.80 × 10.55 mm) was identified as a triplet consisting of a synthetic ruby top and bottom joined by a near-colorless glue layer that surrounded an unidentified center section.

Figure 22. When the cabochon in figure 21 is viewed in profile, unmounted and immersed in methylene iodide, the distinctive layers that make up this assemblage are clearly visible, as are numerous gas bubbles in the near-colorless cement.

Figure 23. Seen through the bottom of the cabochon while it was immersed in methylene iodide, the hexagonal growth structure of the unidentified section is apparent within the cement.
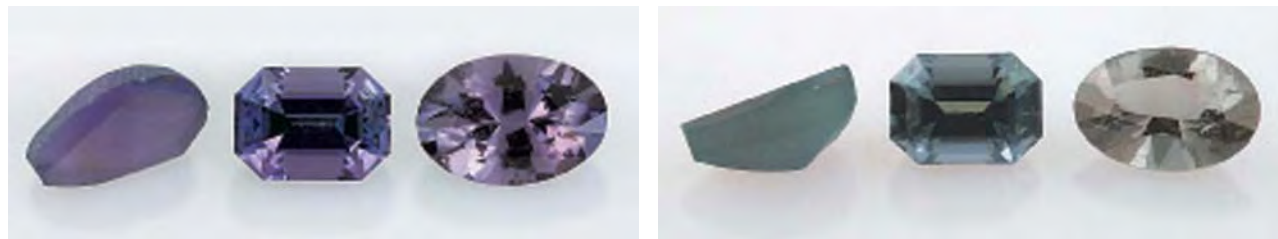
Figure 24. These three cuprian tourmalines from Mozambique (5.47, 5.68, and 5.37 ct) exhibit a strong "reverse" color change from fluorescent light (left) to incandescent light (right).

indicated that it most likely was a thin slice of natural corundum that contained the three directions of rutile needles, or "silk," necessary to create asterism. The conclusion that appeared on the gem identification report read as follows: "Triplet consisting of a synthetic ruby top and a synthetic ruby bottom, joined together with a near colorless cement containing an unidentified center section."

*Siau Fung Yeung
and Wendi M. Mayerson*

Copper-bearing Color-Change TOURMALINE from Mozambique

Color-change tourmaline has been reported in *G&G* on only three prior occasions: dravite from East Africa (Fall 1991 Gem News, pp. 184–185), uvite possibly from East Africa (Fall 2000 Gem News, pp. 270–271), and copper-manganese-bearing elbaite from Nigeria (Fall 2001 Gem News International, pp. 239–240).

Elsewhere in the literature, there are limited reports of color-change tourmalines, which typically proved to be chromium- and vanadium-bearing specimens in the dravite-uvite series (H. Bank and U. Henn, "Colour-changing chromiferous tourmalines from East Africa," *Journal of Gemmology*, Vol. 21, No. 2, 1988, pp. 102–103; A. Halvorsen and B. B. Jensen, "A new colour-change effect," *Journal of Gemmology*, Vol. 25, No. 5, 1997, pp. 325–330).

Noel Rowe of Rough to Cut in San Jose, California, recently submitted to the West Coast laboratory a color-change tourmaline that differed

significantly from those previously described. Viewed table-up, this 5.68 ct transparent emerald-cut stone (11.63 × 8.76 × 7.48 mm) exhibited a distinct color change from purple in fluorescent light to gray–bluish green in incandescent light (figure 24). Particularly notable is the fact that the colors exhibited were the reverse of the usual alexandrite effect: cool colors such as green, blue, or gray in day or fluorescent light and warm colors such as purple, red, or brown in incandescent light. All other previously reported color-change tourmalines followed the usual convention.

This stone was eye-clean, and even with magnification it was exceptionally free of inclusions except for a tiny crystal near the surface of the pavilion and three miniscule needles near the girdle. Although optical properties and Raman analysis proved that this stone was indeed tourmaline (the Raman spectrum was consistent with rubellite in the database), the lack of inclusions and the very unusual phenomenon warranted further investigation.

To facilitate the investigation of this intriguing material, Mr. Rowe and the owner of the stone, Bruce Fry of Mars, Pennsylvania, supplied two additional tourmalines that exhibited similar properties. One was a 5.47 ct pear shape pre-form that had roughly the same color change as the emerald-cut stone. The other was a 5.37 ct oval that had a weaker color change from grayish purple in fluorescent light to gray in incandescent light (again, see figure 24). According to Mr. Fry, these three stones are the only tourmalines of this type that he or his South African suppliers have

ever seen. He stated that the emerald-cut and pear pre-form stones were from Moiane in northern Mozambique, approximately 200 km north of Nampula. The origin of the oval is only known as northern Mozambique. The specimens were alluvial in origin, and at least one of the stones was reportedly mistaken for a low-value iolite after being discovered by a local gold miner. Both the emerald cut and the pear shape pre-form were thought to be from the same lot; although cut recently, they were probably recovered several years ago. The oval was cut from a crystal with a color distribution that included a thin "rind" of pink skin and other small pink zones. Mr. Fry retained a flame-shaped zone of pink when he faceted the stone approximately four years ago.

The pear pre-form had a frosted surface with small areas of the original skin. Although the view into the stone was obscured by the frosted surface, magnification did reveal some sparse "trichites" (interconnected secondary two-phase inclusions) and a couple of fractures extending in from the surface that contained an orangy yellow residue, possibly iron-oxide staining. The stone was vaguely bicolored with a pink zone encompassing approximately half of it toward the tip. The oval also contained trichites, in addition to the pink flame-shaped zone that extended inward from the side. All the stones displayed the strong doubling at facet junctions typical of tourmaline.

The R.I. values of the emerald-cut and oval stones were ω = 1.639–1.640

and ϵ = 1.621 (values for the pear pre-form were unattainable due to the rough surface). The hydrostatic specific gravities ranged from approximately 3.05 to 3.06 for the three samples. All three stones were inert to both long- and short-wave UV radiation. Dichroism was similar in all three—grayish violet to violet and grayish green to pale green—varying mostly in intensity.

To characterize these stones further, GIA senior research associate Sam Muhlmeister performed EDXRF qualitative chemical analysis. Al and Si were the major elements detected; the oval had a minor amount of Mn, while traces of Mn were seen in the other two samples. All the stones also showed traces of Ca, Cu, Ga, and Bi, with the oval showing Zn and Sr, and both the emerald cut and the oval showing some Pb (the presence of which was inconclusive in the pre-form).

The copper content is especially noteworthy. The only other commercially available tourmalines that contain copper are the copper-manganese-bearing elbaites, well-known for their exquisite blue colors, from São José da Batalha, Paraíba, Brazil (and surrounds), and western Nigeria (see, e.g., E. Fritsch et al., "Gem-quality cuprian-elbaite tourmalines from São José da Batalha, Paraíba, Brazil," Fall 1990 *Gems & Gemology*, pp. 189–205; and B. Laurs et al., "More on cuprian elbaite tourmaline from Nigeria," Spring 2002 Gem News International, pp. 99–100). One Nigerian cuprian elbaite that was examined by the Gübelin Gem Lab—a 22.98 ct violet gemstone—also exhibited a color change (C. P. Smith et al., "Nigeria as a new source of copper-manganese-bearing tourmaline," Fall 2001 Gem

News International, pp. 239–240). However, both the dichroism (purple-violet and slightly grayish violet-blue) and the color change (violet to purple) were different from what was seen in the three stones from Mozambique.

It is likely that Cu and Mn, at least in part, are the cause of color in these three specimens (Fritsch et al., 1990). Trace amounts of Pb in these samples could possibly be the result of residue from the polishing process and may not be reliable (D. Dirlam et al., "Liddicoatite tourmaline from Anjanabonoina, Madagascar," Spring 2002 *Gems & Gemology*, pp. 28–53).

The EDXRF analyses helped narrow the list of possible tourmaline species to which these stones belong. The lack of significant amounts of Ca, Fe, and Mg eliminates the calcic tourmalines and several other end members (e.g., dravite). Solely based on the elements detected, the remaining possibilities include the alkali tourmalines elbaite and olenite and the X-site-vacant tourmaline, rossmanite (see, e.g., F. C. Hawthorne and D. J. Henry, "Classification of the minerals of the tourmaline group," *European Journal of Mineralogy*, 1999, Vol. 11, pp. 201–215). However, quantitative chemistry, using a method that would detect lighter elements such as Na and Li, would be necessary to fully characterize these stones and the tourmaline species to which they belong.

Polarized UV-visible spectroscopy (also performed by Sam Muhlmeister) and oriented FTIR spectroscopy were conducted for comparison to other tourmalines. The UV-Vis spectra were very similar to those reported for the cuprian elbaites from the Paraíba mines in Brazil, with broad absorption peaks centered around

485–520 nm (which was attributed to Mn^{3+} in unheated Paraíba tourmalines) and Cu^{2+} absorptions centered around 690 and 895–905 nm in the $E \perp c$ direction and 710–720 and 900–920 nm in the $E \| c$ direction (again, see Fritsch et al., 1990). Although the FTIR spectra were consistent with other tourmalines, determining whether or not subtle differences exist to distinguish these stones would require further study.

Several aspects of these three tourmaline specimens are very intriguing: their strong and distinct color change, the fact that the color change relative to the type of light source is opposite the normal alexandrite effect, the copper content, and the source location in East Africa.

We have no current explanation for the reverse nature of the color change. We are continuing research into this seemingly new variety of tourmaline, with a focus on obtaining quantitative chemistry to more fully characterize this material and determine the species to which it belongs. Quantitative chemical analysis will also provide greater insight into the cause of color in these stones and possibly even clues to the unusual nature of this phenomenon. Perhaps East Africa will become a new source of copper-manganese-bearing change-of-color tourmalines.

CYW

DIAMONDS

An untreated type Ib diamond exhibiting green transmission luminescence and H2 absorption. These contributors recently analyzed a small greenish brownish yellow ("olive yellow") diamond that exhibited green transmission luminescence (figure 1) as well as an unusual combination of absorption features. At first sight, the 0.12 ct diamond did not appear particularly remarkable, except for its UV luminescence, which was green to long-wave and greenish yellow to short-wave UV radiation. However, an infrared spectrum showed that the diamond was a low-nitrogen type Ib/IaA, with the single nitrogen clearly dominating the A-aggregates (figure 2; see specifically the inset showing the 1358–1000 cm^{-1} region). This was surprising, since green luminescence caused by the H3 center (the combination of paired nitrogen [A aggregate] with a vacancy) is commonly observed in type Ia diamonds but seen only very rarely in type Ib diamonds. Furthermore, the extremely low A aggregate concentration would not normally indicate the formation of distinct H3 luminescence. The total amount of nitrogen in the diamond was roughly estimated from the spectrum to be 15 ppm by comparison with samples of known nitrogen content.

A strong "amber center" with its main peak at 4165 cm^{-1} was visible in the near-infrared region of the spectrum (again, see figure 2), indicating a deformation-related coloration. This also was unusual, since the amber center is typical for type Ia brown diamonds colored by deformation and related defects (L. DuPreez, "Paramagnetic Resonance and Optical Investigation of Defect Centres in Diamond," Ph.D. dissertation, University of Witwatersrand, Johannesburg, 1965). In "olive" and brown type Ib diamonds with deformation-related coloration, the main absorption of this defect has been found at 4115 cm^{-1} or as a doublet at 4165 and 4065 cm^{-1} (T. Hainschwang, "Classification and color origin of brown diamonds," Diplôme d'Université de Gemmologie, University of Nantes, France, 2003). A "single" amber-center peak at 4165 cm^{-1} in a type Ib diamond has not previously been described.

The deformation-related color was confirmed by observation in transmitted light between crossed polarizers. The diamond showed very distinct parallel gray to black extinc-
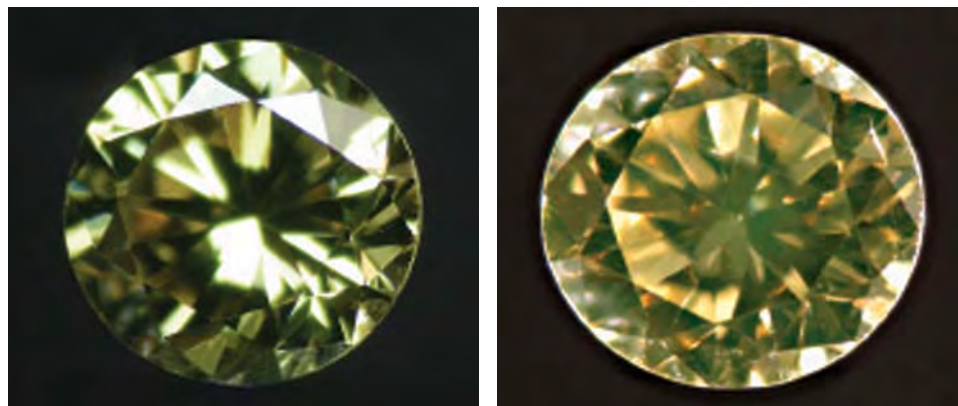

Figure 1. This 0.12 ct diamond, shown on the left in daylight, exhibits green transmission luminescence in dark-field illumination (right), as well as an unusual combination of absorption features. Photos by T. Hainschwang.
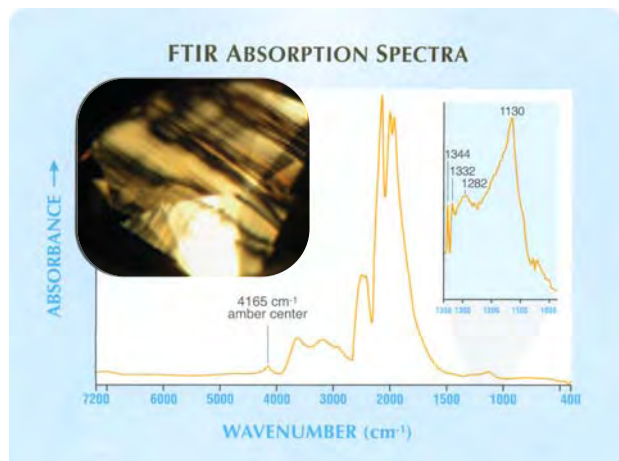
FTIR ABSORPTION SPECTRA

Figure 2. The FTIR spectrum of the diamond in figure 1 reveals that it is a type Ib/IaA, with isolated nitrogen clearly dominating the A-aggregates. The region between at least 5000 and 4165 cm⁻¹ comprises the "amber center," of which the 4165 cm⁻¹ peak is the main feature. The amber center is deformation related; the deformation is apparent in the extinction patterns visible with crossed polarizers (see inset; photo by T. Hainschwang).

VIS-NIR ABSORPTION SPECTRUM

Figure 3. The low-temperature Vis-NIR spectrum of the diamond in figure 1 shows weak absorptions for the H3, NV⁻, and H2 centers, which is an unusual combination for an untreated natural diamond.

tion in two directions along octahedral growth planes, following "olive"-colored graining visible in the stone (figure 2, inset). This colored graining and extinction along the graining are very common features in "olive" diamonds. The order of extinction indicates that the stone is severely deformed and thus not optically isotropic. This is explained by the fact that the dislocations (broken bonds) caused by the deformation interfere with the direct passage of light that would be expected in truly isotropic materials. Even though strain associated with linear extinction and/or interference colors can be found to some degree in practically all diamonds, strong parallel extinction in a colored diamond provides a good indication for deformation-related coloration. Regardless of whether their green coloration is hydrogen- or radiation-related, "olive" diamonds seldom
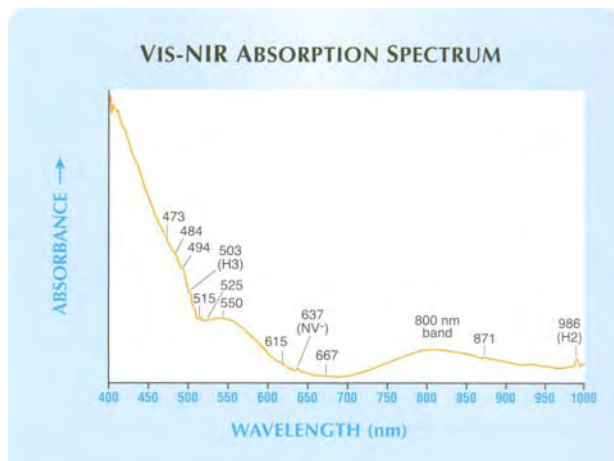
exhibit the strong strain pattern described here.

These observations prompted further analysis of the sample. A low-temperature spectrum was recorded in the visible/near-infrared range, which added to the unusual assemblage of absorption centers found in this diamond. The spectrum exhibited a combination of weak H3 (503 nm), NV⁻ (637 nm), and H2 (986 nm) absorptions with associated structures, plus moderate broad bands at about 550 and 800 nm (figure 3). The H3, NV⁻, and H2 absorption centers are typical of the visible-NIR spectra of HPHT-treated type Ia diamonds (A. T. Collins et al., "Colour changes produced in natural brown diamonds by high-pressure, high-temperature treatment," *Diamond and Related Materials*, Vol. 9, 2000, pp. 113–122), and also can be created in type Ia or Ib diamonds through irradiation followed by annealing (A. M. Zaitsev, *Optical Properties of Diamond: A Data Handbook*, Springer-Verlag, Berlin, 2001, pp. 136–137), although these features typically are moderate to strong in treated-color diamonds.

Despite this correlation, other features indicated unambiguously that the diamond had not been treated by either method, and was indeed natural color. HPHT treatment of a brown-to-olive type Ib diamond, even at very moderate temperatures, would aggregate much of the single nitrogen and destroy the amber center (T. Hainschwang et al., "HPHT treatment of different classes of type I brown diamonds," *Journal of Gemmology*, Vol. 29, 2004 [in press]; A. N. Katrusha et al., "Application of high-pressure high-temperature treatment to manipulate the defect-impurity content of natural diamond single crystals," *Journal of Superhard Materials*, No. 3, 2004, pp. 47–54). Besides the temperature/pressure conditions, the aggregation is influenced by the total nitrogen content and the types of defects present. The combination of factors in

this diamond would enhance nitrogen aggregation under commonly used HPHT conditions. In addition, irradiation of a type Ib diamond followed by annealing would create a very distinct NV⁻ absorption, resulting in pink to purple coloration (E. Bienemann-Küespert et al., *Gmelins Handbuch der Anorganischen Chemie*, Verlag Chemie, Weinheim, Germany, 1967, p. 237). Radiation treatment would also leave other traces, such as the 595 nm and the H1a and possibly H1b absorptions, which were not detected in this diamond.

The authors have recently seen the H2 center in a suite of very rare type Ib diamonds containing large concentrations of single-nitrogen that may exceed 400 ppm. These stones showed no deformation-related features and were distinctly different from the stone reported here. In contrast to these high-nitrogen type Ib diamonds, this is the first type Ib "H2 diamond" we have seen that shows a combination of H3, NV⁻, and H2 centers with classic strain patterns between crossed polarizers and a very low nitrogen concentration. The properties observed for this diamond are, at this point, difficult to explain. The deformation pattern and color distribution indicate octahedral growth and dynamic post-formation conditions. Besides the strong post-growth deformation and associated defects (dislocations, vacancies, and interstitials), the observed features suggest prolonged natural annealing at a low enough temperature to avoid aggregation of the single nitrogen, but nevertheless resulting in the combination of defects noted.

Thomas Hainschwang (gemlab@adon.li)
Gemlab Gemological Laboratory
Vaduz, Liechtenstein

Franck Notari
GemTechLab Laboratory
Geneva, Switzerland

COLORED STONES AND ORGANIC MATERIALS

Gem amphiboles from Afghanistan, Pakistan, and Myanmar. The amphibole group consists of several common rock-forming minerals, as well as many unusual species. Examples that are best known to gemologists are tremolite and actinolite, which as fine-grained aggregates form nephrite. Like most amphiboles, these are opaque, or translucent at best. In the past few years, however, some unusual transparent amphiboles from three localities in Asia have been faceted. These include light yellow richterite from Afghanistan, green pargasite from Pakistan, and brown pargasite and near-colorless edenite from Myanmar. One of these contributors (DB) has obtained facet-quality examples of all these amphiboles from local dealers in Peshawar (Pakistan) and Mogok (Myanmar), and also recently visited one of the deposits.

The Afghanistan richterite was first seen in the Peshawar mineral market in October 2001. The material was sold with sodalite and hackmanite crystals, often

Figure 4. Beginning in late 2001, facet-quality richterite has been recovered from the vicinity of Afghanistan's lapis lazuli deposits. The crystal shown here is 1.9 cm tall, and the oval brilliant weighs 1.72 ct. Courtesy of Dudley Blauwet Gems; photo © Jeff Scovil.

associated on the same specimen. The source was reported to be in the vicinity (i.e., an approximately six- to eight-hours' walk) of the Sar-e-Sang lapis lazuli deposits, which are located in the Kokcha Valley, Badakhshan Province. During 2002, DB saw at least 5 kg of rough material, including some attractive crystals (figure 4); about 20% was facet grade. However, due to the mineral's perfect cleavage, very few stones have been cut. The largest richterite cut by DB weighed 1.86 ct; attempts to cut larger stones have been unsuccessful.

The Pakistan pargasite appeared on the mineral market in the mid-1990s, typically as broken crystals embedded in a marble matrix. Similar material from China was described in the Spring 2002 Gem News International section (p. 97). Due to its attractive green color (figure 5), the Pakistan pargasite is sometimes referred to as "Hunza emerald" by local dealers. DB visited the mining area in November 2003. It is located about 3 km east of the Karakoram Highway bridge that crosses the Hunza River near Ganesh in the Hunza region. The pargasite is found within marble boulders that contain small seams of phlogopite. In addition to the green pargasite, the area has yielded translucent-to-opaque red, pink, and purple-blue corundum (to 7.5 cm) and "maroon," blue, dark brown, and black spinel (to 2.5 cm). Pargasite crystals up to almost 3 cm have been found, sometimes associated with the

dark brown spinel, but transparent material is very rare, yielding faceted stones of less than 1 ct.

The two transparent amphibole species from Myanmar (figures 6 and 7) were purchased by DB in Mandalay in June 2002. The vendor, a geology student from a university in Yangon, reported that both the pargasite and edenite were mined from the well-known Mogok deposit of Ohn Bin. Only a few pieces were available, although several more samples of both minerals turned up in 2003. The largest pargasite and edenite cut by DB weighed 1.78 ct and 0.29 ct, respectively (again, see figures 6 and 7).

To positively identify the specific amphibole species present, one of us (FCH) analyzed the faceted stones pictured in figures 4–7 by electron microprobe. Also analyzed was one additional sample of brown pargasite from Myanmar. Approximately 10 point analyses were obtained from each sample, and their averages were used to calculate the formulas listed in table 1. The mineralogical classification within the amphibole group of each stone was then established using the conventions published by B. E. Leake et al. ("Nomenclature of amphiboles: Report of the subcommittee on amphiboles of the International Mineralogical Association, Commission on New Minerals and Mineral Names," *Canadian Mineralogist*, Vol. 35, 1997, pp. 219–246). All the amphiboles contained relatively high amounts of fluorine. The analyses also revealed that the green pargasite from Pakistan contains traces of vanadium; up to 1.3 wt.% V_2O_3 was reported in similar material by V. M. F. Hammer et al. ("Neu: Grüner Pargasit aus Pakistan," *Lapis*, Vol. 24, No. 10, 1999, p. 41).

Gemological properties were obtained on the same four samples (by SM and EPQ) using standard testing equipment and a gemological microscope; the data are summarized in table 1. The properties of each stone fell within the ranges reported for these amphibole varieties in mineralogical textbooks (see, e.g., W. D. Nesse, *Introduction to Mineralogy*, Oxford University Press, New York, 1991, pp. 277–290). The relatively low R.I. values of the richterite are consistent with its Mg-rich composition (i.e., lacking iron); its properties may overlap those of colorless tremolite. The properties of the pargasites and the edenite also are consistent with the literature—that is, with values reported for hornblende. Material referred to as "hornblende" also includes other closely related species of the amphibole group; because their physical properties may overlap, conclusive identification of these species requires quantitative chemical analysis.

Dudley Blauwet (mtnmin@attglobal.net)
Dudley Blauwet Gems
Louisville, Colorado

Frank C. Hawthorne
University of Manitoba
Winnipeg, Manitoba, Canada

Sam Muhlmeister and Elizabeth P. Quinn
GIA Gem Laboratory, Carlsbad

Figure 5. This vivid green pargasite from Pakistan is colored by vanadium. The specimen is 2.1 cm tall, and the oval brilliant weighs 0.59 ct. Courtesy of Dudley Blauwet Gems; photo © Jeff Scovil.

Figure 6. Transparent yellowish brown pargasite was recently found in Myanmar. The crystal is 1.5 cm tall, and the faceted stone weighs 1.78 ct. Courtesy of Dudley Blauwet Gems; photo © Jeff Scovil.

Figure 7. Myanmar is also the source of facetable edenite, as shown by this 1.4-cm-wide crystal and 0.29 ct round brilliant. Courtesy of Dudley Blauwet Gems; photo © Jeff Scovil.

Recent gem beryl production in Finland. In 1982, a shard of transparent colorless topaz was found at a road construction site near Luumäki in southern Finland. Subsequently, local mineral enthusiasts and gem cutters staked a claim to the source of this stone, a granitic pegmatite running parallel to the road, and initial mining resulted in the discovery of at least one gem beryl pocket.

This deposit subsequently produced some significant crystals and gem material (see S. I. Lahti and K. A. Kinnunen, "A new gem beryl locality: Luumäki, Finland,"

Spring 1993 *Gems & Gemology*, pp. 30–37). The pegmatite was mined until 1995, during the summer seasons. Although several pockets were found in areas adjacent to quartz core zones, none of them contained any beryl mineralization. Indeed, the distribution of the beryl in the pegmatite proved to be quite sporadic.

In the past three years, renewed work at this deposit (now known as the Karelia Beryl mine; figure 8) by a newly formed mining company has yielded some additional production, which recently included what many believe are some of the finest and largest green gem beryls ever found in western Europe (figure 9). This contributor had an opportunity to witness the removal of some of this material during a May 2004 visit to the deposit, which is situated on a small island in one of the 70,000 Finnish lakes. The exact location is Kännätsalo (Finnish for drunken forest), Kivijärvi (Stone Lake), Luumäki, Karelia, Finland.

The new gem beryl pocket had a vertical orientation and measured approximately 2 ∞1.5 ∞4 m. The location of this large cavity in the pegmatite was unusual, in that it was found only 20–40 cm from the hanging wall. The pocket contained two layers of large gem beryls, one near the top and the other about 30 cm from the bottom. Between these layers were found broken translucent beryl crystals (up to 10–15 cm in diameter) of cabochon and carving quality; some areas showed chatoyancy. The beryl in this pocket ranged from light yellow to deep "golden" yellow, and from green-yellow to green.

Most of the gem beryl was found within 10–25 cm of the cavity walls, together with crystals of mica (typically 5–15 cm) and albite (1–8 cm), as well as pocket rubble consisting of broken shards of microcline and, rarely, quartz. A total of more than 110 kg of beryl was produced, with about 30 kg being suitable for faceting. Most of the fac-

TABLE 1. Characteristics of gem amphiboles from Afghanistan, Pakistan, and Myanmar.[a]

Name	Locality	Weight (ct)	Color	R.I.	Birefringence	S.G.	Fluorescence		Internal features[b]
							Long-wave UV	Short-wave UV	
Richterite	Afghanistan	1.72	Light brownish yellow	1.599–1.622	0.023	3.11	Weak orange	Weak yellowish orange	Cavities, fractures, two-phase inclusions
Pargasite	Pakistan	0.59	Yellowish green	1.625–1.640	0.015	3.03	Inert	Very weak yellowish green	Numerous fractures (some along cleavage directions), needles, two-phase inclusions
Pargasite	Myanmar	1.78	Yellowish brown	1.620–1.640	0.020	3.17	Inert	Weak yellow	Numerous three-phase inclusions (some with tension fractures), two-phase inclusions, needles, fractures
Edenite	Myanmar	0.29	Near colorless (very light yellow)	1.612–1.631	0.019	3.14	Inert	Weak yellow	Needles, fractures, three-phase inclusions (some with tension fractures), two-phase inclusions

[a] *None of the samples showed any phosphorescence or any absorption features with a desk-model spectroscope.*

[b] *Microscopy also revealed evidence of clarity enhancement in the 0.59, 1.72, and 1.78 ct samples.*

[c] *Electron microprobe analysis of an additional sample (a grain mounted in epoxy) of yellowish greenish brown potassian fluorian pargasite from Mogok yielded the formula $(Na_{0.58}K_{0.39})Ca_{2.00}(Mg_{3.90}Fe_{0.05}Cr_{0.01}Ti_{0.13}Al_{0.80})(Si_{5.84}Al_{2.16})O_{22}(OH)_{1.13}F_{0.87}$.*

Figure 8. Mining activities have resumed at the gem beryl pegmatite near Luumäki, Finland. Heavy machinery is used to reach the gem-bearing zones, which are then carefully mined by hand to avoid damaging the crystals. Photo by P. Lyckberg.

etable material was found as small (1–3 cm) fragments (figure 10), but some pieces reached 5–8 cm. About 10 kg comprised "flawless" material with no eye-visible inclusions, and in exceptional cases these crystals exceeded 1 kg each. These large stones are of a fine green to yellowish green color, and are rather distinct from the better-known Ukrainian material in terms of both color and morphology. The Finnish crystals are typically etched and striated (but have retained their hexagonal shape), and their terminations are rounded (as pictured by Lahti and Kinnunen,

Chemical composition[c]	Classification
$(Na_{0.60}K_{0.32})(Ca_{1.14}Na_{0.85}Mg_{0.01})(Mg_{4.90}Al_{0.10})$ $(Si_{7.83}Al_{0.17})O_{22}(OH)_{1.59}F_{0.41}$	Potassian fluorian richterite
$(Na_{0.85}K_{0.07})Ca_{2.00}(Mg_{4.18}V_{0.21}Al_{0.61})(Si_{6.25}Al_{1.75})$ $O_{22}(OH)_{1.57}F_{0.43}$	Fluorian vanadian pargasite
$(Na_{0.52}K_{0.43})(Ca_{1.95}Na_{0.03}Fe_{0.02})$ $(Mg_{3.97}Fe_{0.07}Ti_{0.08}Al_{0.88})(Si_{6.05}Al_{1.95})O_{22}$ $(OH)_{1.29}F_{0.71}$	Potassian fluorian pargasite
$(Na_{0.87}K_{0.09})(Ca_{1.80}Na_{0.15}Fe_{0.03}Mg_{0.02})$ $(Mg_{4.45}Ti_{0.01}Al_{0.54})(Si_{6.62}Al_{1.38})O_{22}(OH)_{1.54}F_{0.46}$	Fluorian edenite

Figure 9. In May 2004, several world-class crystals of green gem beryl—some exceeding 1 kg, as shown here—were recovered at the Luumäki pegmatite. Photo by P. Lyckberg.

Figure 10. Most of the Luumäki gem beryl from the May 2004 pocket consisted of relatively small fragments. The inset shows a green beryl weighing approximately 15 ct that was cut in Finland. Photos by P. Lyckberg.

1993). Although it would be possible to cut stones weighing several thousand carats from the largest fine gem crystals, these crystals have been sold as specimens to collectors to preserve their natural beauty.

When present, inclusions in the beryl are similar to those described by Lahti and Kinnunen (1993). For example, a 3 cm golden yellow heliodor studied by this contributor had dozens of parallel channels/tubes along the c-axis, and these were filled by rust-colored clay minerals. None of the beryl was found to contain the clouds of minute inclusions that are typical of Ukrainian beryl.

Approximately 100 large stones (25–50 ct) from the recent production have been cut by Finnish master faceter Reimo Armas Römkä. Most of them are light yellow and some are yellowish green. In addition, about 11,000 round brilliants (10 mm in diameter) have been cut in China. Most of the cut stones are sold into the domestic Finland market.

The 2004 mining season will continue until the severe winter halts activities for the following six months.

Peter Lyckberg (lyckberg@pt.lu)
Luxembourg

Hessonite from Afghanistan. Over the past few years, Afghanistan has become a significant source of gem-quality hessonite (grossular garnet), and some of the material has been found mixed into parcels with other orange to red stones from this region (see Summer 2001 Gem News International, p. 144). To our knowledge, the gemological properties of the Afghan hessonite have not been published, so we were interested to examine several faceted samples and mineral specimens that were recently loaned (and, in some cases, donated) to GIA by Sir-Faraz ("Farooq") Hashmi of Intimate Gems, Jamaica, New York. In addition, Peter Lyckberg loaned six faceted examples for our examination. Mr. Hashmi reported that the hessonite comes from eastern Afghanistan; two known deposits are Munjagal in Kunar Province (producing roughly 1,500–2,000 kg/year of mixed grade) and Kantiwow, Nuristan Province (up to 5,000 kg/year). Most of the clean rough weighs 0.5–1 gram, in colors ranging from yellowish orange to red-orange. Although thousands of kilograms of this garnet have been produced, mining has waned in recent months due to lack of demand in the local market (i.e., in Peshawar, Pakistan) and the migration of miners to the kunzite deposits in the same region of Afghanistan.

The specimens we examined consisted of euhedral garnets that were commonly intergrown with anhedral massive quartz. This assemblage formed within massive garnet that was intergrown with quartz and, less commonly, a green mineral (probably epidote) and another white mineral (possibly wollastonite). This mineral association is typical of a skarn-type deposit formed by contact metamorphism of carbonate rocks by a granitic intrusion. The euhedral grossular crystals typically measured up to 1 cm in diameter, although some partial crystals of larger dimension (up to 4 cm) also were present. The crystals contained abundant fractures, but some had small areas that were transparent enough for faceting.

Figure 11. Afghanistan has produced attractive hessonite over the past few years. These stones, weighing 2.64, 7.39, and 3.51 ct (from left to right), show the range of color that is commonly encountered in this material. Courtesy of Intimate Gems; photo by Maha Tannous.

Three representative faceted stones (2.64–7.39 ct; figure 11) were selected for examination by one of us (EPQ), and the following properties were obtained: color—yellowish orange, orange, and red-orange; diaphaneity—transparent, R.I.—1.739 or 1.740; S.G.—3.63 or 3.64; weak to moderate ADR in the polariscope; and inert to both long- and short-wave UV radiation. Weak absorption bands at 430 and 490 nm were observed with a desk-model spectroscope. Microscopic examination revealed transparent near-color-less crystals (one of which was identified as apatite by Raman analysis), needles, "fingerprints," stringers of parti-cles, fractures, and straight and angular growth lines. One stone showed evidence of clarity enhancement. The R.I. values of these samples are slightly lower than those reported in the literature for hessonite (see R. Webster, *Gems*, 5th ed., rev. by P. G. Read, Butterworth-Heinemann, Oxford, 1994, pp. 201–202). Notably, the three Afghan samples did not show the roiled or oily appearance that is commonly seen in hessonite; nor was this feature noted upon further examination of several additional faceted stones.

BML

Elizabeth P. Quinn
GIA Gem Trade Laboratory, Carlsbad

Interesting abalone pearls. In the Winter 2003 Gem News International section (pp. 332–334), this contributor reported on some interesting pearls that had been loaned by Jeremy Norris of Oasis Pearl in Albion, California. Two of those were unusual specimens from the green abalone *Haliotis fulgens* and the red abalone *H. rufescens*. Mr. Norris recently loaned GIA two additional abalone pearls from the waters off Baja California, Mexico.

One of these pearls was an exceptional example of a

Figure 12. Showing a beautiful array of colors, this 4.90 ct abalone pearl is an exceptional example from the pink abalone H. corrugata. *Courtesy of Jeremy Norris; photo by C. D. Mengason.*

pearl from the pink abalone *H. corrugata*. This 4.90 ct light-toned pearl (11.4 ∞ 8.9 ∞ 6.9 mm) displayed a stun-ning array of colors (figure 12).

The other pearl was a 41.03 ct horn-shaped specimen (36.6 ∞ 23.0 ∞ 14.5 mm) from *H. fulgens*. What was so unusual about this particular pearl was its remarkable resemblance to an eagle's head, complete with eye, brow, and beak structures (figure 13). Such horn shapes—a form typically exhibited by abalone pearls—may be solid, but often they are hollow. This particular specimen was fun-nel shaped, with the narrow end of the hole forming the apparent "eye." The nacre displayed vibrant hues of blue,

Figure 13. This unusual 41.03 ct pearl from the green abalone H. fulgens *has a remarkable resemblance to an eagle's head (left). The funnel-shaped hole, which starts at the wide opening at the back of the "head," and exits out the eagle's "eye," exhibits the same smooth vibrant nacre as the outside of the pearl (right, looking down the wide opening). Courtesy of Jeremy Norris; photos by C. D. Mengason.*
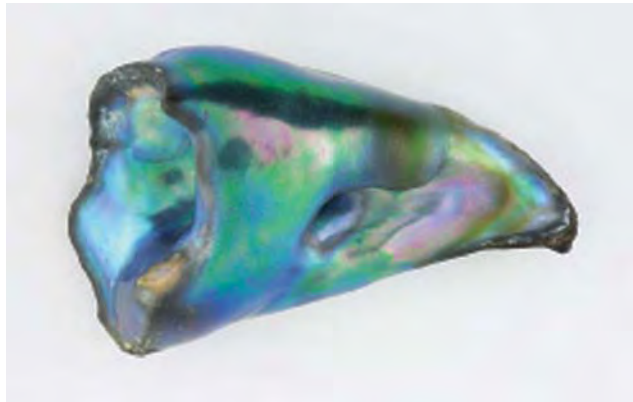
green, and purple-pink, even in the interior (again, see figure 13). For the nacre to have formed so evenly on the inside surfaces of the pearl, Mr. Norris stated that the abalone's nacre-secreting tissue must have passed all the way through the pearl, so that the pearl completely encircled part of the gastropod's anatomy, and in essence entrapped its host. This pearl has wonderful potential for a jewelry designer who could incorporate the bird-like image into a one-of-a-kind creation.

Cheryl Y. Wentzell (cwentzell@gia.edu)
GIA Gem Laboratory, Carlsbad

Rhodonite of facet and cabochon quality from Brazil.
Rhodonite typically occurs as a translucent-to-opaque ornamental stone with an attractive pink color. Trans-

Figure 15. The Brazilian rhodonite samples examined for this study consisted of an oval modified brilliant (1.77 ct) and an oval cabochon (8.55 ct). Courtesy of Joseph Rott; photo by Maha Tannous.

Figure 14. A new find of rhodonite from Minas Gerais, Brazil, has yielded facet- and cabochon-quality material. The faceted stones weigh 1.84 and 8.22 ct, and the cabochons are 9.98 and 32.0 ct. Courtesy of Alan Freidman, Beverly Hills, California; photo © Harold & Erica Van Pelt.

parent facetable material has so far been very rare and has been reported only from Broken Hill, New South Wales, Australia, where it is frequently associated with the closely related mineral pyroxmangite (see H. Bank et al., "Durchsichtiger rötlicher Pyroxmangit aus Broken Hill/Australien und die Möglichkeiten seiner Unterscheidung von Rhodonit [Transparent reddish pyroxmangite from Broken Hill/Australia and the criteria for distinguishing it from rhodonite]," *Zeitschrift der Deutschen Gemmologischen Gesellschaft*, Vol. 22, No. 3, 1973, pp. 104-110). Recently, however, transparent-to-semi-transparent rhodonite also has been found in Minas Gerais, Brazil.

During the February 2004 Tucson gem shows, Joseph Rott (of Tropical Imports, formerly based in New York and now located in Grand Island, Nebraska) showed one of these contributors (BML) some attractive rough and cut examples of Brazilian rhodonite. He said that the material comes from the same region in Minas Gerais that historically has been mined for manganese (see, e.g., F. R. M. Pires, "Manganese mineral paragenesis at the Lafaiete District, Minas Gerais," *Anais da Academia Brasileira de Ciencias*, Vol. 54, No. 2, 1982, p. 463). He also indicated that the deposit contains both rhodonite and pyroxmangite. Although these minerals can be visually indistinguishable and may be intergrown within the same piece, he reported that only minor amounts (if any) of pyroxmangite are known to be present in the gem material from this deposit. Most of the faceted rhodonites are between 1 and 5 ct, although larger gems have been cut; cabochons typically range from 5 to 10 ct (figure 14).

Mr. Rott loaned several rough and cut samples to GIA for examination. Two polished stones were examined by one of us (EPQ), a transparent oval modified brilliant (1.77 ct) and a semi-transparent oval double cabochon (8.55 ct), as illustrated in figure 15. The following properties were recorded: color—orangy red, with moderate pinkish orange and purplish pink pleochroism; R.I.—1.720–1.733 (faceted stone) and 1.73 (spot reading on the cabochon); birefringence—0.013; S.G.—3.69 and 3.66, respectively; and fluo-

Figure 16. The 2.67 ct Brazilian rhodonite in this pendant is set with 111 yellow and 25 pink diamonds (with a total weight of 0.48 and 0.12 carats, respectively). Courtesy of Alan Freidman; photo © Harold and Erica Van Pelt.

As with the Australian material, the main challenge with cutting the Brazilian rhodonite is its perfect cleavage in two directions. This, combined with a Mohs hardness of $5^1/_2–6^1/_2$ and the fact that limited transparent material is available for faceting, means that it will remain a collector's stone. Nevertheless, the availability of even a small amount of faceting-quality rhodonite from the Brazilian source has created interesting opportunities for setting the material into jewelry (figure 16).

Elizabeth P. Quinn (equinn@gia.edu)
GIA Gem Laboratory, Carlsbad

BML

Spessartine and almandine-spessartine from Afghanistan. Beginning in mid-2002, these contributors received occasional reports of new spessartine discoveries in Afghanistan, and a few faceted stones stated to be from this production were seen at the Tucson gem shows in 2003 and 2004. Recently, a multitude of rough and cut samples of this material were loaned (and, in some cases, donated) to GIA by Sir-Faraz ("Farooq") Hashmi of Intimate Gems. Most of these samples were purchased in late 2003, in the mineral bazaar at Peshawar, Pakistan. The dealers reported the garnets were mined from pegmatites in the Darre Pech area of Kunar Province, where they were apparently recovered as a byproduct of mining for kunzite and tourmaline.

The rough material we examined (see, e.g., figure 17) consisted of a 385-gram parcel of loose pieces and two

rescence—inert to very weak red to both long- and short-wave UV radiation. The following absorption bands were observed with the desk-model spectroscope: a strong band at 410 nm, weak lines at 430 and 460 nm, a moderate line at 500 nm, and a wide band at 520–560 nm. Microscopic examination revealed numerous randomly oriented curved needles, cleavage cracks, "fingerprints," and two-phase inclusions in both samples, as well as some transparent brown-yellow euhedral crystals in the cabochon.

The gemological properties are comparable to those reported for rhodonite in the literature (see e.g., R. Webster, *Gems*, 5th ed., rev. by P. G. Read, Butterworth-Heinemann, Oxford, 1994, p. 365). Although some of the properties of rhodonite and pyroxmangite overlap, the relatively low R.I.'s and birefringence of the two samples we examined are indicative of rhodonite. Also, Raman analysis of two spots on the cabochon and one spot on the faceted stone yielded spectra that more closely matched rhodonite than pyroxmangite. EDXRF analyses of the two samples by GIA Gem Laboratory senior research associate Sam Muhlmeister showed major amounts of Si and Mn, as well as traces of Fe and Ca (and possibly Zn in the faceted stone).

Figure 17. Since mid-2002, increasing amounts of spessartine (and some almandine-spessartine) have emerged from Afghanistan. The spessartine in matrix measures at least 3 cm in diameter, and the loose crystals weigh 3.59–15.47 ct. Courtesy of Intimate Gems; photo by Maha Tannous.

Figure 18. This group of yellow-orange to orange spessartines from Afghanistan ranges from 0.78 to 1.68 ct. Courtesy of Intimate Gems; photo by Maha Tannous.

Figure 19. This group of orange-red to dark red almandine-spessartines (0.41–1.28 ct) is reportedly from the same mining area as the orange spessartines in figure 18. Courtesy of Intimate Gems; photo by Maha Tannous.

matrix specimens. One of the specimens was a small crystal of kunzite (2.6 cm long) associated with spessartine and feldspar, while the other consisted of spessartine in a matrix of albite (cleavelandite variety) and K-feldspar that was covered by a thin layer of a porcelaneous clay-like material (again, see figure 17). The spessartine crystal in the latter specimen measured at least 3 cm in diameter, with some areas suitable for faceting. The rough parcel consisted of broken fragments and a few well-formed crystals, as well as pieces that were moderately to heavily corroded (as is typical of spessartine from some pegmatites).

Figure 20. At 12.58 ct, this oval brilliant provides a fine example of a relatively large spessartine from Afghanistan. Courtesy of Mark Kaufman of Kaufman Enterprises, San Diego, California; photo by Maha Tannous.

The faceted examples we examined comprised two distinct color groups. Each group was cut from rough purchased at different times, but represented as being from the same mining area. One group ranged from yellow-orange to orange (figure 18), and the other ranged from orange-red to dark red (figure 19). Two stones from each color group were chosen by one of us (EPQ) for examination. The following properties were obtained: R.I.—1.799 (yellow-orange), 1.802 (orange), and both red stones were above the limits of a standard refractometer; S.G.—4.26 (yellow-orange), 4.28 (orange), and 4.22 (orange-red), and 4.24 (red); fluorescence—all were inert to both long- and short-wave UV radiation; and all had similar absorption spectra when viewed with a desk-model spectroscope. The absorption features consisted of strong bands at 410 and 430 (although these two bands converged in the red stones, creating a cutoff at 440 nm), with weaker bands at 460, 480, 505, 520, and 570 nm. In the two red stones, the 505 and 570 nm bands were more pronounced than they were in the orange stones. This is consistent with their greater inferred iron content, as indicated by their darker and redder color. Based on these properties, the orange-red to dark red garnets are probably a mixture of spessartine and almandine.

Microscopic examination revealed "fingerprints," two-phase inclusions, and needles in all four of the samples. The properties of the yellow-orange to orange stones are comparable to those reported for spessartine from other deposits (see compilation in B. M. Laurs and K. Knox, "Spessartine garnet from Ramona, San Diego County, California," Winter 2001 *Gems & Gemology*, pp. 278–295), except for the higher S.G. values obtained for the Afghan samples in this study.

According to Mr. Hashmi, most of the facetable rough seen thus far in the Peshawar market has weighed less than 2 g, although some 3–5 g pieces were available and the largest clean rough known to him weighed 15 g (a

well-formed crystal). The faceted material has typically ranged up to 2 ct, although a 12.58 ct oval brilliant reportedly from this locality was seen at the 2003 Tucson gem shows (figure 20).

Curiously, faceted examples of this spessartine look very similar to the hessonite that also has come from eastern Afghanistan in recent years (see entry on pp. 258–259 of this section). In fact, Mr. Hashmi cautioned that some rough parcels he has examined contained both types of garnets.

Elizabeth P. Quinn
GIA Gem Laboratory, Carlsbad

BML

Gem tourmaline from Congo. Africa has long been an important source of gem tourmaline; of particular interest are the countries of Nigeria, Namibia, Zambia, and Mozambique. In recent years, however, the Democratic Republic of the Congo (DRC, formerly known as Zaire) has occasionally yielded attractive gem rough and collector-quality crystals. While information on the exact sources in the DRC was not available to these contributors, the appearance and composition of these tourmalines indicates they are derived from granitic pegmatites.

The Central African pegmatite province includes numerous pegmatite fields in a broad region encompassing Uganda, Rwanda, Burundi, the eastern DRC, northern Zambia, western Kenya, and western Tanzania. Most of these pegmatites are categorized in the rare-metal class and are associated with Early Proterozoic granites (800–1,000 million years old; V. Ye. Zagorsky et al., *Miarolitic Pegmatites*, in Vol. 3 of B. M. Shmakin and V. M. Makagon, Eds., *Granitic Pegmatites*, Nauka, Siberian Publishing Firm RAS, Novosibirsk, Russia, 1999 [in Russian]). In the eastern DRC, the pegmatites are located in the Nord-Kivu, Sud-Kivu, and Katanga provinces (N. Varalamoff, "Central and West African rare-metal granitic pegmatites, related aplites, quartz veins and mineral deposits," *Mineralium Deposita*, Vol. 7, 1972, pp. 202–216). These deposits have been mined for decades for cassiterite (Sn) and industrial beryl (Be), but miarolitic pegmatites that host gem-quality tourmaline, beryl, and other minerals are apparently uncommon in the DRC.

In mid-2000, gem dealer John Patrick (El Sobrante, California) obtained about 200 g of variously colored DRC tourmaline through an African supplier. The supplier indicated the material came from the Virunga region north of Goma (Nord-Kivu Province). Mr. Patrick donated three green/pink crystals (2.5–4.0 cm long) and five multicolored slabs (1.5–2.9 cm wide) to GIA for research purposes. The slabs had irregular outlines and were concentrically zoned around the c-axis in pink and green; one sample had a blue core. All of these samples were semitransparent due to fluid inclusions and fissures, as are typically seen in tourmaline.

Figure 21. Transparent tourmalines, for the most part green to blue, recently have been recovered from the Democratic Republic of the Congo. These crystals, up to 4 cm long, are courtesy of New Era Gems; photo by Maha Tannous.

More recently, an undisclosed locality in the DRC has yielded transparent prisms of mostly green-to-blue tourmaline (figure 21). Steve Ulatowski (New Era Gems, Grass Valley, California) first obtained this material in mid-2003, and he estimates that about 20–30 kg/month were produced in early 2004. Since then, however, production appears to have diminished. Mr. Ulatowski purchased about 3 kg of the rough, of which 30% was facetable (see, e.g., figure 22), 60% was cabochon grade, and 10% was bead quality. The largest clean piece of gem rough he acquired weighed approximately 30 grams, although stones faceted from the

Figure 22. These tourmalines (5.78 and 15.94 ct) were cut from material similar to that in figure 21. These stones were faceted by Thomas Trozzo (Culpeper, Virginia). Photo by C. D. Mengason.

Figure 23. Heating experiments were conducted on the bottom portions of these four crystals of DRC tourmaline, while the top untreated portions were retained for comparison. All samples were heated in air as follows (from left to right, with weight of original crystal in parentheses): 427°C over a period of 5 hours (31.61 ct), 482°C over 6 hours (34.84 ct), 566°C over 8 hours (19.11 ct), and 621°C over 9 hours (19.89 ct). No appreciable change in the green-to-blue colors was seen in any of the heated portions, but abundant microcracks significantly reduced their transparency. Donated to GIA collection (nos. 30834–30837) by New Era Gems; photo by Maha Tannous.

Figure 25. The attractive color zoning shown by these DRC tourmalines (up to 3.6 cm long) ranges from pink to greenish yellow to yellowish green at the pyramidal terminations. Courtesy of William Larson; photo by Maha Tannous.

prismatic crystals typically weighed 3–5 ct. A small proportion of the crystals had a slightly waterworn appearance, but most showed no evidence of alluvial transport. Most of the tourmaline was green, although some blue-green, yellow-green, and rare bright pink material also was produced.
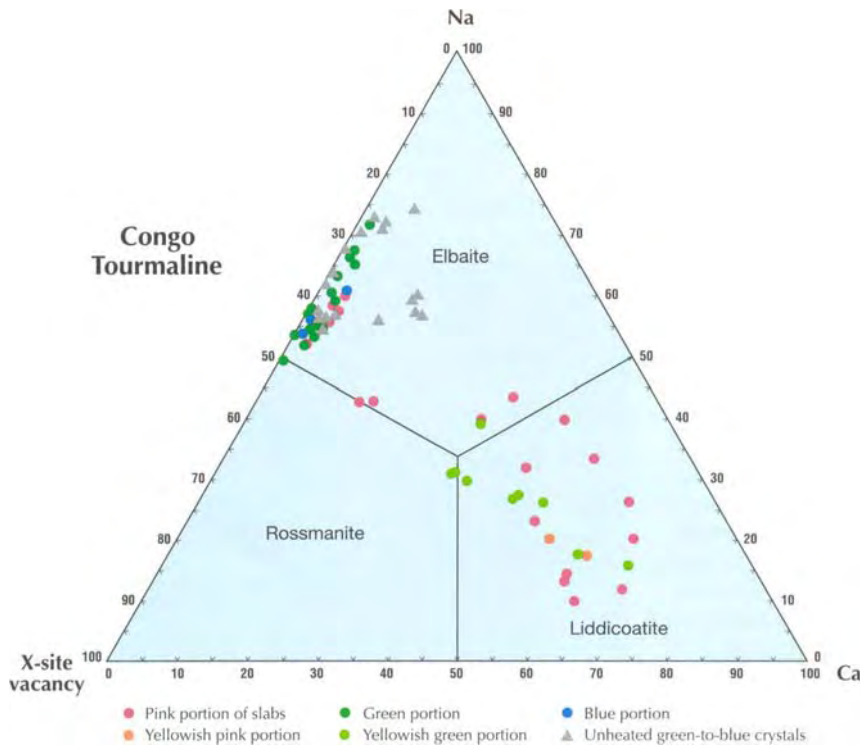
Figure 24. Electron-microprobe analyses of five multicolored slabs and the four green-to-blue tourmalines (before heating) from the DRC showed that they were predominantly elbaite and liddicoatite. In addition, rossmanite was found in two analyses (overlapping) of a yellowish green area, and one each of a pink and a green area of the slabs. These points fall very close to the boundaries with elbaite and liddicoatite and only barely cross into the rossmanite field. The color of each data point roughly approximates the color of the area analyzed. There is no correlation between X-site occupancy and color.

Mr. Ulatowski reported that the overdark gem rough does not respond well to heat treatment. To demonstrate this, he heated portions of four green-to-blue crystals in air at temperatures ranging from 427 to 621°C for 5–9 hours. A comparison to the unheated portions of these crystals revealed no appreciable change in color, as well as diminished transparency of all samples due to abundant microcracks (figure 23).

To investigate the composition of the DRC tourmaline, the five multicolored slabs and eight green-to-blue samples (i.e., the four clipped crystals in figure 23, before and after heating) described above were analyzed by electron microprobe at the University of New Orleans. The slabs were analyzed in core-to-rim traverses of 9–13 points each, and the green-to-blue samples had either core-to-rim or along-rim traverses of 5 points each. Figure 24 shows that most compositions ranged from elbaite to liddicoatite. Of note, however, are four analyses (from green, yellowish green (2), and pink portions of the slabs) that fell just slightly into the rossmanite field. All of the green-to-blue samples consisted of elbaite, whereas the slabs were elbaite ± liddicoatite (with the latter found in two of the five slabs). As expected from our previous analyses of gem tourmaline (see, e.g., Winter 2002 Gem News International, pp. 356–357), there was no relationship between the color and the tourmaline species.

However, significant variations were seen among the chromophoric elements Fe and Mn in the multicolored slabs (see the *G&G* Data Depository at www.gia.edu/gemsandgemology). Traces of vanadium (up to 0.10 wt.% V_2O_3) also were commonly found in the slabs, but Ti was rarely found (up to 0.06 wt.% TiO_2) and no Cr or Bi was detected. The green-to-blue samples likewise had appreciable Fe and Mn, but they had slightly higher traces of Ti and no detectable V, Cr, or Bi.

Another example of attractive Congolese tourmaline, but with much different coloration, is shown in figure 25. These gem-quality prisms are mostly pink, grading into greenish yellow and then yellowish green at their pyramidal terminations. According to William Larson (Pala International, Fallbrook, California), these crystals also were produced in recent years from the DRC. Clearly, they show the potential for the DRC to become a more important source of gem tourmaline in the future.

BML

William "Skip" Simmons and Alexander Falster
University of New Orleans, Louisiana

SYNTHETICS AND SIMULANTS

Dyed horn as an amber imitation. A necklace with 46 rounded beads of a translucent yellow-brown material was sent to the SSEF Swiss Gemmological Institute for identification (figure 26). The 50-cm-long necklace was purchased in Africa, where it was represented as amber.

Figure 26. This necklace of dyed horn beads (20–22 mm in diameter) was sold as amber in Africa. Photo by H. A. Hänni, © SSEF.

However, despite its general resemblance to amber, some of its details were suspicious. A closer look at the surface revealed a peculiar structure and yellow color concentrations (figure 27). Due to the number of beads on the strand and their rough surfaces, it was not possible initially to obtain S.G. or R.I. values. An infrared spectrum taken from a small powder sample was consistent with horn, although our reference spectrum did not indicate the

Figure 27. A closer look at one of the beads in figure 26 shows features inconsistent with amber, although the rough surface made gemological testing difficult. Width of view is approximately 15 mm; photomicrograph by H. A. Hänni, © SSEF.
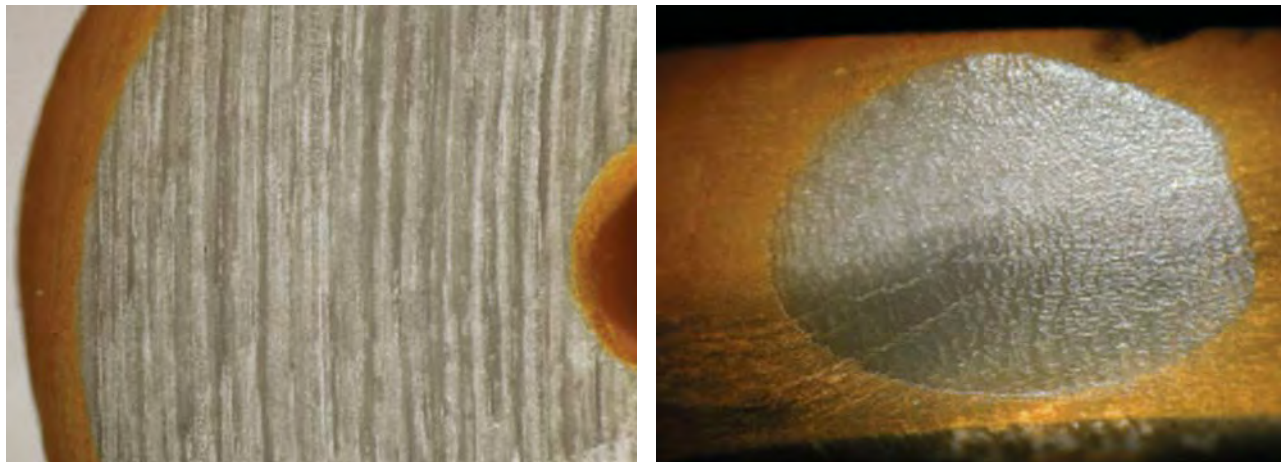
Figure 28. Polished areas of this imitation amber bead show that the structure (both parallel and perpendicular to the "grain") is consistent with horn. The yellow color is clearly restricted to a thin surface layer. In each, width of view is approximately 1 cm; photomicrographs by H. A. Hänni, © SSEF.

species origin (e.g., cow, deer, etc.). The spectrum also provided evidence of a yellow dye.

With the client's permission, we removed one of the beads and polished several areas on the surface to study the growth structure. The S.G. of this bead was measured hydrostatically as 1.27, which is consistent with horn but not amber. R.I. measurements on the polished areas were not possible because of the porosity of the material. A Raman spectrum of the original surface showed clear peaks related to the yellow dye (at 1402, 1434, 1144, 1188, 1609 cm^{-1}, in order of decreasing intensity). The most prominent FTIR peaks were at 1660 and 1540 cm^{-1}. The polished areas showed that the structure of the material was characteristic of horn and the yellow pigmentation was restricted to a thin outer layer (figure 28).

Amber imitations such as this have been described in the past. R. Webster reported that dyed bull horn beads have been marketed as "red amber" in various parts of Africa (*Gems*, 5th ed., rev. by P. G. Read, 1994, p. 597).

HAH

Fake inclusions in quartz, "Made in Brazil." Quartz is well known for its attractive and varied inclusions, and specimens with distinctive inclusions can fetch high prices from collectors. However, this demand also encourages the manufacture of fakes and imitations. Brazil is one of the largest producers of quartz specimens with unusual inclusions, and it is also where this contributor encountered some interesting new faked "inclusions" in July 2004.

Figure 29. These quartz cabochons contained unusual "inclusions" that proved to be manufactured fakes. The largest cabochon is 6 cm long. Photo by J. Hyrsl.

Figure 30. The faked inclusions form interesting patterns, and appear to emanate from areas of naturally occurring mica or chlorite within the quartz. Photo by J. Hyrsl.

The first examples were seen in Governador Valadares, where a local dealer had a parcel of 19 specimens that he had bought for a high price in Teófilo Otoni. All of the specimens were cut as cabochons and contained naturally occurring inclusions of mica or chlorite near their base (figure 29). These cabochons also contained very unusual coral-like features, which appeared to grow from the micaceous inclusions (figure 30). The branches were up to ~30 mm long and 3 mm thick, occurring both singly and in groups. Their color varied, with green, brown, pink, and yellow examples seen; a few even showed multiple colors. In two specimens, it was apparent that small portions of the "branches" were not completely filled by the colored material.

Figure 31. On the base of the cabochon in figure 30, the filled holes were seen to be covered with pieces of feldspar. The glue used to attach the feldspar could be indented by a needle; it fluoresced yellowish green when exposed to UV radiation. Photo by J. Hyrsl.
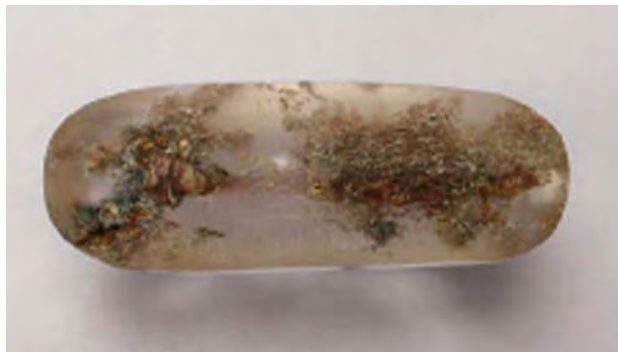
Two days later, when this contributor visited Teófilo Otoni, the mystery surrounding these cabochons was solved. Several colleagues had numerous examples of this material. They were familiar with the person who was fabricating them, and reported that the "branches" were drilled into the cabochons and then filled with a mineral powder, probably mixed with glue, via a syringe. The filled holes were then covered with small pieces of feldspar and quartz mixed with glue, and sometimes "sealed" with a larger piece of feldspar (figure 31).

The glue was soft when poked with a sharp needle, and showed weak yellowish green luminescence to UV radiation (stronger with long-wave UV). The unique shape of the inclusions, sometimes incomplete filling, and especially the presence of glue on the base of the cabochons provide evidence for the artificial origin of these inclusions.

Jaroslav Hyrsl (hyrsl@kuryr.cz)
Kolin, Czech Republic

TREATMENTS

Dyed cultured pearls fading on exposure to heat. Due to the popularity (and expense) of natural-color dark cultured pearls, dyed-color cultured pearls (figure 32) are quite common in the marketplace. Although the risks of dam-

Figure 32. After the pendant in this suite of cultured pearl jewelry was accidentally left on the dashboard of a car during several days of hot weather, it showed noticeable fading when compared to its original color (as represented by the earrings here). The fading of the treated color was likely due to dehydration of the conchiolin and possibly delamination of the nacre. Natural-color black pearls may also fade on exposure to prolonged heat. Photo by Maha Tannous.

aging pearls through harsh cleaning methods are fairly well known (see, e.g., D. D. Martin, "Gemstone durability: Design to display," Summer 1987 *Gems & Gemology*, pp. 63–77), excessive heat can also cause fading.

The cultured pearl jewelry suite in figure 32 was acquired by a GIA staff member during the 2003 Tucson gem shows ("Cultured pearls with diamond insets," Spring 2003 Gem News International, p. 56). During a recent stretch of hot weather in southern California, the pendant was accidentally left on the dashboard of a car for several days. When recovered, the cultured pearl's color displayed noticeable fading.

The pendant was examined by one of these contributors (SE) using EDXRF spectroscopy, which detected the presence of silver in the cultured pearl. This indicates that it had been treated with silver nitrate to create the dark color.

Although K. Nassau (*Gemstone Enhancement*, 2nd ed., Butterworth-Heinemann, London, 1994, pp. 171–172) reported that the color induced through silver nitrate dyeing is "non-fading," exposing any pearl—whether natural or treated color—to prolonged heat (such as that generated inside a closed car) is likely to be detrimental to the color. It would not be surprising for the color to fade due to dehydration of the conchiolin and possibly delamination of the nacre.

This example serves to underscore the fact that all pearls must be treated with care.

Thomas W. Overton (toverton@gia.edu)
GIA, Carlsbad

Shane Elen
GIA Research, Carlsbad

MISCELLANEOUS

Masterpieces of American Jewelry Exhibition. "Jewelry, like all true art, can be a remarkable expression of an entire culture," said Judith Price, president of the National Jewelry Institute (NJI). Her words are beautifully reflected in the NJI's inaugural exhibition, "Masterpieces of American Jewelry," which will be hosted by the American Folk Art Museum in New York City from August 20, 2004 to January 23, 2005. During a tour of the exhibition, this contributor was impressed by the artful displays and overall presentation of the show.

This exhibit, the first museum show to focus exclusively on the jewelry history of the U.S., emphasizes the creativity and artistry of American jewelry from the late 1700s to the 1980s. More than 120 dazzling pieces are displayed, most of which were selected by Ralph Esmerian, curator of this exhibit, vice-chairman of NJI, and chairman of the Folk Art Museum. Included are unique creations that were crafted by American designers, manufactured in American workshops, or retailed by American firms such as Tiffany & Co. and Harry Winston. Also on display are pieces from foreign jewelers such as Cartier,

Van Cleef, and Bulgari, that were designed, manufactured, and distributed in the United States.

The show focuses on five major themes common throughout America's jewelry history: Americana, nature, humor, pastimes, and high style. The Americana section pays tribute to the American spirit, with pieces that depict victories in the War of 1812 or a single American flag. The Nature section showcases 19th-century nature-inspired pieces such as the exotic Tiffany orchid brooches. Disney charm bracelets designed by Cartier, a New York Yankees watch by Hamilton, a sailing ship pin by Marcus & Co., and ballerina brooches by Van Cleef & Arpels (figure 33) are featured in the Humor and Pastimes sections. The High-style exhibit includes photographs of women who distinguished themselves by their personal styles.

Figure 33. Among the highlights of the "Masterpieces of American Jewelry" exhibition is this miniature ballerina brooch (7 × 4 cm) designed in 1940 by Maurice Duvalet for Van Cleef & Arpels, New York. It is set with rubies, emeralds, and diamonds in platinum. Courtesy of Masterpieces of American Jewelry *(by J. Price, Running Press, Philadelphia, 2004).*

On display are Jacqueline Kennedy Onassis' gold cuffs by Van Cleef & Arpels and Joan Crawford's diamond bracelet by Raymond C. Yard.

"Masterpieces of American Jewelry" is truly a masterpiece worth seeing, and the companion book by Judith Price will enthrall readers. For more information, visit www.folkartmuseum.org or e-mail info@folkartmuseum.org.

Siau Fung Yeung (siaufung.yeung@gia.edu)
GIA Gem Laboratory, New York

ANNOUNCEMENTS

G&G beryllium diffusion article wins AGS Liddicoat journalism award. "Beryllium diffusion of ruby and sapphire," published by John Emmett and co-authors in the Summer 2003 *Gems & Gemology*, has received the American Gem Society's Richard T. Liddicoat Journalism Award in the Jewelry Industry/Trade Reporting class. This award was developed in remembrance of GIA Chairman Richard T. Liddicoat to honor journalists who have made exceptional contributions to the understanding of gemology, as well as the ideals of ethics, education, and consumer protection. *Gems & Gemology* previously won the inaugural 2003 Liddicoat Journalism Award in the same category for "Photomicrography for Gemologists" by John I. Koivula in the Spring 2003 issue (see Fall 2003 Gem News International, p. 248).

Visit *Gems & Gemology* in Tucson. Meet the editors and take advantage of special offers on subscriptions and back issues at the *G&G* booth in the Galleria section (middle floor) of the Tucson Convention Center during the AGTA show, February 2–7, 2005.

GIA Education's traveling Extension classes will offer hands-on training in Tucson with "Gem Identification" (January 31–February 4) and "Advanced Gemology" (February 5). To enroll, call 800-421-7250, ext. 4001. Outside the U.S. and Canada, call 760-603-4001.

The GIA Alumni Association will host a Dance Party in Tucson on February 4, featuring a silent auction, an industry awards presentation, and a live auction. To reserve tickets, call 760-603-4204 or e-mail events@gia.edu.

Exhibits

Pearls at the Royal Ontario Museum. "Pearls: A Natural History," a traveling exhibition tracing the natural and cultural history of pearls organized by the American Museum of Natural History (New York) in collaboration with the Field Museum (Chicago), will be on display at the Royal Ontario Museum in Toronto from September 18, 2004 to January 9, 2005. Among the many exhibits will be displays on pearl formation and culturing, as well as historical pearl jewelry that once belonged to Great Britain's Queen Victoria and Marie Antoinette of France. Visit www.rom.on.ca.

Carnegie Gem & Mineral Show. Held November 19–21, 2004, at the Carnegie Museum of Natural History, Pittsburgh, Pennsylvania, this show will feature sapphires in special exhibits and invited museum displays. Visit www.carnegiemuseums.org/cmnh/minerals/gemshow.

Mineralien Hamburg. The International Show for Minerals, Fossils, Precious Stones, and Jewellery will take place in Hamburg, Germany, on December 3–5, 2004. Special exhibitions will feature pearls and carved mineral and gem materials from China. Visit www.hamburg-messe.de/mineralien.

Conferences

Rapaport International Diamond Conference 2004. Held October 12, this conference will take place in New York and feature an insider's look at the international diamond and jewelry industry. Visit www.diamonds.net/conference.

CGA Gemmology Conference 2004. The Canadian Gemmological Association is holding its annual conference at the Terminal City Club in Vancouver on October 22–24. Contact Donna Hawrelko at 604-926-2599 or donnahawrelko@hotmail.com.

Pegmatites at GSA. A topical session titled "Granitic Pegmatites: Recent Advances in Mineralogy, Petrology, and Understanding" will be held at the annual meeting of the Geological Society of America in Denver, Colorado, November 7–10, 2004. The meeting will also feature a session covering advanced mineral characterization techniques. Visit www.geosociety.org/meetings/2004.

Antwerp Diamond Conference. The 3rd Antwerp Diamond Conference, presented by the Antwerp Diamond High Council (HRD), will take place in Antwerp on November 15–16, 2004. The conference will focus on synthetic diamonds as well as on strategies to promote consumer confidence in natural diamond. Visit www.hrd.be.

Diamond Synthesis and History. To commemorate the 50th anniversary of the successful repeatable synthesis of diamond, the H. Tracy Hall Foundation is organizing a one-day symposium on "Diamond Synthesis and History" on December 16, 2004, in Provo, Utah. The conference will focus on high-pressure research and equipment development. Visit www.htracyhall.org/Symposium.htm.

GemmoBasel 2005. The first open gemological conference in Switzerland will be presented by the SSEF Swiss Gemmological Institute at the University of Basel April 29–May 2. Among the events scheduled is a field trip to a Swiss manufacturer of synthetic corundum and cubic zirconia. Visit http://www.gemmobasel2005.org or contact gemlab@ssef.ch.

Book **REVIEWS**

Blood from Stones: The Secret Financial Network of Terror

By Douglas Farah, 225 pp., publ. by Broadway Books, New York, 2004. US$24.95

In 1999, the U.S. government attempted to cut the purse strings of the Taliban and al Qaeda by freezing some $240 million in assets. Forced to look outside the conventional banking system, al Qaeda leaders turned to untraceable commodities they could easily transport and exchange to fund terrorist operations. Were diamonds part of their financial network?

In *Blood from Stones*, investigative reporter Douglas Farah claims that in the late 1990s, al Qaeda began buying up millions of dollars of better-quality rough diamonds in Sierra Leone. In exchange for these "blood diamonds," al Qaeda operatives allegedly paid cash to warlords from the Revolutionary United Front (RUF), a group then in the midst of waging a decade-long civil war in Sierra Leone. Known for its many atrocities, the RUF operated with the backing of former Liberian leader and U.N.-indicted war criminal Charles Taylor. Farah maintains that the diamonds were then smuggled to Antwerp, where they entered the supply chain. The arrangement armed the RUF and added to Taylor's personal fortune, and in return al Qaeda was given a secret source of funding. According to Farah, the Lebanon-based Hezbollah organization had made similar inroads into Sierra Leone's diamond trade in the early 1980s.

Farah, the former West African bureau chief for the *Washington Post*, says he "stumbled on" the diamond trail shortly after the September 11 attacks. His investigation began over lunch when one of his sources, a Taylor associate named Cindor Reeves, casually asked, "What is Hezbollah?" Reeves explained that a group of Arab diamond clients had invited him to watch videos of Hezbollah suicide bombings. When Farah later showed him photos of known al Qaeda operatives published in *Newsweek*, Reeves immediately recognized them as men he had taken to the diamond fields of Sierra Leone. Farah held a secret meeting with a group of RUF commanders, who confirmed the identification. In November 2001, he broke the story on the front page of the *Post*.

In addition to the decades of corrupt rule in Sierra Leone and neighboring Liberia, the author lays blame on the U.S. Central Intelligence Agency for overlooking compelling evidence of a diamonds-terrorism link. Farah also criticizes the diamond industry for failing to take "serious measures" to eliminate conflict diamonds, suggesting that it was more interested in lobbying to water down the Clean Diamond Trade Act passed in 2001. He charges the World Diamond Council (WDC) with doing "little of substance" and downplays the effectiveness of its Kimberley Process Certification Scheme in policing the diamond supply chain.

Diamonds do not figure in the latter half of the book, which is a primer on al Qaeda's funding tactics. The author shows how al Qaeda has used *hawala*, an informal exchange system based on trust between brokers, to launder funds raised through Islamic charities and a host of petty scams. The book concludes with an unsettling picture of the barriers to combating terrorism, most notably shrinking counterterrorism budgets and bureaucratic infighting among U.S. government agencies.

The author's fast-paced, straightforward reporting is at its strongest in portraying the West African nightmare created by a network of corrupt political leaders, arms smugglers, and drugged-out child soldiers. While the section on al Qaeda fundraising operations is thorough and well documented, the alleged diamonds-terrorism connection that inspired the book's title is less so. Farah's story relies too heavily on the accounts of characters associated with Taylor and the RUF, and he abruptly drops the argument halfway through the book.

Indeed, the question of a possible link between the diamond trade and al Qaeda is still in dispute. Since the publication of *Blood from Stones*, the final report from the National Commission on Terrorist Attacks, known as the 9/11 Commission, cleared the diamond trade of links to al Qaeda. This finding was welcomed by the WDC but disputed by United Nations war-crimes prosecutors and the human rights group Global Witness. Yet with the end of Sierra Leone's civil war in January 2002, Charles Taylor's exile under international pressure in August 2003, and the implementation of the Kimberley Process the following month, few could deny that prospects for peace and stability in the West African diamond trade are brighter today.

STUART OVERLIN
Gemological Institute of America
Carlsbad, California

Starting to Collect Antique Jewellery

By John Benjamin, 191 pp., illus., publ. by Antique Collectors' Club, Woodbridge, England, 2003. US$25.00*

The challenges of collecting antique jewelry can be overwhelming. To make wise purchases, the collector must be armed with a good working knowledge of gems, metals, manufacturers, manufacturing styles, jewelry periods, and much more. With this guide, Mr. Benjamin succeeds in giving the reader specific information on all of these topics, as well as a broad overview of antique jewelry categories that will be helpful to the novice collector.

The book is comprised of 19 chapters, including "Gemmology and Gems in Antique Jewellery," "The Evolution of Jewellery from Early Times to the 18th Century," "Cameos and Intaglios," "Reviving History in the 19th Century," and "Fabergé, Tiffany, and Cartier." References for further reading are provided at the end of each chapter so readers may expand on their studies of selected topics. The book is generously illustrated with photographs of antique jewelry that range from the very simple to the most sumptuous. Illustrations from old jewelry catalogs are also included.

Especially appealing to this reviewer were the chapters on "Enamels" and "Jewels of Sentiment and Love," as they are areas of personal interest, but the entire book is filled with valuable information, such as why ironwork jewelry became popular, what features to look for in a cameo, and how platinum was integral to the development of the "garland" style of jewelry. Other useful features are short biographies of notable jewelers and a compendium that briefly discusses valuations, fakes, restorations, and cleaning.

Many enthusiasts find that they are drawn to specific areas of antique jewelry and focus their collections accordingly. *Starting to Collect Antique Jewellery* can help beginning collectors decide which areas interest them most, and it should be required reading for anyone thinking of starting an antique jewelry collection.

JANA E. MIYAHIRA-SMITH
Gemological Institute of America
Carlsbad, California

Starting to Collect Antique Silver

By Ian Pickford, 192 pp., illus., publ. by Antique Collectors' Club, Woodbridge, England, 2003. US$25.00

This visually appealing book, written by antique silver expert Ian Pickford, covers a wide range of areas related to collecting and caring for antique silver.

The author first discusses early silver sources, and how silver items and coins from other regions began to accumulate in Britain as international trade grew. Since silver was often melted down during times of economic hardship, problems associated with variations in metal content arose. The first solution was implemented in 1238, when sterling silver (.925) was established as the standard and wardens were appointed to test, assess, or assay silver. Pieces not up to the standard were destroyed. Later, the hallmarking system enacted by King Edward I in 1300 set a standard for coinage and goldsmithing.

Mr. Pickford details the evolution of this marking system, which essentially was the first form of consumer protection and now allows us to date and identify pieces of British silver with accuracy. The reader is never bored; scattered throughout are many interesting bits of related trivia, such as the origin of the expression "born with a silver spoon," silver's anti-bacterial properties, and why the price of silver dropped significantly with technological changes in the photographic industry. Entire chapters cover manufacturing techniques, highlight prominent maker marks, and take in-depth looks at various utility items and vessels. Items covered include spoons, candlesticks, tea and coffee items, drinking vessels, boxes, and small collectibles. The numerous high-quality photos and illustrations clearly demonstrate what a collector should look for on a particular piece. The author strives to clear up any misunderstandings regarding plating, and covers areas of concern such as fakes, forgeries, and alterations.

Although this book is geared toward collecting British silver and only offers a few American examples, it is an essential and informative book for any novice or serious silver collector.

MARY MATHEWS
Gemological Institute of America
Carlsbad, California

Within the Stone

By Bill Atkinson, 180 pp., illus., publ. by Browntrout Publishers, San Francisco, CA, 2004. US$39.95*

The first impression of *Within the Stone* is one of beauty—it hits you immediately with the cover photos. A close-up photograph of a fine dendritic agate from Madagascar adorns the front and draws your interest. The back cover features an intriguing photo of pietersite, a brecciated rock composed primarily of fragmented hawk's-eye and tiger's-eye quartz. These images draw you in, and that initial impression of beauty stays with you throughout the entire book.

Although this is not a scientific work or gemological text as such, the pleasure it conveys to the reader satisfies the curiosity we all have for nature and makes us want to explore this natural world beyond the limits of the 72 magnificent illustrations provided. The original poems and essays by noted artists and scientists that accompany each of the full-page photos add to the unique experience of this book as well.

Twenty-six different rocks and minerals are illustrated. The most widely pictured subjects are jasper, agate, petrified wood, and pietersite, so the breadth of material covered is not extensive. These are photomacrographs taken with a camera and bellows mounted on a copy stand, as opposed to photomicrographs taken through a microscope. The magnification range is 1× to 9×, and the polished rock and mineral subjects vary from 1

to 10 inches (2.5–25 cm) in width. For this reviewer, this approach is part of what is so special about the book. As a photomicrographer, I can also see in each image several different areas that would have been captured wonderfully with the higher magnifying power of a microscope. From either perspective, the selection of subjects is excellent.

Gemologists and earth scientists will find additional enjoyment in the "Rock Descriptions" chapter, written by well-known mineral authorities Si and Ann Frazier and Robert Hutchinson, which describes the mineralogical and gemological aspects of each of the illustrated subjects. The book closes with brief explanations on how the photographs were taken, and how the book itself was made. Nature is never perfect, but near perfection was achieved in these photos using careful gray-scale balancing with a digital gray card for each subject. The computer-scanned transparencies and the direct digital captures were also "cleaned up and refined in Adobe Photoshop."

Besides being a pleasure to read and study, this book also serves as an art catalogue, since all of the photos are available as large matted and signed fine-art prints. With its large (12 × 11 inch) format, *Within the Stone* is visually impressive. Mr. Atkinson refers to the book as "a beautiful work of art," and I agree completely. It will be enjoyed by anyone with a fondness for our natural world.

JOHN I. KOIVULA
Gemological Institute of America
Carlsbad, California

Gems and Jewels: A Connoisseur's Guide

By Benjamin Zucker, 248 pp., illus., publ. by Overlook Press, New York, NY, 2003. US$60.00

Since this book's original publication in 1984, the field of gemology has exploded with ever-increasing scientific sophistication, not to mention a succession of dizzying discoveries

from Canada's subarctic to the tropical depths of the South Pacific. Readers seeking relief from photoluminescence spectra and the geopolitical dramas facing today's gem markets will find welcome respite in Benjamin Zucker's reissued *Guide*.

Each of the chapters is dedicated to a single gem, beginning with the "Big Four" followed by pearl, amber, lapis lazuli, jade, turquoise, opal, and garnet. To address the subtitle's promise, Zucker introduces readers to each gem's distinguishing features. Though emphasis is placed on top-grade color and geographic provenance, the author also discusses chemical variances and microscopic characteristics.

More than 200 color photographs illustrate the qualitative aspects of fine gemstones as well as their recovery from earth and sea. Though inconsistent in composition and photographic quality, the illustrations include many historical and rarely seen pieces as well as notable gemstone objects and jewelry dating back to the Bronze Age. The exceptionally well-chosen color photos aptly serve this labor-of-love's emphasis on historical references and geographic origins.

Gem lovers with a pulse will quickly find their interest piqued by the book's description of extraordinary pieces residing in far-flung museums. As is the case throughout most of the book, collections from Europe, the Near East, and elsewhere in Asia are featured more prominently than North American treasures.

Changes to this new edition include a bounty of new photos and substantial text revisions, all supported by an updated introduction and index. While some readers may note occasional outdated terminology and omissions (such as a very thin discussion of Chinese freshwater cultured pearls in an otherwise thorough chapter on that organic material), the book is ideal for those seeking a descriptive and less quantitative approach to gem appreciation from a well-traveled and respected connoisseur.

MATILDE PARENTE
Indian Wells, California

OTHER BOOKS RECEIVED

The Tourmaline. *By A. C. Hamlin, 107 pp., illus., originally publ. by James R. Osgood & Co., Boston, MA, 1873; republished by Rubellite Press, New Orleans, LA, 2004, US$75.00.* **The History of Mount Mica.** *By A. C. Hamlin, 123 pp., illus., originally publ. by Augustus Choate Hamlin, M.D., 1895; republished by Rubellite Press, New Orleans, LA, 2004, US$85.00.*

Until now, these two classic works on tourmaline were available only through rare-book dealers. Fortunately for tourmaline aficionados, they have recently been republished as faithful reproductions—even including the original punctuation, spelling (with errors), formatting, and "feel." The hardbound covers also mimic the originals, as custom dies were created for the stamping and embossing process. Color plates in both books were meticulously matched to those found in original copies and are printed on high-quality paper.

The Tourmaline, which contains four color plates, chronicles the early history, world localities known at the time, and physical properties (particularly color) of this mineral. Approximately one-third of the book is devoted to the characteristics of tourmaline from Mt. Mica (Maine), including the crystal forms, colors, and specific localities at this historic deposit. In closing, the author offers some creative ideas on the origin of gems in general.

The History of Mount Mica contains eight drawings, five black-and-white photos (including a panoramic pull-out image), and color plates showing drawings of 43 tourmaline crystals from this locality. These plates, which occupy the latter half of the book, document the impressive color variations in tourmaline from Mt. Mica. The text provides a detailed account of the mining and production at this classic locality, from its discovery in 1820 until the mid-1890s.

BRENDAN M. LAURS
Gemological Institute of America
Carlsbad, California

Gemological **ABSTRACTS**

2004

COLORED STONES AND ORGANIC MATERIALS

The changing opal market. P. B. Downing, *Lapidary Journal*, Vol. 57, No. 7, 2003, pp. 62–66.

The opal market has seen many changes in the last 10 years. There has been a major decline in the production of natural opal from Australia, and the new non-Australian (e.g., Ethiopia, British Columbia) sources have not provided adequate replacement. At the same time, worldwide demand, especially from Japan, has weakened while prices have increased. The response to the reduced supply and high prices has been a reshaping of the market for opal. As a result, the market is now seeing more opal doublets, inlay, and intarsia in jewelry, as well as more opal synthetics and simulants.

Most common today are inexpensive "boulder opal" doublets (thin pieces of opal—usually darkened to simulate black opal—cemented to a brown ironstone base); cutters can easily produce four doublets from the same opal that would normally yield only one solid cabochon. However, boulder doublets are fragile and must be bezel set to reduce the risk of chipping. Another type of doublet, assembled primarily in Lightning Ridge, Australia, consists of thicker slices of opal with a common opal (potch) backing. These are cut in a dome shape with thicker edges that are less prone to chipping. Inlay jewelry became more popular in the 1990s. Inlay, like intarsia, conserves opal, as the rough used is only about 1–2 mm thick. Inlay and intarsia jewelry are currently being mass-produced in Asia.

Synthetic opal is gaining acceptance. The new Gilson Created Opal is difficult to distinguish from natural opal and is now used in quality jewelry. Opal simulants in a wide variety of colors are also becoming increasingly available. *MT*

Crystallographic position of Mn^{3+} in violet tourmaline. R. V. Shabalin and B. B. Shkurski, *Gemological Bulletin*, No. 9, 2003, p. 26–30 [in Russian with English abstract].

A tourmaline from Madagascar with an unusual violet color (type vB 8/2 in the GIA color notation) and characterized by a predominant absorption peak at 560 nm was investigated using X-ray diffraction analysis, electron microprobe analysis, and energy calculations with a Tanabe-Sugano diagram. This color was unique in a collection of more than 40 colored tourmalines available to the authors.

This tourmaline has a surplus of Al (7.73 formula units), which fully occupies the Z crystallographic positions. Thus, Mn^{3+} ions, which prefer the Z positions and cause an absorption at 515 nm, were required to occupy Y crystallographic positions, which resulted in the 560 nm absorption peak. Fe^{3+}, Li, and Al were also found in the Y positions, whereas Na and Ca occurred in the X positions. Small absorption peaks at 450 and 415 nm were caused by electron transitions due to Fe^{3+} and Mn^{2+}, respectively. Ti, Mg, and K were not detected by electron microprobe analysis. *BMS*

An interesting Australian abalone pearl. S. M. B. Kelly and G. Brown, *Australian Gemmologist*, Vol. 21, No. 12, 2003, pp. 498–501.

A detailed, illustrated description is given of a large crescent-shaped abalone pearl (95.79 ct) recovered from a black lip abalone (*Haliotis rubra*) from waters off Clay Head, northern New South Wales. The fleshy body of the abalone was so distorted by the size and shape of the pearl that the shell had to be broken for the pearl to be recovered. The multicolored iridescent nacre on the pearl was unevenly distributed, so it could only be considered to be of low-medium quality. *RAH*

Relationship between the groove density of the grating structure and the strength of iridescence in mollusc shells. Y. Liu, K. N. Hurwit, and L. Tian, *Australian Gemmologist*, Vol. 21, No. 10, 2003, pp. 405–407.

The iridescence of mollusk shells and pearls is caused by diffraction. A previous study showed that the strength of iridescence of a *Pinctada margaritifera* shell is qualitatively related to the groove density of the diffraction-grating structure formed by its aragonite tiles. In this study, the groove density of a shell of the pearl-producing *Pinctada maxima* was examined and found to be intermediate between the groove densities of the outer and inner surfaces of *P. margaritifera*; the strength of its iridescence was also intermediate. In general, a groove density in the range of 80–300 grooves per millimeter can produce iridescence in the visible-wavelength range; a density of 300 grooves per millimeter yields the strongest iridescence, whereas a density of 80 grooves per millimeter rarely produces iridescence. The authors conclude that the strength of the iri-

descence of a mollusk shell is directly related to the groove density of the diffraction-grating structure, and not to the species of mollusk. *RAH*

Rock-forming moissanite (natural α-silicon carbide). S. Di Pierro, E. Gnos, B. H. Grobety, T. Armbruster, S. M. Bernasconi, and P. Ulmer, *American Mineralogist*, Vol. 88, Nos. 11–12, 2003, pp. 1817–1821.

The possibility of silicon carbide occurring as a natural terrestrial mineral has been the subject of scientific controversy for nearly a century. This article reports the discovery of a unique volcanic rock that contains moissanite (6H polytype) as a significant mineral component (8.4% by volume). The rock was found accidentally as a beach pebble in an unpopulated region along the coast of Turkey about 150 km northwest of Izmir. The source outcrop of this pebble has not yet been located. The grayish blue rock exhibits a homogeneous, porphyritic texture consisting of fine-grained brucite, calcite, and magnesite along with larger macrocrysts of quartz and moissanite. The bulk whole-rock chemistry is somewhat similar to that of a kimberlite.

The moissanite crystals are hexagonal, 0.2–1.5 mm in size, and blue or black in color, with a metallic luster. Some crystals are transparent and display a subadamantine luster. They have a platy, tabular shape dominated by pinacoid (001) crystal faces. About one-third of the crystals examined contain one (or more on rare occasions) rounded black metallic inclusions of several phases, including Si and, in lesser amounts, various Fe-silicides. When viewed with transmitted light in thin section, the moissanite grains range from colorless to light or dark blue to almost black. Some crystals are pleochroic, and some are likely to be twinned. Optically they are uniaxial positive. A few grains exhibited yellow, blue, and red cathodoluminescence. The crystals are very homogeneous chemically, with no elements (besides Si) detected above background levels by electron microprobe analysis.

The authors present various kinds of evidence to suggest this rock is a naturally occurring specimen, and not the product of any industrial or scientific process. They conclude that the rock most likely formed at ultra-high-pressure conditions in the upper mantle or transition zone, and was brought to the Earth's surface during a volcanic eruption. *JES*

DIAMONDS

Diamonds: Time capsules from the Siberian mantle. L. A. Taylor and M. Anand, *Chemie der Erde: Geochemistry*, Vol. 64, No. 1, 2004, pp. 1–74.

In this invited review, the authors report their systematic studies on diamondiferous eclogite xenoliths from Siberia. The steps in investigating these are: (1) high-resolution computed X-ray tomography of the xenoliths to give 3-D

images that relate the minerals of the xenolith to their diamonds; (2) detailed dissection of the entire xenolith to reveal the diamonds inside, followed by characterization of the setting of the diamonds within their enclosing materials; and (3) extraction of diamonds from the xenolith to facilitate further investigation of the diamonds and their inclusions. In this last step, it is important to record carefully the nature and relative positions of the inclusions in the diamonds to maximize the number of inclusions that can be exposed simultaneously on one polished surface. Once the diamonds have been extracted, cathodoluminescence imaging is performed on polished surfaces to reveal the internal growth zones of the diamonds and the spatial relationship of the mineral inclusions to these zones. In addition, infrared analyses of nitrogen aggregation and carbon and nitrogen isotopic analyses are performed on the diamonds. Such multiple lines of evidence indicate the ultimate crustal origin for the majority of mantle eclogites. Similar pieces of evidence, particularly from $\delta^{13}C$ in P-type diamonds and $\delta^{18}O$ in peridotitic garnets, suggest that at least some of the mantle peridotites, including diamondiferous ones, as well as inclusions in P-type diamonds, may have a crustal protolith as well. *RAH*

DTC sightholders. P. Insch, *Rough Diamond Review*, No. 3, December 2003, pp. 13–15.

As a result of the economic hardships brought on by the Great Depression, consumer demand for diamonds declined drastically in the 1930s. In 1934, De Beers created the Central Selling Organisation (CSO, now known as the Diamond Trading Co. [DTC]) to stabilize the market by effectively directing the flow of rough diamonds to the marketplace through a single-channel system. Central to this system were "sightholders" (select dealers and manufacturers in international cutting centers), who were allocated rough diamonds every 10 weeks at a "sight." This system worked well for several decades because De Beers supplied, via the DTC and its predecessor, 80% of all gem-quality rough diamonds sold worldwide.

Recently, De Beers, which currently supplies 50–60% of global production, revamped their single-channel marketing system into an updated Supplier of Choice initiative designed to increase consumer demand for diamond jewelry and facilitate effective competition of diamonds with other luxury goods. Currently, there are about 80 sightholders in this new rough diamond marketing format as opposed to 125–300 in previous decades. Several criteria are considered in the selection process for new sightholders: financial standing; market position; distribution, marketing, technical, and manufacturing abilities; and adherence to the *Best Practice Principles* of the DTC. Sightholders keep contracts with the DTC for two years, after which they must reapply to maintain their sightholder status.

Three factors determine the type and volume of goods offered the sightholder: (1) the sightholder's effectiveness in marketing diamonds and diamond jewelry; (2) the size and quality of diamonds requested by the sightholder for the next six-month period; and (3) the predicted availability of diamonds in the next period. Once all of these factors are assessed, De Beers gives each client an "intention to offer" list of the goods that client can expect. There are minimum prices for each box, and the sightholder (or a representative) may reject all or part of them. *JS*

Seeking the origin of carbon in diamond. P. Cartigny, *Rough Diamond Review*, No. 3, December 2003, pp. 39–42.

The study of carbon isotope variations in natural diamonds is important to our understanding of how diamonds formed. The isotopic ratio of ^{13}C to ^{12}C, expressed as $\delta^{13}C$ and reported as per mil (‰), is a deviation from an international standard for which $\delta^{13}C=0$. The $\delta^{13}C$ values for diamonds range from –38.5 to +2.7‰; however, two distinct $\delta^{13}C$ distributions occur. One spans the broad range of –38.5 to +2.7‰, whereas the second is restricted to a narrow band of –8 to –2‰. These distinct $\delta^{13}C$ distributions, incorporated in systematic studies of diamond's physical properties and inclusions, are associated with two types of diamonds, eclogitic and peridotitic, respectively. Each type originates from different sources in the earth.

Eclogitic diamonds form from sedimentary carbon recycled from the surface of the earth and subducted into the mantle. Peridotitic diamonds form in the mantle from carbon originally in that location. Notwithstanding the above explanations with respect to the two sources of carbon in diamond, some uncertainties and ambiguities exist (e.g., data from nitrogen isotopes) that have encouraged some researchers to favor a single source of carbon for both types of diamond. *DMK*

Spectroscopic and morphological characteristics of diamonds from the Grib kimberlite pipe. R. M. Mineeva, A. V. Speranskii, S. V. Titkov, O. M. Zhilicheva, L. V. Bershov, O. A. Bogatikov, and G. P. Kudryavtseva, *Doklady of the Russian Academy of Sciences, Earth Science Section*, Vol. 394, No. 1, 2004, pp. 96–99.

Diamonds from the new (discovered in 1980) diamondiferous province in the Arkhangel'sk district of northwestern Russia contain an extremely high content of rounded rhombododecahedral and tetrahexahedral, as well as cubic, crystals compared to diamonds from Yakutia (Siberia). Generally, Arkhangel'sk crystals are nearly colorless with pale yellow and brown tints. Details of the crystal morphology of 15 crystals are tabulated together with data on their paramagnetic centers. Compared with diamonds from other pipes in the Arkhangel'sk district, those from the Grib kimberlite have a lower content of Group 1 diamonds with a predominance of $P1$ centers. The majority of the Grib diamonds are classified as Group 2 with a predominance of $P2$ centers. The Grib kimberlite also con-

tains more *N*2-bearing Groups 3 and 4 diamonds compared to other kimberlites in the province. Since *N*2 centers in diamond crystals form during plastic deformation, the authors conclude that this epigenetic process (i.e., plastic deformation) had a greater effect on diamonds from the Grib pipe than it did on those from other pipes in the Arkhangel'sk district. *RAH*

GEM LOCALITIES

Der Pegmatit von Anjahamiary bei Fort Dauphin, Madagaskar [The Anjahamiary pegmatite near Fort Dauphin, Madagascar]. F. Pezzotta and M. Jobin, *Lapis*, Vol. 29, No. 2, 2004, pp. 24–28 [in German].
This zoned granitic pegmatite is situated about 80 km northwest of Fort Dauphin (Taolagnaro) in southeastern Madagascar, far from the well-known and highly productive gem pegmatite province in the central part of the country. It was first worked in the 1930s and has been exploited intermittently since then by different owners. After the discovery of a large tourmaline pocket in 1991, Somema, a Madagascan company, began exploration in the area as well as gem production from the tourmaline-bearing zones of the pegmatite. The tourmalines are mainly deep to pale pink and grayish blue to intense blue. A preliminary chemical analysis indicated that the blue parts are liddicoatite and the pink parts are rossmanite. Although the colors of some of the blue crystals resemble those of Paraíba tourmalines, the analysis did not detect any copper. *RT*

Genesis of amethyst geodes in basaltic rocks of the Serra Geral Formation (Ametista do Sul, Rio Grande do Sul, Brazil): A fluid inclusion, REE, oxygen, carbon, and Sr isotope study of basalt, quartz, and calcite. H. A. Gilg, G. Morteani, Y. Kostitsyn, C. Preinfalk, I. Gatter, and A. J. Strieder, *Mineralium Deposita*, Vol. 38, No. 8, 2003, pp. 1009–1025.
Amethyst geodes occur abundantly in a basalt lava flow (40–50 m thick) of Lower Cretaceous age in the Ametista do Sul region of the state of Rio Grande do Sul in southern Brazil. This area is famous for the production of amethyst both as geodes and cutting material. The geodes, typically spherical cap-shaped and sometimes vertically elongate up to 6 m in largest dimension, display an outer rim of celadonite followed inwards by agate, colorless quartz, and finally amethyst crystals. Occurrences of calcite and gypsum are also common within the geodes.

In this study, chemical and isotopic composition as well as fluid inclusion data were analyzed to better understand the conditions of geode formation. The authors suggest that their genesis most likely occurred as the result of a two-stage process. During the initial magmatic stage, numerous cavities are thought to have formed within the cooling lava from an immiscible fluid phase of lower den-

sity and viscosity than the surrounding basaltic magma. In a second, post-magmatic stage, the cavities were then filled with amethyst and other minerals (thus becoming geodes) at temperatures of less than 100°C, as determined by fluid inclusion and stable isotope data. These minerals crystallized from a circulating gas-poor aqueous fluid of meteoric origin that leached the necessary constituents from highly reactive interstitial glass in the host basalt. This infilling process is thought to have continued for an extended period of time (perhaps 40–60 million years) after the eruption of the basaltic lava. *JES*

Jurassic to Miocene magmatism and metamorphism in the Mogok metamorphic belt and the India-Eurasia collision in Myanmar. M. E. Barley, A. L. Pickard, K. Zaw, P. Rak, and M. G. Doyle, *Tectonics*, Vol. 22, No. 3, 2003, pp. 4-1–4-11.
For centuries, the Mogok Stone Tract in north-central Myanmar has been famous as a source of ruby, sapphire, peridot, spinel, and a wide variety of other gems. This abundance of gem minerals originates mainly from the Mogok metamorphic belt (MMB), a 50-km-wide zone of marbles, schists, and gneisses that are intruded by granites and pegmatites. Northward, this belt can be traced to the eastern edge of the Himalayas, whereas to the south it extends into Thailand. Because of its location, the MMB occupied a key position in the tectonic evolution of the region that witnessed the convergence and collision of fragments of the Paleozoic Gondwana and Eurasia continents, culminating in the collision of India and the uplift of Tibet and the Himalayas.

This article presents results from high-resolution ion-microprobe analyses of grains of zircon that had been collected in granitic rocks along the MMB. The resulting U-Pb ages suggest a complex magmatic and metamorphic history for the MMB, ranging from the Jurassic to the Miocene, that both pre-dates and post-dates the collision of India with the southern margin of Eurasia. Earliest zircon ages of about 170 million years (My) were obtained from strongly deformed granitic orthogneisses. Overgrowths on zircons give an age of about 43 My that is thought to represent metamorphic recrystallization during a period of thickening of the Earth's crust and associated metamorphism following the initial collision of India and Eurasia (65 to 55 My). The authors conclude that the MMB played a key role in the network of deformation zones that accommodated strain during the northward movement of India and the resulting extrusion and rotation of Indochina. *JES*

Lambina opalfield: An update. J. Townsend, *Australian Gemmologist*, Vol. 21, No. 12, 2003, pp. 490–494.
The Lambina opal field, 10 km south of the Lambina Homestead, in the remote northern part of South Australia, has been a significant producer of precious opal only in the last decade (e.g., the value of the production has ranged between $A7.3 and 10.2 million annually since 1999). At

Lambina, opalized sandstone is accompanied by opal introduced into cracks, in nodules, and replacing marine snails, belemnites, and bivalves. Good-quality opal from this locality includes white (light) opal and crystal opal that displays good play-of-color; about 50% of the opal does not fluoresce under long-wave ultraviolet light. Emphasis is placed on the possible influence of paleochannels as conduits for water movement (and hence silica movement) and the deposition of opal adjacent to these ancient channels.

RAH

Les gisements de corindon: Classification et genèse [Corundum deposits: classification and origin] and **Les placers à corindon gemme [Gem corundum placer deposits].** V. Garnier, G. Giuliani, D. Ohnenstetter, and D. Schwarz, *Le Règne Minéral*, No. 55, 2004, pp. 7–35 and 36–47 [in French with English abstract].

Several classifications of corundum have been proposed based on crystal habits, geologic settings and origin of the deposits, lithology of the host rocks, and chemical composition (only rubies). These authors propose an improved classification based on (a) the lithology of the host rocks and (b) deposit types. In general, the two articles deal with primary and secondary deposits, respectively.

Primary deposits are divided into two main groups: magmatic and metamorphic. These two groups are further divided into subtypes, each of which is discussed in detail using typical deposits as examples. Magmatic deposits comprise mainly basalts, such as those in Australia and Thailand/Cambodia, but also syenite xenoliths in basalts (Loch Roag, Scotland), syenites (Garba Tula, Kenya), and mafic intrusions (Yogo Gulch, Montana). The metamorphic deposit subtypes are: (1) pegmatitic intrusions in mafic, ultramafic, and carbonate rocks and their associated metasomatic rocks (Umba, Tanzania; Andranondambo, Madagascar); (2) marbles (Mogok, Myanmar; Hunza, Pakistan); (3) gneisses, granulites, and charnockites (Mysore, India; Ratnapura/Elahera, Sri Lanka); (4) amphibolites (Longido, Tanzania; North Carolina); and (5) anatexites (Morogoro, Tanzania).

The discussion of secondary deposits is basically a comprehensive description of the customary classification of such deposits into eluvial/colluvial, alluvial, and littoral deposits and their exploitation. Deposits in New South Wales (Australia), Vietnam, Ilakaka (Madagascar), and Tunduru (Tanzania) are discussed in detail. The article contains several maps and diagrams and is richly illustrated.

RT

Rare gem mineral deposits from Brazil. Part 2: Lazulite and scorzalite. M. L. de Sá C. Chaves, J. Karfunkel, A. H. Horn, and D. B. Hoover, *Australian Gemmologist*, Vol. 21, No. 10, 2003, pp. 390–399.

Lazulite and scorzalite constitute a complete solid-solution series between the magnesium and iron end members of the lazulite group. Although they are valued for their fine blue color, their relatively low hardness ($\sim5\frac{1}{12}$–6) and rarity in gem quality make them of interest primarily to collectors of rare gems. This paper identifies the Brazilian deposits where these lazulite-group minerals occur, discusses their genesis, and gives details of their gemological characteristics. Representative chemical analyses are given for lazulite-scorzalite series minerals from the Minas Gerais and Rio Grande do Norte areas. Most specimens are translucent to opaque, best suited for cutting en cabochon; transparent crystals are small (most faceted stones weigh < 1 ct) and typically have cracks and "feathers" that cause them to fracture during cutting.

RAH

Spectroscopic and related evidence on the coloring and constitution of New Zealand jade. C. J. Wilkins, W. C. Tennant, B. E. Williamson, and C. A. McCammon, *American Mineralogist*, Vol. 88, No. 8/9, 2003, pp. 1336–1344.

Nephrite jade has long been known to occur at several locations along the west-central coast of the South Island of New Zealand, where it is recovered from rivers as cobbles and boulders. The authors documented material from several deposits by chemical analysis and several spectroscopic techniques. Nephrite is a near mono-mineralic rock consisting of randomly oriented, felted masses of microscopic needles of actinolite/tremolite. The analyzed samples were generally similar in chemical composition except for variations in iron content, as well as the presence of trace elements such as chromium and nickel. The color of these samples could not be directly correlated to differences in composition.

Infrared spectra confirmed that the samples were composed principally of nephrite; chromian margarite (calcium mica) was also identified in several samples. Optical absorption spectra were consistent with those in the published literature. The Fe^{3+}/Fe^{2+} ratio increased for samples that were more highly weathered (which typically have a brown surface coloration of hydrated iron oxide that, in turn, is sometimes altered to a whitish rim if the material was exposed to more acidic weathering conditions). The black appearance of some samples is due to dispersed minute grains of a black opaque mineral (such as magnetite or chromite).

JES

INSTRUMENTS AND TECHNIQUES

An assessment of nuclear microprobe analyses of B in silicate minerals. H. Skogby, P. Kristiansson, and U. Hålenius, *American Mineralogist*, Vol. 88, No. 10, 2003, pp. 1601–1604.

Boron is a widespread but uncommon element in the Earth's crust. It is an important chemical component in certain gem minerals (e.g., tourmaline) and a minor element in many others (e.g., some olivine, sillimanite,

idocrase, muscovite). Because it is a light atomic-weight element, boron cannot be detected by standard electron microprobe analysis; as a result, the extent of its incorporation in many silicate minerals is uncertain. This article describes an alternative quantitative method for the microanalysis of the boron content in minerals over a wide concentration range. The method involves measurement of alpha particles released by this element when it undergoes a nuclear reaction involving a proton. The method requires access to a beam of 600–800 keV protons produced by a proton accelerator. The authors present results of their analyses of several minerals with B concentrations in the range of 1.9–8.8 wt.%, and discuss the advantages and possible applications of this nuclear microprobe method for analyzing boron concentrations in silicate minerals. *JES*

Large OPL™ diffraction grating spectroscope. T. Linton, A. Cumming, and K. Hunter, *Australian Gemmologist*, Vol. 21, No. 10, 2003, pp. 410–412.

This article describes a new, larger version of the well-known OPL diffraction grating spectroscope. Both are easy to use, have a fixed slit width and a fixed focus, and are capable of producing high resolution and a wide linear spectrum. However, the new instrument enables increased resolution of finer spectral features, as well as a 30% increase in the height of the spectra. The quality of the images of complex absorption spectra obtained from the large OPL instrument matched the quality of those produced by most other prism spectroscopes and was superior in some cases (e.g., it was easier to observe the 450/460 nm absorption that typifies blue Australian basaltic sapphire, and the wider red spectrum allowed more accurate and easier recognition of absorptions in that spectral region).

Gemologists who require vision correction may encounter difficulties using this instrument, because the spectral image viewed through the eyepiece lens of a fixed-focus spectroscope is set for users with "normal vision acuity." However, the authors provide an ingenious solution to this problem through the use of plastic lenses obtained from inexpensive "reading glasses." Numerous other practical suggestions are made, such as with regard to illumination, a stand to hold the spectroscope, and the use of a polarizing filter to increase resolution. The large OPL spectroscope is recommended for teaching purposes and for the practicing gemologist, as it will show most spectra that are required for gemological investigations.

MWF

The petrographic microscope: Evolution of a mineralogical research instrument. D. E. Kile, *Mineralogical Record, Special Publication No. 1*, 2003, 96 pp.

The petrographic microscope is an instrument that is designed to observe and measure the optical properties of minerals as a means of identifying them, in both unpolarized and polarized light. For over a century, it has been an essential tool in the development of the related sciences of mineralogy and petrography. This beautifully illustrated special supplement to the *Mineralogical Record*, written by a research chemist at the U.S. Geological Survey in Boulder, Colorado, presents a history of the petrographic microscope from the beginnings of optical mineralogy in the 1600s. It opens with descriptions of the main components of a petrographic microscope and of the optical properties of minerals that can be observed with it. Then the parallel historical evolution of the instrument and optical mineralogy are traced by citing the contributions of many individuals. Numerous color photographs illustrate this evolution with changes in the design of the microscope. The manufacturing of these instruments is also described, as are many specifically developed accessories (e.g., the quartz wedge, waveplate, and universal stage). The final section discusses the evaluation and restoration of antique petrographic microscopes. This extensive and thorough article is recommended reading for anyone interested in the development of optical mineralogy, which forms much of the basis for the tools and techniques of gem identification. *JES*

Possibilities of laser ablation–inductively coupled plasma–mass spectrometry for diamond fingerprinting. M. Resano, F. Vanhaecke, D. Hutsebaut, K. De Corte, and L. Moens, *Journal of Analytical Atomic Spectrometry*, Vol. 18, No. 10, 2003, pp. 1238–1242.

A homogenized 193 nm excimer laser with a flat-top beam profile is capable of controlled ablation of diamonds, and the sensitivity of ICP-MS suffices for the determination of more than 10 elements. For this study, 31 diamonds from four mines (Premier, Orapa, Udachnaya, and Panda) were ablated in eight different spots for 30 seconds, and the median of eight integrated signals was taken as the representative value for statistical analysis. Under these conditions, the total mass of material removed from a single diamond was ~16 µg (leaving a crater diameter of 120 µm).

Nine elements were selected for fingerprinting purposes (Al, Hg, Na, Ni, Pb, Sb, Sn, Ti, and Zn), and various pattern recognition techniques (ternary plots, cluster analysis, and partial least-squares analysis) were used to classify the data. For example, distinct differences in the diamonds from the four mines were observed when data for Ni, Ti, and Pb were plotted on ternary diagrams. These results are considered as promising, especially for the partial least-squares approach, provided that appropriate data standardization is carried out. The authors emphasize the practical difficulties associated with determining the provenance of diamonds by this multi-element technique—particularly for alluvial diamonds that may be transported vast distances from their primary sources.

RAH

JEWELRY RETAILING

Hot rocks. T. Treadgold, *BRW* [Business Review Weekly, Australia], Vol. 26, No. 20, 2004, pp 98–101.

As smaller diamonds and Chinese freshwater cultured pearls find favor in the mass markets, the rich are opting for bigger and better diamonds and pearls. As a result, producers of Australia's high-quality South Sea cultured pearls are maintaining their standards as supplies of lesser qualities of cultured pearls increase steadily, causing prices to erode. Australian producers, who are limited by government quotas, must command a premium price for their goods or face financial ruin. Last year, Australian cultured pearls accounted for 1% of total world production by volume but 30% by value.

Production of larger, high-quality diamonds is declining, creating a shortage and higher prices. Wealthy consumers are competing for such goods, while prices for mass-market diamonds have been languishing because less-affluent consumers are more price conscious. Brands, including BHP Billiton's CanadaMark diamonds which originate from the Ekati mine in Canada, are succeeding in creating a premium-brand consciousness in that country.

RS

SYNTHETICS AND SIMULANTS

Fe and Ni impurities in synthetic diamond. Y. Meng, M. Newville, S. Sutton, J. Rakovan, and H.-K. Mao, *American Mineralogist*, Vol. 88, No. 10, 2003, pp. 1555–1559.

The distribution and incorporation mechanisms of Fe and Ni impurities in General Electric Co. HPHT-grown synthetic diamond crystals were studied using synchrotron X-ray fluorescence (XRF) microanalysis and X-ray absorption near-edge structure (XANES) spectroscopy. The crystals were small (~700 μm) and were selected from standard industrial grit product in which Fe and Ni were used as catalysts. Nickel is dispersed as atoms either in the diamond lattice or in interstitial sites. It is concentrated in the {111} growth sectors relative to the {100} sectors. In contrast, iron exists as micro-aggregate inclusions with no observable growth-sector correlations. Further, the Fe is oxidized to the ferrous (Fe^{2+}) valence state and is very likely bonded with oxygen as FeO. *JES*

Features of beryllium aluminate crystal growth by the method of horizontally oriented crystallization. V. V. Gurov, E. G. Tsvetkov, and A. G. Kirdyashkin, *Journal of Crystal Growth*, Vol. 256, No. 3–4, 2003, pp. 361–367.

Synthetic chrysoberyl, including its variety alexandrite, has been grown mainly by the Czochralski pulling method. A new technique developed in Russia for growing single crystals of synthetic chrysoberyl—the horizontally oriented crystallization (HOC) method—has two main advantages over the Czochralski technique. One is the ability to use large molybdenum crucibles (in the form of "boats" up to 100×35 mm made from sheet molybdenum 0.2–0.3 mm thick) instead of expensive iridium crucibles. Another is that the process is relatively simple, with the oriented seed plate being moved horizontally through the melting zone at the rate of 1.5–3 mm/hr. In addition to the crystallization container, the other main component of the HOC apparatus is a resistance heating system consisting of tungsten coils that allows the growth of crystals with a melting point above 2000°C.

Synthetic chrysoberyl crystal ingots grown by the HOC method are elongated along the [100] direction; their size and geometry are determined by the shape of the boat-like crystallization container. The crystals have growth striations, localized zones of gas-melt inclusions, and numerous metallic inclusions composed of minute molybdenum crystals. Synthetic chromium-doped alexandrite crystals grown by the HOC method have several advantages over those produced by the Czochralski technique; for example, their chromium content is nearly constant along the length of the entire synthetic alexandrite crystal. *TL*

Growth of 15-inch diameter sapphire boules. C. P. Khattak, P. J. Guggenheim, and F. Schmid, in R.W. Tustison, Ed., *Window and Dome Technologies VIII, Proceedings of SPIE*, Vol. 5078, 2003, pp. 47–53.

This article describes the world's largest transparent synthetic sapphire boules, which weigh approximately 84 kg and measure 380 mm (15 inches) in diameter. They are being produced on a routine basis by the Heat Exchanger Method (HEM) at Crystal Systems Inc. in Salem, Massachusetts. These crystals are grown for use as special optical windows in military and other high-technology applications where high optical quality, compositional purity, and uniformity of physical properties are of crucial importance. The use of very pure starting materials for the crystallization process has resulted in a synthetic sapphire product with impurity levels that are very near the detection limit of the Glow Discharge Mass Spectroscopy (GDMS) technique (~5 ppm or less for the impurity elements). Efforts are underway to grow 500-mm-diameter synthetic sapphire boules by this same technique. *JES*

35 years on: A new look at synthetic opal. A. Smallwood, *Australian Gemmologist*, Vol. 21, No. 11, 2003, pp. 438–447.

Within a few years after the structure of synthetic opal was established in 1964, Pierre Gilson Laboratories in France produced the first truly synthetic opal. The history of the early days of synthetic opal manufacture is reviewed in this paper. The more recent production of synthetic and imitation opals from Japan, Russia, and China is described and their gemological properties are listed. Natural opal will

phosphoresce, but synthetic opals will not; the observation of a "lizard skin" pattern and no UV photoluminescence (i.e., the absence of phosphorescence) will confirm that an opal is synthetic. Dark varieties of synthetic opal will readily absorb a drop of water on the surface. Mention is made of industrial applications whereby the same-sized silica lepispheres of synthetic opal are coated with carbon; subsequent etching out of the silica leaves a series of ordered "shells" of carbon for use in so-called "photonic" devices that trap certain wavelengths of light. *RAH*

TREATMENTS

Change of cathodoluminescence spectra of natural diamond with HPHT treatment. H. Kanda and K. Watanabe, *Diamond and Related Materials*, Vol. 13, No. 4–8, 2004, pp. 904–908.

The recent introduction of high pressure, high temperature (HPHT) treatments to change the colors of natural diamonds from brown to colorless or to yellowish green has generated a persistent demand for new gemological identification techniques. To that end, several natural diamonds (mostly type IIa) were examined before and after HPHT treatment (6 GPa, 2000°C) using cathodoluminescence spectroscopy over the range 220–320 nm to evaluate changes induced by HPHT processes.

Three luminescence bands—2BD(G), 2BD(F), and 5RL—were found to decrease dramatically in intensity during HPHT treatment. For comparison, the band intensities were normalized to free-exciton (FE) lines, which are common in type IIa diamonds and not affected by HPHT treatment. The authors attribute the 2BD bands to plastic deformation on the basis of their association with mosaic strain patterns. The 5RL band is reportedly due to natural irradiation (i.e., α-particles) and quickly disappears with heating. Whereas the presence of the 2BD and 5RL bands in association with FE lines suggests that a diamond has not been HPHT treated, the absence of the bands is not diagnostic evidence for treatment because the bands do not occur in all type IIa diamonds.

Christopher M. Breeding

MISCELLANEOUS

Depositional placer accumulations in coarse-grained alluvial braided river systems. J. P. Burton and P. Fralick, *Economic Geology*, Vol. 98, No. 5, 2003, pp. 985–1001.

Economically significant deposits of certain minerals, including gems such as diamonds and corundum, occur as alluvial placers along braided river systems. The study reported here was based on field work at several uranium or gold placers in Canada, and on results obtained from laboratory experiments of moving sediment-water mixtures designed to simulate flowing rivers. The object was to identify the fundamental conditions present in gravel-dominated river systems that act to maximize the concentration of heavy minerals in alluvial deposits.

Alluvial placers form along *bars*, that is, ridge-like accumulations of sand, gravel, or other material at certain locations in a river where a decrease in the velocity of the moving water allows for deposition of the transported sediment load. Although similar in their geologic setting, two processes control the concentration of ore in placer deposits. Erosional placers are produced by preferential removal by the flowing water of light minerals from the mineral assemblage in a deposit. In contrast, depositional placers are formed by the preferential deposition of heavy minerals from the mixed assemblage of sediments moving past the site. Along a particular river system, both processes will simultaneously occur in different parts of the river channel, and will shift position over time. Erosion and deposition work together to produce a placer, and the dominance of one process over the other defines the placer type.

Data from this study indicate that a number of conditions are necessary, or at least desirable, for heavy minerals to accumulate in coarse-grained sediments. These conditions include:

1. A low proportion of granule to small pebble-size rock fragments in the alluvium

2. A very heavy mineral population with a hydraulic behavior in the flowing water that more closely resembles that of the pebble population compared to that of the quartz sand

3. Velocities of the flowing water capable of removing the coarse-grained quartz sand by suspension

4. A change in the slope of the river that creates a zone where the heavy mineral population can no longer be transported by the flowing water and is deposited

5. Infrequent major flooding events that would destroy placer deposits

6. Possible preconcentration of the heavy mineral population upstream in the river

These conditions, plus the presence of economically valuable minerals in the sediment load, control the formation of exploitable placers deposits in longitudinal bars in braided river systems.

JES